



**WetSpa Extension,  
A GIS-based Hydrologic Model for  
Flood Prediction and Watershed Management**

Documentation and User Manual

**Y.B. Liu, and F. De Smedt**

Department of Hydrology and Hydraulic Engineering  
Vrije Universiteit Brussel  
Pleinlaan 2, 1050 Brussel, Belgium

March 2004

Updated:  
July 2008 by Jef Dams  
February 2009 by Ali Safari  
February 2009 by Elga Salvadore

# **WetSpa Extension, A GIS-based Hydrological Model for Flood Prediction and Watershed Management Documentation and User Manual**

**Yongbo Liu and Florimond De Smedt**

Department of Hydrology and Hydraulic Engineering, Vrije Universiteit Brussel

Pleinlaan 2, 1050 Brussels, Belgium

Email: [yongbliu@vub.ac.be](mailto:yongbliu@vub.ac.be), [fdesmedt@vub.ac.be](mailto:fdesmedt@vub.ac.be)

**Abstract:** A GIS-based distributed watershed model, WetSpa Extension, has been under development suitable for use of flood prediction and watershed management on catchment scale. The model is physically based and simulates hydrological processes of precipitation, snowmelt, interception, depression, surface runoff, infiltration, evapotranspiration, percolation, interflow, groundwater flow, etc. continuously both in time and space, for which the water and energy balance are maintained on each raster cell. Surface runoff is produced using a modified coefficient method based on the cell characteristics of slope, land use, and soil type, and allowed to vary with soil moisture, rainfall intensity and storm duration. Interflow is computed based on the Darcy's law and the kinematic approximation as a function of the effective hydraulic conductivity and the hydraulic gradient, while groundwater flow is estimated with a linear reservoir method on a small subcatchment scale as a function of groundwater storage and a recession coefficient. Special emphasis is given to the overland flow and channel flow routing using the method of linear diffusive wave approximation, which is capable to predict flow discharge at any converging point downstream by a unit response function. The model accounts for spatially distributed hydrological and geophysical characteristics of the catchment and therefore is suitable for studying the impact of land use change on the hydrological behaviours of a river basin.

**Keywords:** Watershed modelling, WetSpa, GIS, Runoff, Flood prediction

## TABLE OF CONTENTS

ABSTRACT	i
TABLE OF CONTENTS	ii
LIST OF TABLES	v
LIST OF FIGURES	vi
1. MODEL DESCRIPTION	1
1.1 MODEL HISTORY	1
1.1.1 WetSpa	1
1.1.2 WetSpass	2
1.1.3 WetSpa Extension	3
1.2 MODEL CONSTRUCTION	4
1.2.1 Model objectives	4
1.2.2 Model structure	5
1.2.3 Model assumptions	6
1.2.4 Model limitations	7
1.3 DATA PREPARATION	9
1.3.1 Digital data	9
1.3.2 Hydro-meteorological data	12
2. MODEL FORMULATION	14
2.1 PRECIPITATION	14
2.2 INTERCEPTION	15
2.3 SNOWMELT	18
2.4 RAINFALL EXCESS AND INFILTRATION	19
2.5 DEPRESSION AND OVERLAND FLOW	21
2.5.1 Formulation of depression storage	21
2.5.2 Mass balance of depression storage	23
2.5.3 Formulation of overland flow	23
2.6 WATER BALANCE IN THE ROOT ZONE	24
2.7 EVAPOTRANSPIRATION FROM SOIL	25
2.7.1 Potential evapotranspiration	25

2.7.2	Actual evapotranspiration	28
2.8	PERCOLATION AND INTERFLOW	29
2.9	GROUNDWATER STORAGE AND BASEFLOW	32
2.10	OVERLAND FLOW AND CHANNEL FLOW ROUTING	34
2.10.1	Flow response at a cell level	34
2.10.2	Flow response at a flow path level	36
2.10.3	Flow response of the catchment	38
2.11	SUBCATCHMENT INTEGRATION	38
2.12	CATCHMENT WATER BALANCE	40
3.	PARAMETER IDENTIFICATION AND MODEL EVALUATION	43
3.1	DEFAULT PARAMETERS	43
3.1.1	Parameters characterizing soil texture classes	43
3.1.2	Parameters characterizing land use classes	44
3.1.3	Potential runoff coefficient	46
3.1.4	Depression storage capacity	50
3.2	GLOBAL PARAMETERS	53
3.3	MODEL EVALUATION	58
4.	MODEL OPERATION	61
4.1	PROGRAM INSTALLATION	61
4.2	PROGRAM DESCRIPTION	62
4.2.1	Avenue scripts and their tasks	62
4.2.2	Lookup tables	63
4.2.2	Fortran programs and their tasks	64
4.3	GIS PRE-PROCESSING	64
4.3.1	Surface grid preparation	64
4.3.2	Soil based grid preparation	68
4.3.3	Land use based grid preparation	69
4.3.4	Potential runoff coefficient and depression storage capacity	70
4.3.5	Flow routing parameters	70
4.3.6	Thiessen polygon	71
4.3.7	Drainage systems for a complex terrain	72

4.4	CREATION OF INPUT FILES	73
4.4.1	Input file of time series	73
4.4.2	Global parameters and spatial output specifications	76
4.5	MODEL CALIBRATION AND VERIFICATION	79
4.5.1	Calibration and verification processes	79
4.5.2	Parameter adjustment	83
4.5.3	Parameter sensitivity	84
4.6	MODEL OUTPUT	86
4.6.1	Intermediate output	86
4.6.2	Final output	88
4.6.3	Post processing of model outputs	92
5.	CASE STUDY: CASE 1: BISSEN CATCHMENT, LUXEMBOURG	93
5.1	Description of the study area	93
5.2	Data available	95
5.3	Basin delineation and parameter determination	98
5.4	Model calibration and validation	101
5.5	Discussion	105
6.	CONCLUDING REMARKS	108
	REFERENCES	112

## LIST OF TABLES

Table 3.1. Default parameters characterizing soil textural classes	43
Table 3.2. Default parameters characterizing land use classes	45
Table 3.3. Potential runoff coefficient for different land use, soil type and slope	47
Table 3.4. Slope constant $S_0$ for determining potential runoff coefficient	48
Table 3.5. Impervious percentages associated with selected land use classes	49
Table 3.6. Depression storage capacity for different land use, soil type and slope	51
Table 4.1. Sample file of precipitation series p.txt	74
Table 4.2. Sample file of potential evapotranspiration series pet.txt	74
Table 4.3. Sample file of temperature series t.txt	75
Table 4.4 Sample file of discharge series q.txt	75
Table 4.5. Template of global model parameters	76
Table 4.6. Template of spatial output specifications	77
Table 4.7. Parameter sensitivity for model calibration	85
Table 4.8. Sample output file of mean.txt	86
Table 4.9. Parts of output file uh_cell_h.txt	87
Table 4.10. Sample output file of q_tot.txt	88
Table 4.11. Sample output file of q_sub.txt	89
Table 4.12. Sample output file of balance.txt	90
Table 4.13. Parts of output file runoff.asc	90
Table 4.14. Model evaluation result evaluation .txt	91
Table 5.1. Default parameter values in the PET formula for different land use	97
Table 5.2. Data available and characteristics of the Bissen catchment	98
Table 5.3. Statistics and model performance for the calibration/validation period	103
Table 5.4. Water balance estimation at Bissen for the whole simulation period	106

## LIST OF FIGURES

Fig. 1.1. WetSpa model structure	2
Fig. 1.2. Schematic of a hypothetical grid cell for WetSpa	3
Fig. 1.3. Structure of WetSpa Extension at a pixel cell level	6
Fig. 2.1. Annual variation of grass interception storage capacity	17
Fig. 2.2. Relationship between rainfall excess coefficient and soil moisture content	20
Fig. 2.3. Sketch of depression storage as a function of excess rainfall	22
Fig. 2.4. Graphical presentation of excess rainfall and overland flow	24
Fig. 2.5. Graphical presentation of soil water balance	24
Fig. 2.6. Observed and simulated daily EP at Ukkel for the year 1997	27
Fig. 2.7. Simulated hourly EP with $EP_d = 3m$	27
Fig. 2.8. Graphical presentation of soil evapotranspiration	29
Fig. 2.9. Effective hydraulic conductivity as a function of moisture content	30
Fig. 2.10. Flow path response functions with different $t_i$ and $\sigma_i^2$	37
Fig. 3.1. Potential runoff coefficient vs. slope for forest and different soil types	48
Fig. 3.2. Depression storage capacities vs. slope for grass and different soil types	52
Fig. 4.1. Schematic view of the model's project folders	61
Fig. 4.2. Screenshot of surface menu	65
Fig. 4.3. Screenshot of parameter menu	68
Figure 5.1. Location of the Bissen catchment	93
Figure 5.2. Watershed topography of Bissen	94
Figure 5.3. Land use map of Bissen	94
Figure 5.4. Soil type map of Bissen	94
Figure 5.5. River network and Thiessen polygons of Bissen	94
Figure 5.6. Hydraulic radius of Bissen	99
Figure 5.7. Runoff coefficient of Bissen	99
Figure 5.8. Mean travel time to the basin outlet of Bissen	100
Figure 5.9. Standard deviation of flow time to the basin outlet of Bissen	100
Figure 5.10. Observed and calculated flow at Bissen for the floods in Dec. 1999	102
Figure 5.11. Observed and calculated hourly flow at Bissen for the year 1999	104
Figure 5.12. Peak $Q_m$ Vs Peak $Q_c$ selected from the whole simulation period	104
Figure 5.13. Observed and calculated hourly flow frequency curves at Bissen	105

## **1. MODEL DESCRIPTION**

Recent development of GIS and remote sensing technology makes it possible to capture and manage a vast amount of spatially distributed hydrological parameters and variables. Linking GIS and the distributed hydrological model is of rapidly increasing importance in studying the impact of human activity on hydrological behaviours in a river basin. Ideally, watershed models should capture the essence of the physical controls of topography, soil and land use on runoff production as well as the water and energy balance. Distributed parameter hydrological models are typically structured in characterizing watershed conditions such as topography, soil type, land use, drainage density, degree of soil saturation, and rainfall properties, for which it is advantageous to use the data currently available in GIS format. This report describes such a model, called WetSpa Extension.

### **1.1 Model History**

*The WetSpa Extension is based on the previously developed WetSpa model, and is parallel to another extension WetSpaSS. A brief introduction of these two models is given below.*

#### **1.1.1 WETSPA**

*WetSpa is a physically based and distributed hydrological model for predicting the Water and Energy Transfer between Soil, Plants and Atmosphere on regional or basin scale and daily time step developed in the Vrije Universiteit Brussel, Belgium (Wang et al., 1997 and Batelaan et al., 1996). The model conceptualizes a basin hydrological system being composed of atmosphere, canopy, root zone, transmission zone and saturation zone. The basin is divided into a number of grid cells in order to deal with the heterogeneity. Each cell is further divided into a bare soil and vegetated part, for which the water and energy balance are maintained. Figure 1.1 shows schematically the considered hydrological processes. Water movement in the soil is simplified as one-dimensional vertical flow, including surface infiltration, percolation and capillary rise in the unsaturated zone and recharge to groundwater. The model was designed to simulate the Hortonian overland flow and the variable source area concept of runoff generation. In order to have a more realistic representation of the interaction between surface runoff and groundwater storage,*

a groundwater flow model is integrated, for which the groundwater balance in the saturated zone is described by the two-dimensional Dupuit-Forchheimer horizontal flow equation. Under appropriate boundary conditions, the water table position is determined with a finite difference scheme for each grid cell, and explicitly for each time step. The model was designed for scientific research with time resolution of minutes. This brings difficulties to the model in practical application due to the data available.

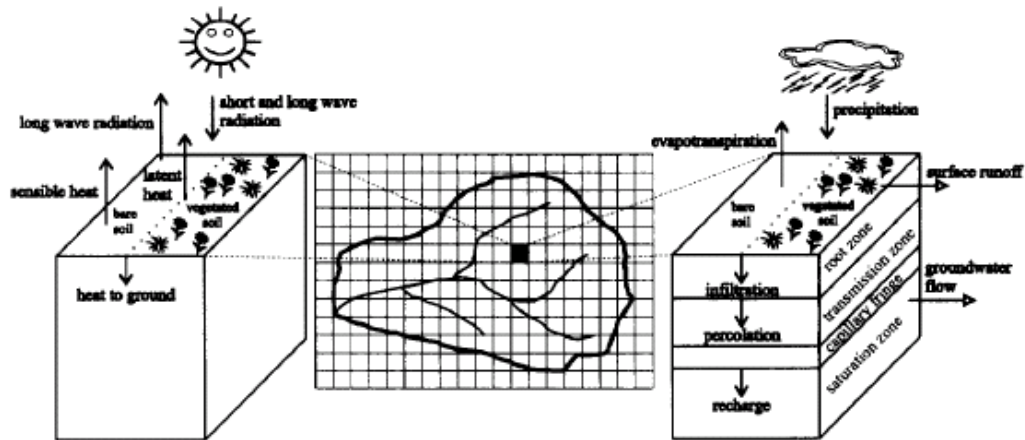
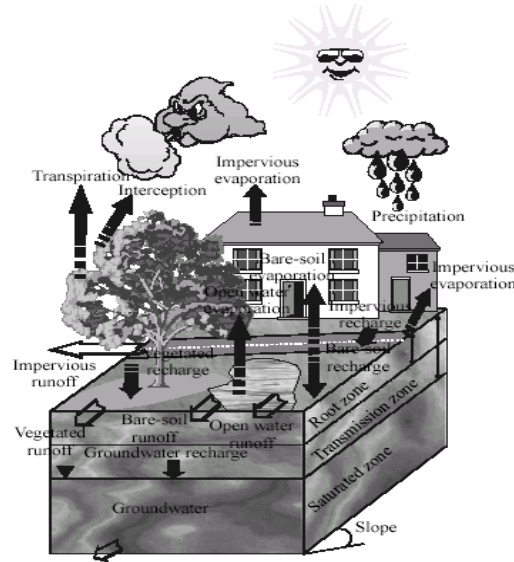


Fig. 1.1. WetSpa model structure

### 1.1.2 WETSPASS

For the estimation of long-term spatial patterns of the groundwater recharge, that could be used as input in regional groundwater flow models and for the analysis of regional groundwater flow systems, a simplified model WetSpa was developed by Batelaan & De Smedt (2001) based on WetSpa. WetSpa stands for Water and Energy Transfer between Soil, Plants and Atmosphere under quasi-Steady State conditions, which is GIS based, spatially distributed hydrological model for calculating the spatially distributed yearly and seasonal evapotranspiration, surface runoff, and groundwater recharge. The model accounts for the spatial variation in the groundwater recharge, which is the result of distributed land use, soil type, slope, etc. Figure 1.2 gives a schematic water balance of a hypothetical grid cell for WetSpa from Batelaan & De Smedt (2001). The total water balance for a cell in a spatially distributed grid is split up in independent water balances for vegetated, bare-soil, open-water and impervious parts of the grid cell. This allows

accounting for the non-uniformity of the land use depending on the resolution of the grid cell. The processes in each part of a grid cell are set in a cascading way. This means an order of occurrence of the processes, after the precipitation event, is assumed. Defining such an order is a prerequisite for the seasonal time scale with which the processes are quantified.



**Fig. 1.2.** Schematic of a hypothetical grid cell for WetSpa

### 1.1.3 WETSPA EXTENSION

The WetSpa Extension, described in this report, is a GIS-based distributed hydrological model for flood prediction and water balance simulation on catchment scale, which is capable of predicting outflow hydrograph at basin outlet or any converging point in a watershed with a variable time steps (De Smedt et al., 2000; Liu et al., 1999, 2002, 2003). The model aims not only at predicting flood, but also investigating the reasons behind it, especially the spatial distribution of topography, land use and soil type. Comparing with the original WetSpa model, the major changes involved in this extension are:

- 1) The time resolution of all hydrological processes is changed to a variable time scale (minutely, hourly, daily, etc.) in order to meet the specific requirement of flood prediction.
- 2) The flow routing component for both overland flow and channel flow are incorporated using the method of linear diffusive wave approximation.

- 3) *The component of shallow subsurface lateral flow is added to the original model simulating interflow by the method of kinematic approximation.*
- 4) *The component of snowmelt modelling is added to the original model simulating snowmelt by the degree-day approach.*
- 5) *The hydrological process of depression storage is taken into account being one of the major losses of initial abstraction.*
- 6) *Groundwater flow simulation is performed on small subcatchment scale by the method of linear reservoir for the simplification of model parameterization.*
- 7) *Some model formulas are modified in order to make the model more physically based and capable of using readily available data.*
- 8) *All default parameter values involved in the model lookup tables are recalibrated based on the literature review and practical case studies.*
- 9) *Model programs using ArcView Avenue and Fortran language are developed, which makes use of spatial inputs and gives spatial outputs as well.*

This manual is designed to provide a brief description of the components in the WetSpa Extension. It also describes the program structure, the guideline for estimating model parameters, the base maps required to represent a catchment, as well as the input and output datasets for model calibration and validation. The ArcView scripts, lookup tables and Fortran programs, as well as the sample input and output files are included in the ArcView project in the enclosed diskette. Operating instructions and any revisions can be found in the project help script.

## **1.2 MODEL CONSTRUCTION**

### **1.2.1 Model objectives**

- 1) To provide a comprehensive GIS-based tool for flood prediction and watershed management on catchment scale, which is compatible with GIS technology and remote sensing information.
- 2) To enable the use of the model for simulation of the spatial distribution of hydrological processes, such as runoff, soil moisture, groundwater recharge, etc.

- 3) To enable the use of the model for analysis of land use change and climate change impacts on hydrological processes.
- 4) To provide for a distributed model that can operate on cell scale and a variable time step, and a semi-distributed model on small subwatershed scale.
- 5) To provide a platform on which the future water quality and soil erosion models can be developed at multiple scales.

### **1.2.2 Model structure**

The model uses multiple layers to represent the water and energy balance for each grid cell, taking into account the processes of precipitation, interception, snowmelt, depression, infiltration, evapotranspiration, percolation, surface runoff, interflow and groundwater flow. The simulated hydrological system consists of four control volumes: the plant canopy, the soil surface, the root zone, and the saturated groundwater aquifer. The precipitation that falls from the atmosphere before it reaches the ground surface is abstracted by canopy interception storage. The remaining rainfall reached to the ground is separated into two parts depending on the land cover, soil type, slope, the magnitude of rainfall, and the antecedent moisture content of the soil. The first component fills the depression storage at the initial stage and runs off the land surface simultaneously, while the remaining part infiltrates into the soil. The infiltrated part of the rainfall may stay as soil moisture in the root zone, move laterally as interflow or percolate further as groundwater recharge depending on the moisture content of the soil. Drainage water from a given cell flows laterally depending on the amount of groundwater storage and the recession coefficient. The percolation out of the soil layer is assumed to recharge the groundwater storage. Interflow from the root zone is assumed to contribute overland flow and routed to the watershed outlet together with surface runoff. The total runoff from each pixel cell constitutes the sum of the surface runoff, the interflow and the groundwater flow. Evaporation takes place from intercepted water, depressed water and the soil surface, while transpiration takes place from the plant through root system in the soil layer, and a small part from the groundwater storage. The water balance for the interception storage includes precipitation, evaporation and through fall. The water balance for the depression storage includes through fall, infiltration, evaporation and surface runoff. The water balance for the

soil column includes infiltration, evapotranspiration, percolation, and lateral subsurface runoff. The water balance for the groundwater storage includes groundwater recharge, deep evapotranspiration, and lateral groundwater flow. Figure 1.3 shows schematically the model structure at a pixel cell level.

The simple structure in Figure 1.3 is used in the model because the emphasis here is on developing and testing parameterizations for the root zone. Excess runoff, infiltration, evapotranspiration, interflow and percolation estimates are point calculations. Different slope, land use and soil properties in different grid cells of a watershed result in different amounts of excess runoff when subjected to the same amount of rainfall. The routing of runoff from different cells to the watershed outlet depends on flow velocity and wave damping coefficient using the method of diffusive wave approximation. Although the spatial variability of land use, soil and topographic properties in a watershed are considered in this model, the groundwater response is modelled on small subcatchment scale for the convenience of model parameterization and model simulation. Two alternatives for determining groundwater flow are used in the model, simulating groundwater flow with a simple linear reservoir method and non-linear reservoir method. All model equations are specifically chosen to maintain a physical basis and well supported by previous studies. The inputs to the model are precipitation and potential evapotranspiration (PET).

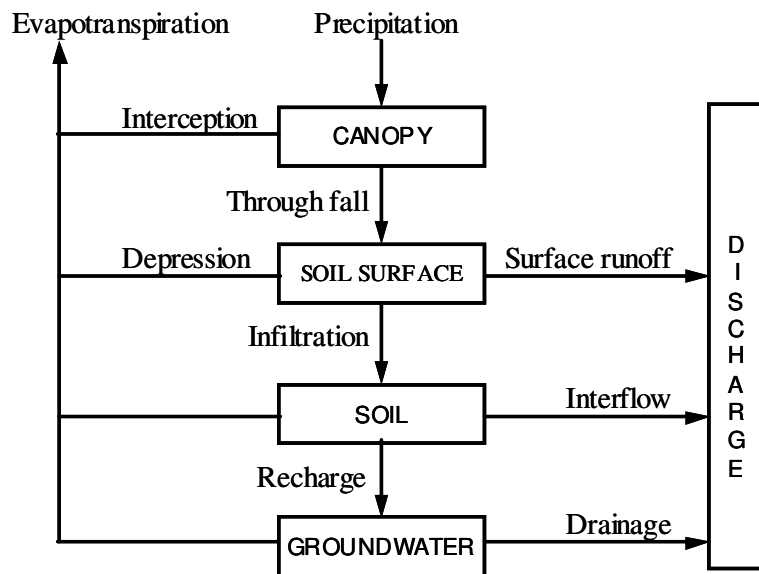


**Fig. 1.3.** Structure of WetSpa Extension at a pixel cell level

Temperature data are needed if snow accumulation and snowmelt occur during the simulation period. The digital maps of topography, land use and soil type are used to derive all necessary spatial distributed model parameters. The main outputs of the model are river flow hydrographs and spatially distributed hydrological characteristics, such as soil moisture, infiltration rates, groundwater recharge, surface water retention or runoff, etc.

### **1.2.3 Model assumptions**

- 1) Soil characteristics and landscape are isotropic and homogeneous for a single raster cell.
- 2) Canopy cover and ground cover are homogeneous for a single raster cell.
- 3) Precipitation is spatially homogeneous within a raster cell.
- 4) The form of Hortonian overland flow is valid for most of the areas.
- 5) Evapotranspiration is neglected during a rainstorm and when the soil moisture is lower than residual soil moisture.
- 6) Deep evapotranspiration takes place when soil is dry, and is restricted by the amount of effective groundwater storage.
- 7) Soil moisture content is homogeneous in a single cell, while the groundwater storage is uniformly distributed on small subcatchment scale for each time step.
- 8) Water flows along its pathway from one cell to another, and cannot be partitioned to more than one adjacent raster cell.
- 9) The method of linear diffusive wave approximation is valid for routing of both overland flow and channel flow.
- 10) Hydraulic radius is location dependent, varies with flood frequency, but remains constant over a flood event.
- 11) Interflow occurs when soil moisture content is higher than field capacity and can be estimated by Darcy's law and kinematic approximation.
- 12) The water losses during overland and channel flow, as well as the losses of deep percolation are not important.

#### **1.2.4 Model limitations**

*Hydrological modelling is an attempt to simulate real hydrological processes through the use of input data describing physical characteristics of the system, a set of algorithms to transform input data to output of interest, and simplifying assumptions to limit the scope of the model. Model limitations must be considered in running the model and interpreting its output. Followings are the major limitations associated with model simulation.*

- 1) WetSpa Extension runs with a continuous input data series. Therefore, the check of continuity and reliability must be carried out in the phase of data preparation. If missing data exist in the precipitation or PET series, artificial interpolation must be done for the time period. For the purpose of continuous model evaluation, negative values are taken the place in case of missing flow records.*
- 2) The land use categories are grouped, for which some of the categories might be somewhat ambiguous. For instance, the category agriculture may include farmsteads, lawns, disturbed areas, idle land, and other land uses that are not identifiable as one of the other specified land use categories. Further more, the annual crop rotation is not taken into account in the model. On the other hand, lower level highways and country roads are not modelled uniquely, but are combined within the rural residential category, this may reduce the amount of runoff and alter the flow direction expected from these areas.*
- 3) Values assigned to any raster or grid cell represents an average value over the area of each cell. The greater the variability over the cell, the greater will be the error induced through the use of an average value. Therefore, the grid size should be well defined. A small grid size may better represent the variability of physical watershed characteristics, but leads to more memory cost and time consumption during the model simulation, especially for large watersheds. Balance should be made between the model accuracy and computer efficiency.*
- 4) The time resolution should be well defined. As for instance, it is not feasible to predict flood using hourly or daily scale for a very small watershed, where excess water may flow out within the first time step. In this case, a shorter time interval should be chosen, if field measurements are available.*
- 5) The snow accumulation and snowmelt are modelled in a simple way by the degree-day*

*coefficient method, where the redistribution of snow pack, the influence of aspect, local slope, land use, etc., to the snowmelt are not into account.*

- 6) WetSpa Extension generates runoff by an empirical-based modified coefficient method rather than from equations more closely representing physical processes. Though definitely a limitation, the use of the method has its advantages of close linking runoff with cell characteristics such as slope, land use, soil type and moisture content, and has a great potential to predict the impact of land use change on hydrological behaviours in the watershed.*
- 7) The impervious fractions for urban areas are set subjectively depending upon cell size, since no detailed measurements are available. For instance, for a 50X50 m grid, 30% is set for residential area, 70% for commercial and industrial area and 100% for major communication lines, parking lots, etc. This may not actually reflect the real world and may bring errors to model result.*
- 8) WetSpa Extension employs many default parameters, which are interpolated from the literature and used over the entire catchment. Due to the vast variation range, parameters such as hydraulic conductivity, roughness coefficient, etc. may change greatly when applying the model to another place with quite different environment. Therefore, model calibration is preferable, and this brings difficulties in model parameterization in an un-gauged river basin.*
- 9) WetSpa Extension simulates groundwater flow on small subcatchment scale. It estimates the groundwater flow and groundwater storage for each small subcatchment at each time step, but cannot predict the spatial distribution of groundwater table, as well as its variation during the simulation period.*
- 10) WetSpa Extension assumes that the groundwater table is below the root zone. This constrains the use of the model in wetland areas.*

### **1.3 DATA PREPARATION**

The preparation of the database for WetSpa Extension to a specific watershed implies the determination of the complete drainage structure of the watershed, the spatial distribution of land use classes and soil types, as well as the collection of available hydro-meteorological data related to the project.

### **1.3.1 Digital data**

The model uses geo-spatially referenced data as input for deriving model parameters, which includes most data types supported by ArcView, such as coverage, shape file, grid and ASCII file. Image can be used for reference within a view, but is not used directly by the model. The digital maps of topography, land use and soil type are 3 base maps used in the model, while other digital data are optional depending upon the data available and the purpose and accuracy requirement of the project.

#### **1) Digital Elevation Model (DEM)**

The raster-type DEM, generated from point or contour topographic map, is preferred in order to be compatible with other remotely sensed data. The spatial and elevation resolutions should be fine enough to capture the essential information allowing taking care of the effects of spatial variability of the watershed characteristics on its hydrological response. In practice, the chosen resolution must allow adequate representation of the actual topography and accurate determination of the watershed area, its river network, and its subwatersheds. In the absence of large water surfaces (lakes, reservoirs, ponds, etc.) and large plains with little or no elevation variation, processing of the DEM is relatively straightforward. After filtering of the initial data to detect and remove erroneous extreme values, the slope, aspect, flow direction, flow length and flow accumulation of each grid cell are determined. Over flat areas, no slope and, hence, no direction can be computed. Also, the DEM may contain artificial pits from which no water can flow out. These specific problems have to be reserved by modifying elevations artificially to lead to flow directions as accurate as possible on any of the cells. Next, the identification of river network is performed by assuming that all cells draining more than a specified upstream area are part of that network. More or less detailed river networks can be identified, depending on the selected upstream threshold area. Finally, the stream links, stream orders and the subwatersheds corresponding to these river reaches are identified.

#### **2) Land use and soil types**

Land use information is an important input to the WetSpa Extension, which is normally obtained from high-resolution remotely sensed data for the same area as the DEM, and

with the same grid cell size. For hydrological simulation purpose, all land use classes initially determined are grouped together into 14 WetSpa classes significantly distinguished from each other on the basis of their effect on hydrological processes, namely crop, short grass, evergreen needle leaf tree, deciduous needle leaf tree, deciduous broad leaf tree, evergreen broad leaf tree, tall grass, irrigated crop, bog marsh, evergreen shrub, deciduous shrub, bare soil, impervious area and open water surface. Each of these classes is characterized by quantitative attributes. The groups may vary according to the algorithms used in the model. For instance, only 5 classes are considered in defining potential runoff coefficient and depression storage capacity, i.e. crop, grass, forest, bare soil and urban areas. For simulation purpose, the percentage of bare soil and impervious areas are estimated for each grid cell based on the high-resolution land use map.

Soil types of the catchment are obtained from the soil information furnished by soil maps. The soil code system used in WetSpa Extension is based on the soil texture triangle developed by the United States Department of Agriculture (USDA), which is characterized by its percentage of clay, silt and sand, ranging from the fine textures (clay), through the intermediate textures (loam); and the coarser textures (sand). Therefore, the original soil coverage map has to be converted to a raster map with WetSpa soil codes in the phase of data preparation. The grid must be adjusted to the same grid structure as the DEM and limited to the same area by using the mask grid of the catchment. The reclassification can be done within GIS framework, which makes use of a reclassification table prepared in ArcInfo GIS or ArcView Spatial Analyst. This work must be done with caution in order to make the conversion as accurate as possible. The soil properties and hydraulic characteristics of those soil types are considered constant in the present version of the model. Default values are interpolated from literature as described in section 3.1, but users can substitute any other more appropriate values for them.

### 3) Optional digital data

Other optional digital data that can be used in the model include point coverage or shape file of gauging station locations, line coverage or shape files of stream network and major traffic lines, polygon coverage or shape files of boundary and sewer systems,

etc. These data are of great help in delineating watershed drainage path network, estimating spatial rainfall distribution, as well as properly determining model routing parameters. If two or more rain gauges exist in or around the catchment with measured data, the Thiessen polygon weighting method is then introduced to calculate the rainfall distribution, for which the weighting factors are computed for each grid cell and subwatershed. Otherwise, a uniform rainfall distribution is assumed over the catchment. The internal streamflow gauges can be used in the watershed discretization process, for which the watershed is split at those locations where gauges are present. This makes it possible to compare measured and computed flow hydrographs at a point or series points. The coverage of official river network and catchment boundary is a very important geo-referenced data, which can be combined within GIS in delineating watershed drainage network, particularly for meandering rivers in flat areas. Usually, from the topographic information present in a DEM, it is quite difficult to represent watershed boundary and meandering rivers in plain areas. To account those cases, data coming from the hydrographical layer of digital maps (boundary, rivers, lakes, ponds, etc.) are used in combination with the DEM to identify drainage areas, find input and output cells for water bodies, and make any necessary corrections to flow directions in order to have the river reaches flow where they should and to be able to estimate the flow length closer to reality. For hydrological modelling in a complex terrain, such as an urban or suburban watershed, the sewer systems, communication lines, artificial channels, etc. are important elements in drainage structure configuration, and govern flow direction more strongly than the derived aspect at a local scale. Since most of these barriers are not sufficient to be represented in a DEM, additional procedures in term of deriving more realistic flow direction map are performed using GIS overlaying technique in the model, where the general flow direction map is overlaid by the sewer flow direction map, the communication line flow direction map and the river flow direction map subsequently. This allows water draining from the sewer areas at its outlet and water crossing communication lines at the concave points to join the river. The altered flow direction map is then used for further drainage structure delineation.

### 1.3.2 Hydro-meteorological data

The basic input requirements for the WetSpa Extension consist of model parameters, initial conditions, meteorological data and streamflow data for model calibration and validation. The basic meteorological data requirements are rainfall and PET. Temperature data are optional used for simulation of snowmelt. In the case of calculating PET by the Penman-Monteith equation, additional meteorological data are required, including air temperature, radiation, relative humidity and wind speed. In this section, the meteorological and hydrological data are described. The model parameters and initial conditions are described in the subsequent sections.

#### 1) Rainfall

Rainfall is the fundamental driving force and pulsar input behind most hydrological processes. Rainfall-runoff models are particularly sensitive to the rainfall input and any errors in estimates are amplified in streamflow simulations. The input rainfall series must be in the same interval as the model running step. For instance, hourly rainfall data are required for each rain gauge when modelling in an hourly scale. In many cases, rainfall data at certain stations are in a daily scale rather than an hourly scale. These data can be used by disaggregating according to the temporal structure of rainfall of the neighbouring hourly reference rain gauges. The Thiessen polygon method is then used to estimate areal rainfall during model simulation. Depending upon the objective of the study and on the time scale of the catchment response, the time resolution of rainfall input can be enlarged to a daily scale or reduced to a finer resolution corresponding to the model time scale. The rainfall data are treated as accumulated totals so that the rainfall associated with any particular time is the rainfall volume since the end of last time step.

#### 2) Potential evapotranspiration

WetSpa Extension requires PET data as one of the inputs with the same time interval as rainfall series, which can be obtained from field measurement or estimated by physical or empirical equations. Normally, daily values of PET are sufficient, for which the value is either averaged to an hourly value or disaggregated with a simple empirical equation as a function of hour as described in section 2.7. If only one measuring station is available, the PET data can be uniformly applied to the whole study area for a small

catchment. Otherwise, the value should be revised for different virtual stations according to the local meteorological and geophysical conditions, especially when modelling in mountainous areas. The areal PET is estimated using the Thiessen polygon method. The evapotranspiration data are treated as accumulated totals so that the evapotranspiration associated with any particular time is the evapotranspiration volume since the end of last time step.

3) Discharge ( $\text{m}^3/\text{s}$ )

For the purpose of model calibration and evaluation, observed discharge data at the basin outlet with the same time interval as the precipitation series are required for visual comparison and statistical analysis. The discharge data at internal gauging sites are optional for model verification. Data conversion to another time scale is necessary according to the simulation time step. The discharge data at any particular time is the average discharge since the end of last time step.

4) Optional meteorological data

Temperature data are required when snow accumulation and snowmelt occur in the catchment. Normally, daily average temperature data are sufficient in simulating snow processes. Anyhow, the temperature data should keep the same time interval as the precipitation series. If the Penman-Monteith equation is chosen to calculate the PET, when there is no measured data available in the study area, the data of air temperature, short wave radiation, relative humidity, and wind speed are required in the model, which can be obtained from the routine meteorological stations.

## **2. MODEL FORMULATION**

WetSpa Extension is a distributed, continuous, physically based model describing the processes of precipitation, runoff and evapotranspiration for both simple and complex terrain. It is a distributed model because the watershed and channel network are represented by a grid of mesh. Each cell is described by its unique parameters, initial conditions, and precipitation inputs. It is continuous model because it has components describing evapotranspiration and soil water movement between storms, and therefore can maintain water and energy balance between storms. It is physically based because the

mathematical models used to describe the components are based on such physical principles as conservation of mass and momentum. In this section, a brief description about the model formulation involved in the processes of interception, snowmelt, depression, infiltration, surface runoff, evapotranspiration, percolation, interflow and groundwater flow are presented.

## **2.1 PRECIPITATION**

Rainfall is a fundamental component of any hydrological model. As precipitation is commonly measured at fixed rainfall stations, either interpolation or extrapolation of the existing data is required to obtain information at a specific location in a catchment. The spatial distribution of rainfall is often estimated by the elementary techniques from a set of fixed rainfall gauges, while the temporal distribution is ignored by averaging the rainfall over a predetermined period. The crudest method for estimating the precipitation over a region is to plot contours of equal precipitation with the assistance of a structured grid. The average precipitation is computed between successive isohyets. This method is difficult to realize for each modelling time step with sparse precipitation data, although the task of plotting isohyets is automated with the advance of GIS technology.

A common interpolation approach is the Thiessen polygons, which is also the method used in the current version. In this approach, areas closest to a rainfall gauge adopt the rainfall recorded at that gauge. This results in constant rainfall regions with discontinuities between regions. In addition, there is no justification in assuming that point rainfall measurements provide reliable estimates of precipitation in the surrounding region.

The Thiessen polygon method assigns an area called a Thiessen polygon to each gage. The Thiessen polygon of a gage is the region for which if we choose any point at random in the polygon, that point is closer to this particular gage than to any other gage. In effect, the precipitation surface is assumed to be constant and equal to the gage value throughout the region. A FORTRAN code is developed to calculate mean areal precipitation over each subbasin using Thiessen polygon method, when model is intended to run in semi-distributed mode. Also, the same method is used for calculating mean areal evapotranspiration and temperature for subbasins.

Recall that, for the fully distributed modelling, Model2 program does not use output

file of the aforementioned developed code for the subbasins mean precipitation as well as evapotranspiration and temperature, since it is cell-based not subbasin-based.

## 2.2 INTERCEPTION

Interception is that portion of the precipitation, which is stored or collected by vegetal cover and subsequently evaporated. In studies of major storm events, the interception loss is generally neglected. However, it can be a considerable influencing factor for small or medium storms and water balance computations would be significantly in error if evaporative losses of intercepted precipitation were not included.

### 1) Mass balance of the interception storage

Interception is a complicated process, which is affected by the storm characteristics, the species of vegetation, percentage of canopy cover, growth stage, season, and wind speed, etc. Interception loss is higher during the initial phase of a storm and approaches zero thereafter. In WetSpa Extension, the rainfall rate is reduced until the interception storage capacity is reached. If the total rainfall during the first time increment is greater than the interception storage capacity, the rainfall rate is reduced by the capacity. Otherwise, all rainfall is intercepted in the canopy, and the remainder of interception is removed from the rainfall in the following time increments. The equation can be expressed as

$$I_i(t) = \begin{cases} I_{i,0} - SI_i(t-1) & \text{for } P_i(t) > I_{i,0} - SI_i(t-1) \\ P_i(t) & \text{for } P_i(t) \leq I_{i,0} - SI_i(t-1) \end{cases} \quad (2.2)$$

where  $I_i(t)$  is the interception loss at cell  $i$  over the time interval (mm),  $I_{i,0}$  is the cell interception storage capacity (mm),  $SI_i(t-1)$  is the cell interception storage at time step  $t-1$  (mm), and  $P_i(t)$  is the cell precipitation amount (mm). The mass balance of interception storage at a pixel cell is computed as:

$$SI_i(t) = SI_i(t-1) + I_i(t) - EI_i(t) \quad (2.3)$$

where  $SI_i(t-1)$  and  $SI_i(t)$  are cell interception storage at time step  $t-1$  and  $t$  (mm),  $EI_i(t)$  is the cell evaporation from interception storage (mm).  $EI_i(t) = 0$  when interception

storage is zero, or during the storm event.  $EI_i(t) = SI_i(t-1)$  under the condition of  $P_i(t) = 0$  and  $EP > SI_i(t-1) > 0$ , in which EP is the potential evaporation (mm). And  $EI_i(t) = EP$  for the rest conditions.

## 2) Seasonal variation of interception storage capacity

Interception storage capacity is a function of leaf area index and vegetal species. Evidently, it varies with season in temperate regions. Typical values can be found in the literature (Horton, 1919; Clark, 1940; Lull, 1964; Simons, 1981; Rowe, 1983). Through physical analysis and interpolations, a lookup table of maximum and minimum interception storage capacity corresponding to summer and winter extremes for different vegetation types are established (Table 3.2). Specifically, the interception storage capacity of crop is set to 0.8 mm during growing season and null for the rest. For wetting losses on impervious areas, the adsorption storage capacity is set to 0.5 mm (Bauwens et al., 1996). Since the interception storage capacity varies continuously with time, a simple sine-shaped variation curve is proposed for the convenience of model programming. The empirical equation is similar as that of estimating daily potential evaporation based on statistical analysis of long-term measurements (De Smedt, D., 1997), and is written as

$$I_{i,0} = I_{i,\min} + (I_{i,\max} - I_{i,\min}) \left[ \frac{1}{2} + \frac{1}{2} \sin \left( 2\pi \frac{d - 87}{365} \right) \right]^b \quad (2.4)$$

in which  $I_{i,\min}$  is the minimum interception storage capacity at cell  $i$  (mm),  $I_{i,\max}$  is the maximum interception storage capacity (mm), and  $d$  is the day of the year. The exponent  $b$  controls the shape of the variation curve, and can be adjusted according to the local conditions. Hourly interception storage capacity is assumed to be constant during a day in the model. Therefore, the interception storage capacity is only a function of the date. Figure 2.1 gives a graphical presentation for the annual variation of grass interception storage capacity, for which the minimum and maximum interception capacity is 0.5 and 2.0 mm respectively, and the exponent  $b$  is set to 1.35.

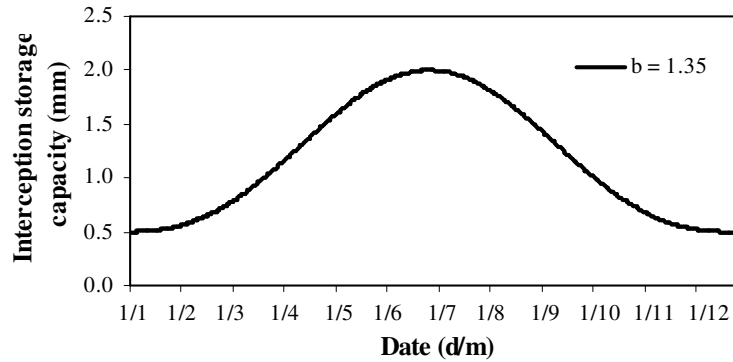


**Fig. 2.1.** Annual variation of grass interception storage capacity

By substituting Eq. (2.2) to Eq. (2.3), the interception loss and interception storage at each time step can be estimated. No interception loss exists when the interception storage capacity is achieved, and all precipitation reaches ground surface. The intercepted water in canopy loses by evaporation and returns to the hydrological cycle with potential evaporation rate modified by a correction factor. Although interception losses may be highly significant in the annual water balance, it is relatively unimportant for flood-producing storms.

### 2.3 SNOWMELT

Snow accumulation and melt are important hydrological processes in river basins, where the snow pack acts as storage in which precipitation is retained during the cold season and subsequently released as melt water during the warmer season. The snowmelt is incorporated within WetSpa Extension. This component is optional and temperature data is required additionally if the snow routine is selected.

The conceptual temperature index or degree-day method (Martinec et al., 1983) is widely used in snowmelt modelling, in which the full energy balance is replaced by a term linked to air temperature. It is physically sound in the absence of short wave radiation, when much of the energy supplied to the snow pack is atmospheric long wave radiation. Its reliance on daily temperature and precipitation data make it useful for modelling snow processes in regions with a lack of regular snow observations, or historical periods with limited data. In WetSpa Extension, an additional snowmelt caused by the advective heat

transferred to the snow pack by precipitation is also considered. The total snowmelt is calculated as

$$M_i = C_{snow}(T_i - T_0) + C_{rain}P_i(T_i - T_0) \quad (2.5)$$

where  $M_i$  is the daily snowmelt at cell  $i$  (mm/day),  $T_i$  is the cell daily mean temperature ( $^{\circ}\text{C}$ ),  $T_0$  is a threshold temperature (usually  $0^{\circ}\text{C}$ ),  $C_{snow}$  is the degree-day or melt factor (mm/ $^{\circ}\text{C}$ /day), and  $C_{rain}$  is a degree-day coefficient regarding to the heat contribution from rainfall (mm/mm/ $^{\circ}\text{C}$ /day). Specifically, temperature, precipitation and snow cover often vary significantly within a mountainous catchment, and in many cases, the hydro-meteorological information from mountainous areas is quite sparse. To account for the large variations in temperature with altitude, the reference series is adjusted for each grid cell by the lapse rate correction

$$T_i = T_{ref} + (H_i - H_{ref})\beta \quad (2.6)$$

where  $T_{ref}$  is the temperature at the reference station ( $^{\circ}\text{C}$ ),  $H_i$  and  $H_{ref}$  are the height at cell  $i$  and at the reference station, and  $\beta$  is the temperature lapse rate.

The degree-day coefficient implicitly represents all terms of the energy budget that account for the mass balance of a snow pack, and is therefore highly variable over time (Singh et al., 2000), and different between vegetation types (Kite & Kouwen, 1992). However, a constant value is used in the current version for simplicity. This factor can be determined by field experiments, or will have to be obtained by calibration otherwise. Moreover, the degree-day method by definition is only valid for daily melt simulations, whereas simulations for short time intervals require finer temporal resolutions. In this case, a fully energy balance module is suggested, and it will be incorporated in the future version.

## 2.4 EXCESS RAINFALL AND INFILTRATION

Excess rainfall, or effective rainfall, is that part of rainfall in a given storm, which falls at intensities exceeding the infiltration capacity of the land surface. It may stay temporarily on the soil surface as depression, or become direct runoff or surface runoff at the watershed outlet after flowing across the watershed surface under the assumption of Hortonian

overland flow. Direct runoff forms the rapidly varying portions of watershed hydrographs and is a key component for estimating the watershed response.

Infiltration is the downward flow of water into the soil defined as the quantity of rainfall that does not contribute to surface runoff. Under normal conditions, the infiltration rate is mainly a function of: (1) rainfall characteristics, (2) surface conditions, (3) soil characteristics, (4) initial moisture content of the soil, etc. It is desirable to relate loss rates to physical characteristics of the watershed in a continuous simulation so that loss rates may be computed as a function of catchment characteristics and soil moisture conditions during a model simulation. In WetSpa Extension, a modified coefficient method for estimating surface runoff and infiltration processes is used relating runoff and infiltration with topography, soil type, land use, soil moisture, and rainfall intensity. The equations can be expressed as

$$PE_i(t) = C_i [P_i(t) - I_i(t)] \left[ \frac{\theta_i(t)}{\theta_{i,s}} \right]^a \quad (2.7)$$

$$F_i(t) = P_i(t) - I_i(t) - PE_i(t) \quad (2.8)$$

in which  $PE_i(t)$  is the rainfall excess on cell  $i$  over the time interval (mm),  $F_i(t)$  is the cell infiltration (mm),  $I_i(t)$  is the interception loss (mm),  $\theta_i(t)$  is the cell soil moisture content at time  $t$  ( $m^3/m^3$ ),  $\theta_{i,s}$  is the soil porosity ( $m^3/m^3$ ),  $a$  is an exponent related with rainfall intensity (-), and  $C_i$  is the cell potential rainfall excess coefficient or potential runoff coefficient (-). This parameter  $C_i$  has a rather stable regularity under ideal conditions. Default rainfall excess coefficients for different slope, soil type and land cover are taken the reference from the literature (Kirkby 1978, Chow et al. 1988, Browne 1990, Mallants & Feyen 1990, and Fetter 1980). Based on the physical analysis and linear interpolations of these values, a look up table is then established (Table 3.3), relating potential rainfall excess coefficient to the different combinations of slope, soil type and land use. The rainfall excess is closely related with the relative soil moisture content. No rainfall excess when soil is dry, and actual rainfall excess coefficient approaches to the potential value when soil moisture content close to saturation, under which the infiltrated water is considered to be used for percolation, evapotranspiration and lateral interflow. The exponent in the formula is a variable reflecting the effect of rainfall intensity on the rainfall

excess coefficient. The value is higher for low rainfall intensities resulting less surface runoff, and approaches to 1 for high rainfall intensities. The threshold value can be defined during model calibration. If  $a = 1$ , a linear relationship is assumed between rainfall excess and soil moisture. The effect of rainfall duration is also accounted by the soil moisture content, in which more excess produces due to the increased soil moisture content. Figure 2.2 shows the relationship between actual rainfall excess coefficient, relative soil moisture content and potential rainfall excess coefficient with an exponent of 2.0.

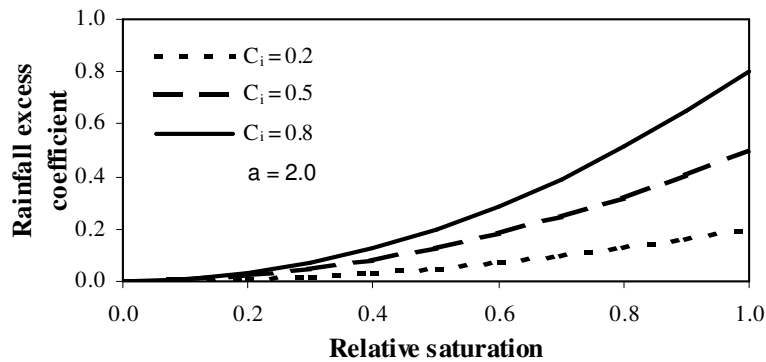


**Fig. 2.2.** Relationship between rainfall excess coefficient and soil moisture content

## 2.5 DEPRESSION AND OVERLAND FLOW

Precipitation that reaches the ground may infiltrate, or get trapped into several small depressions, which is retained in puddles, ditches, and on the ground surface. As soon as rainfall intensity exceeds the local infiltration capacity, the rainfall excess begins to fill depression. Water held in depression at the end of rain either evaporates or contributes to soil moisture and subsurface flow by the following infiltration. Depression storage may be of considerable magnitude and may play an important role in hydrological analysis. Stock ponds, terraces, and contour farming etc. tend to moderate flood by increasing depression storage. Depression losses usually occur during the initial period of the storm and are negligible after a certain time. Factors that affect depression storage include: (1) nature of terrain; (2) slope, the more slope gradient, the less depression losses; (3) type of soil surface, the more sandy soil, the more depression losses; (4) land use, the more woody land

use, the more depression losses; (5) antecedent rainfall, the more soil water content, the less depression storage; and (6) time, for which depression losses decrease with time. Depression is considered included in the potential rainfall excess coefficient in the WetSpa Extension, in order to emphasize its effects on surface runoff production, particularly for the rough surfaces and for small flood events. Therefore, default potential rainfall excess coefficient should be determined cautiously from the literature values, taking the influence of interception and depression into account.

### 2.5.1 Formulation of depression storage

Due to the extreme variability of affecting factors, it is very difficult to specify a general relationship for the depression losses. In WetSpa Extension, a simple empirical equation suggested by Linsley (1982) is used to estimate depression storage:

$$SD_i(t) = SD_{i,0} \left( 1 - \exp\left(-\frac{PC_i}{SD_{i,0}}\right) \right) \quad (2.9)$$

in which  $SD_i(t)$  is the cell depression storage at time  $t$  (mm),  $SD_{i,0}$  is the cell depression storage capacity (mm), and  $PC_i$  is the accumulative excess rainfall on the soil surface (mm). The concept of Eq. (2.9) is that both overland flow and depression storage occurs simultaneously, allowing some of the water delivering as overland flow, even if excess rainfall is less than the depression storage capacity. A sketch of  $SD_i(t)$  as a function of  $PE_i$  is shown in Figure 2.3.

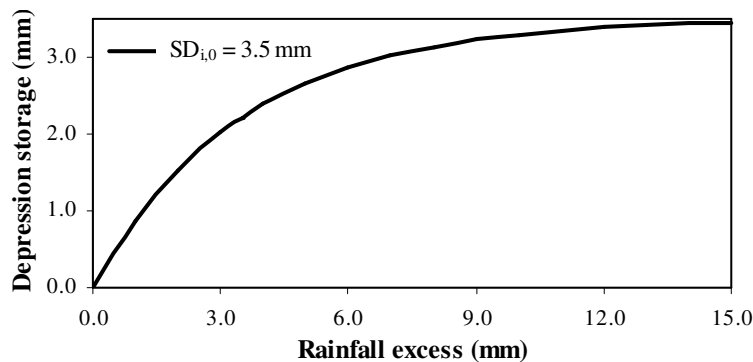


**Fig. 2.3.** Sketch of depression storage as a function of excess rainfall

The increment of depression storage can be obtained by derivation of t both side of Eq. (2.9) as

$$\Delta SD_i(t) = PE_i(t) \exp\left(-\frac{PC_i}{SD_{i,0}}\right) \quad (2.10)$$

where  $\Delta SD_i(t)$  is the increment of depression storage at cell i over the time interval (mm), and  $PE_i(t)$  is the excess rainfall for the time increment (mm). Considering that the rainfall is interrupted between storm events, the accumulative excess rainfall can be estimated based on Eq. (2.9), which is the excess rainfall at present time step plus an excess rainfall corresponding to the depression storage at last time step.

$$PC_i = PE_i(t) + SD_{i,0} \ln\left(-\frac{SD_i(t-1)}{SD_{i,0}}\right) \quad (2.11)$$

Obviously,  $PC_i$  equals  $PE_i(t)$  when depression storage at last time step,  $SD_{t-1}$ , is zero, and becomes a very large value when  $SD_i(t-1)$  approaches to  $SD_{i,0}$ , leading to a very small depression storage increment,  $\Delta SD_{i,t}$ , from Eq. (2.10).

The capacity of depression storage,  $SD_{i,0}$ , is mainly affected by landform, soil type and vegetation. Based upon the analysis and linear interpolation of the typical values collected in the literature (ASCE, 1969; SINCE, 1972; Sheaffer, 1982), and default values in other popular hydrological models, a lookup table for default depression storage capacity is set up, according to the categories and classes of slope, land use and soil type (Table 3.6), which is similar as the lookup table of potential rainfall excess coefficient.

### 2.5.2 Mass balance of depression storage

As discussed above, the depressed water on soil surface will be depleted by evaporation directly or infiltrated into the soil after the rainstorm. The mass balance of depression storage can be expressed as

$$SD_i(t) = SD_i(t-1) + \Delta SD_i(t) - ED_i(t) - F_i(t) \quad (2.12)$$

where  $ED_i(t)$  and  $F_i(t)$  are cell evaporation and infiltration from depression storage for the time increment after the rainstorm (mm).  $ED_i(t) = 0$  when  $P_i(t) > 0$  or  $SD_i(t-1) = 0$ .  $ED_i(t) =$

$EP - EI_i(t)$ , when  $P_i(t) = 0$  and  $SD_i(t-1) \geq EP - EI_i(t)$ , in which  $EP$  and  $EI_i(t)$  are the potential evaporation and the evaporation from the cell interception storage (mm).  $ED_i(t) = SD_i(t)$  when  $P_i(t) = 0$  and  $0 < SD_i(t) < EP - EI_i(t)$ . The infiltration from depression storage after rainstorm can be estimated using Eq. (2.7) and Eq. (2.8) by taking the remaining depression storage as the amount of rainfall on the ground surface.

### 2.5.3 Formulation of overland flow

Recall that the excess rainfall is a sum of overland flow and the change of depression storage, the amount of overland flow over the time interval,  $RS_i(t)$  (mm), can be written as

$$RS_i(t) = PE_i(t) \left[ 1 - \exp\left(-\frac{PC_i}{SD_{i,0}}\right) \right] \quad (2.13)$$

Eq. (2.13) assumes that both overland flow and depression storage occur simultaneously as described in Figure 2.4, for which the overland flow approaches to zero when the accumulative excess rainfall is very small, and approaches to  $PE_i(t)$  when the depression storage closes to its capacity. This is different with the assumption that overland flow begins only after the depression storage capacity is reached as the dashed line shown in the figure.

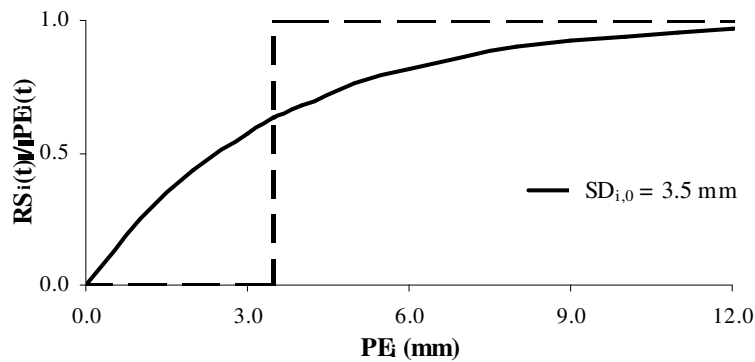


**Fig. 2.4.** Graphical presentation of excess rainfall and overland flow

## 2.6 WATER BALANCE IN THE ROOT ZONE

Soil moisture storage is the actual quantity of water held in the soil at any given instant, usually applied to a soil layer of root depth. Based on the different soil water content, the moisture storage can be divided into saturation capacity, field capacity, plant wilting point, residual soil moisture, etc. WetSpa Extension calculates water balance in the root zone for each grid cell. Soil water is fed by infiltration and removed from the root zone by evapotranspiration, lateral interflow and percolation to the groundwater storage, as described in Figure 2.5.

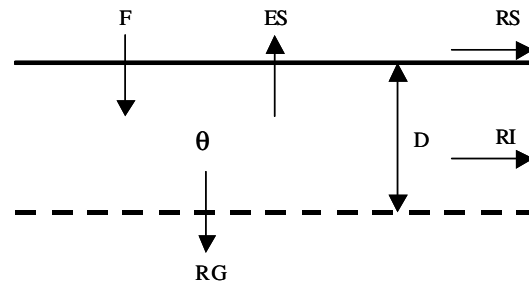


**Fig. 2.5.** Graphical presentation of soil water balance

The moisture storage in the root zone is expressed by a simple balance equation as

$$D_i [\theta_i(t) - \theta_i(t-1)] = F_i(t) - ES_i(t) - RG_i(t) - RI_i(t) \quad (2.14)$$

in which  $\theta_i(t)$  and  $\theta_i(t-1)$  are cell soil moisture content at time step  $t$  and  $t-1$  ( $m^3/m^3$ ),  $D_i$  is the root depth (mm);  $F_i(t)$  is the infiltration through soil surface for the time increment (mm), including the infiltration during the rainstorm and the infiltration from depression storage after the rainstorm (mm),  $ES_i(t)$  is the actual evapotranspiration from the soil for the time increment (mm),  $RG_i(t)$  is the percolation out of root zone or groundwater recharge (mm), and  $RI_i(t)$  is the interflow or lateral shallow subsurface flow out of the cell for the time increment (mm).

## **2.7 EVAPOTRANSPIRATION FROM SOIL**

### **2.7.1 Potential evapotranspiration (PET)**

PET is defined as the quantity of water vapour, which could be emitted by a plant or soil surface per unit area and unit time under the existing conditions without water supply limit.

The WetSpa model requires the measured PET in the basin as an input. Identical to precipitation, PET is usually measured at meteorological stations or estimated using numerical and experimental methods i.e. Penman-Monteith equation. Spatial distribution of the PET is done in the same way as for the precipitation, using the Thiessen polygon approach.

Most advanced measuring stations provide pan evaporation measurements. These measurements combine the effect of temperature, humidity, wind speed and sunshine on the PET. The potential evaporation can be estimated with the pan evaporation multiplied by a pan coefficient.

The main influencing factors to the potential evaporation are: (1) solar radiation, providing energy or heat; (2) wind speed, transporting the moisture away from the surface, and (3) specific humidity gradient in the air above the water surface, being the driving forces for diffusion of water vapour. This means if no PET measurements are available equations incorporating previous mentioned variables can be used to estimate the PET. The FAO-56 Penman-Monteith equation (Allen et al., 2000) is recommended as an appropriate formula for PET estimations. The calculations of the potential evapotranspiration, if no measurements are available, have to be done outside the WetSpa model.

### **2.7.2 Actual evapotranspiration**

Without considering the evaporation from interception storage and depression storage, actual evapotranspiration is defined as the sum of the quantities of water vapour evaporated from the soil and the plants when the ground is at its actual moisture content. Thus, if soil is fully saturated, then it is expected that the actual evapotranspiration rate equals to the PET rate. However, if the soil or vegetation is water stressed, the evapotranspiration will be less than potential evapotranspiration. Influencing factors to the actual evapotranspiration

include weather, vegetation and soil condition, etc. Since the actual evapotranspiration is governed by the availability of water, soil moisture content becomes a crucial factor, which is determined by water recharge and the soil characteristics.

In the WetSpa Extension, evapotranspiration consists of four parts: (1) evaporation from interception storage, (2) evaporation from depression storage, (3) evapotranspiration from soil, and (4) evapotranspiration from groundwater storage. It is assumed that water evaporates to the atmosphere in a cascade way, i.e. from interception storage, depression storage, soil matrixes, and groundwater storage consequently. The evaporation from interception storage and depression storage has been described in section 2.2 and 2.5, and the groundwater contribution to the evapotranspiration will be described in section 2.9. The actual evapotranspiration from soil and plant is calculated for each grid cell using the relationship developed by Thornthwaite and Mather (1955) as a function of PET, vegetation and its growing stage, and moisture content in the cell

$$ES_i(t) = \begin{cases} [c_v EP - EI_i(t) - ED_i(t)] \left[ \frac{\theta_i(t) - \theta_{i,w}}{\theta_{i,f} - \theta_{i,w}} \right] & \text{for } \theta_{i,w} \leq \theta_i(t) < \theta_{i,f} \\ c_v EP - EI_i(t) - ED_i(t) & \text{for } \theta_i(t) \geq \theta_{i,f} \end{cases} \quad (2.18)$$

where  $ES_i(t)$  is the actual soil evapotranspiration for the time increment (mm),  $c_v$  is a vegetation coefficient determined by land use classes varying throughout the year,  $\theta_i(t)$  is the cell average soil moisture content at time  $t$  ( $m^3/m^3$ ),  $\theta_{i,f}$  is the soil moisture content at field capacity ( $m^3/m^3$ ), and  $\theta_{i,w}$  is the soil moisture content at plant permanent wilting point ( $m^3/m^3$ ). It can be concluded from Eq. (2.18) that when the sum of interception and depression storage is greater than the PET, all evaporation comes from the interception and depression storage with a potential rate. When the sum of interception and depression storage is less than the amount of PET, all the remaining storage evaporates at this time step, and there is a part of evapotranspiration from the soil layer depending on the soil moisture content. For the simulation between storm events, actual evapotranspiration is mainly from the soil and plant, which varies linearly between PET when soil moisture content is at or above field capacity, and zero when soil moisture content is below the wilting point. A graphical presentation of soil evapotranspiration is given in Figure 2.8, in

which  $\theta_{i,s}$  is the soil porosity ( $\text{m}^3/\text{m}^3$ ). For the cell in urban areas, soil evapotranspiration is reduced by 70 % to account for impervious surface covers the impervious areas, and is calculated by cell evapotranspiration times the pervious percentage.

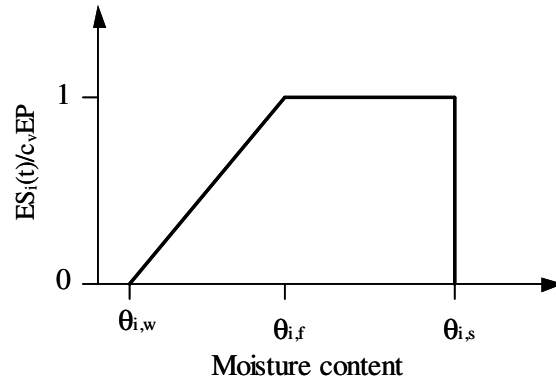


**Fig. 2.8.** Graphical presentation of soil evapotranspiration

## 2.8 PERCOLATION AND INTERFLOW

Percolation or groundwater recharge refers to the natural process by which water is added from soil water zone to the saturation zone of the aquifer. Groundwater recharge is an important component in the root zone water balance, which connects the soil water and the saturated groundwater. The main influencing factors to the groundwater recharge are the hydraulic conductivity, root depth, and water content of the soil. In WetSpa Extension, percolation out of root zone is assumed to pass directly to the groundwater reservoir, and estimated based on the Darcy's law, being the product of hydraulic conductivity and the gradient of hydraulic potential. When an assumption is made that the pressure potential only varies slightly in the soil, its gradient can be approximated to zero, and the percolation is controlled by gravity alone (Famiglietti and Wood, 1994). Based on this assumption, the percolation amount out of root zone is simply specified as the hydraulic conductivity corresponding to the average effective saturation in the respective soil layer. The Brooks and Corey relationship between hydraulic conductivity and effective saturation is used to define percolation, which is simply (Brooks and Corey, 1966)

$$RG_i(t) = K_i[\theta_i(t)]\Delta t = K_{i,s} \left[ \frac{\theta_i(t) - \theta_{i,r}}{\theta_{i,s} - \theta_{i,r}} \right]^A \Delta t \quad (2.19)$$

where  $RG_i(t)$  is the percolation out of root zone over the time interval (mm),  $K_i[\theta_i(t)]$  is the effective hydraulic conductivity corresponding to the average soil moisture content at time  $t$  (mm/h),  $\Delta t$  is the time interval (h),  $K_{i,s}$  is the cell saturation hydraulic conductivity (mm/h),  $\theta_{i,s}$  is the soil porosity ( $m^3/m^3$ ),  $\theta_{i,r}$  is the cell residual moisture content ( $m^3/m^3$ ), and  $A$  is the pore disconnectedness index, calculated by the equation  $A = (2+3B)/B$ , in which  $B$  is the cell pore size distribution index.

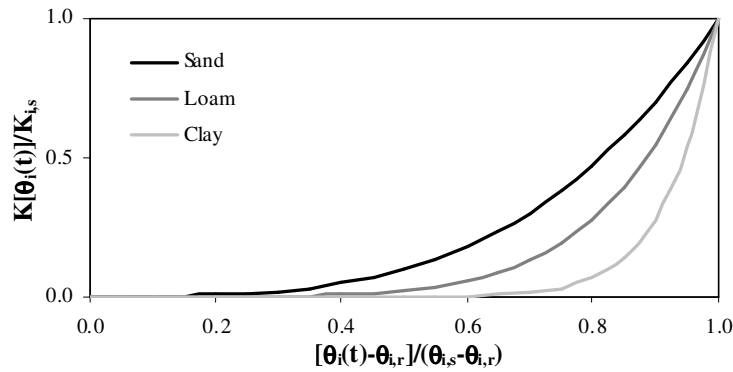


**Fig. 2.9.** Effective hydraulic conductivity as a function of moisture content

Figure 2.9 gives a graphical presentation for the effective hydraulic conductivity as a function of moisture content for three different soil types: sand, loam and clay. It can be seen that the effective hydraulic conductivity varies with moisture content exponentially, reaching a maximum, the saturated conductivity, when soil is completely saturated, and zero when soil becomes dry.

Interflow, or shallow subsurface lateral flow, is also a key component in the soil water balance. It is defined as the water which infiltrates the soil surface and moves laterally through the upper soil layers until it enters a channel, which includes litter flow, return flow, unsaturated through flow, saturated through flow and so on, but excludes the saturated groundwater flow. Due to the delayed flow time, interflow usually contributes to the falling limb of a flood hydrograph, but it may also be a part of peak discharge at the

basin outlet, particularly for the areas with steep slope and forest cover in humid or temperate regions. Factors that influence the amount of interflow include: (1) physical properties and depth of the soil, for which coarse texture leads to more vertical flow, while fine texture or layered soil results in resistance to vertical flow and interflow may some time occur quickly; (2) vegetation cover and land use, which are directly related to the maintenance of infiltration capacity and the conditioning effect of organic material on soil structure, bulk density and porosity; (3) topography, for which the slope gradient is a major factor determining the amount and the velocity of interflow; (4) soil moisture content, for which higher moisture content tends to generate more interflow; and (5) lithology and climate of the study area. In WetSpa Extension, interflow is assumed to occur after percolation and cease when soil moisture is lower than field capacity. The quantity of interflow out of each cell is calculated from Darcy's Law and the kinematic approximation; i.e. the hydraulic gradient is equal to the land slope at each cell

$$RI_i(t) = k_i D_i S_i K[\theta_i(t)] \Delta t / W_i \quad (2.20)$$

in which  $RI_i(t)$  (mm) is the amount of interflow out of the cell over the time interval  $\Delta t$  (h),  $D_i$  is the root depth (m),  $S_i$  is the cell slope (m/m),  $K[\theta_i(t)]$  (mm/h) is the cell effective hydraulic conductivity at moisture content  $\theta_i(t)$  ( $m^3/m^3$ ),  $W_i$  is the cell width (m), and  $k_i$  (-) is a scaling factor depending on land use, used to consider stream density and the effects of organic matter and root system on horizontal hydraulic conductivity in the top soil layer. Apparently, rapid interflow may generate in areas with high moisture, steep slope and well vegetation, while little is produced for other areas with Eq. (2.20). For modelling simplification, interflow is assumed to join the surface runoff at the nearest channels or gullies serving as a supplementary discharge to the stream flow during and after storm event without further divisions among down slope neighbours. Soil hydraulic characteristics, such as porosity, field capacity, residual saturation, hydraulic conductivity, and so on, are collected from the literature, and used as default values in the WetSpa Extension (Table 3.1).

## 2.9 GROUNDWATER STORAGE AND BASEFLOW

Groundwater storage is defined as the quantity of water in the zone of saturation including that part of such stage when water is entering and leaving storage. Groundwater storage capacity refers to the volume of saturated groundwater that can be alternatively extracted and replaced in the deposit under natural conditions. Normally, the groundwater discharge forms a base flow to the hydrograph at basin outlet. Groundwater storage capacity is governed by the thickness and extent of the aquifer and its porosity, while the movement of groundwater is governed by the hydraulic gradient and the hydraulic conductivity of the aquifer.

For the purpose of streamflow prediction, an estimate must be made of flow from the groundwater storage into the stream for each time step. Since little is known about the bedrock, the simple concept of a linear reservoir is used to estimate groundwater discharge on a small subcatchment scale, while a non-linear reservoir method is optional in the model with storage exponent of 2 (Wittenberg and Sivapalan, 1999). The groundwater outflow is added to any runoff generated to produce the total streamflow at the subcatchment outlet. The general groundwater flow equation can be expressed as

$$QG_s(t) = c_g [SG_s(t)/1000]^m \quad (2.21)$$

where  $QG_s(t)$  is the average groundwater flow at the subcatchment outlet ( $m^3/s$ ),  $SG_s(t)$  is the groundwater storage of the subcatchment at time  $t$  (mm),  $m$  (-) is an exponent,  $m = 1$  for linear reservoir, and  $m = 2$  for non-linear reservoir,  $c_g$  is a groundwater recession coefficient taking the subcatchment area into account, has a dimension of ( $m^2/s$ ) for linear reservoir and ( $m^{-1}s^{-1}$ ) for non-linear reservoir, which is dependent upon area, shape, pore volume and transmissivity of the subcatchment, and can be estimated from recession portions of streamflow hydrographs if measurement data at the subcatchment outlet are available. For each subcatchment, the groundwater balance can be expressed as

$$SG_s(t) = SG_s(t-1) + \frac{\sum_{i=1}^{N_s} [RG_i(t)A_i]}{A_s} - EG_s(t) - \frac{QG_s(t)\Delta t}{1000A_s} \quad (2.22)$$

where  $SG_s(t)$  and  $SG_s(t-1)$  are groundwater storage of the subcatchment at time step  $t$  and  $t-1$  (mm),  $N_s$  is the number of cells in the subwatershed,  $A_i$  is the cell area ( $m^2$ ),  $A_s$  is the

subcatchment area ( $m^2$ ),  $EG_s(t)$  is the average evapotranspiration from groundwater storage of the subcatchment (mm), and  $QG_i(t)$  is the groundwater discharge ( $m^3/s$ ).

The component of evapotranspiration from groundwater storage is considered in the WetSpa Extension, which may be produced by deep root system or by capillary drive in the areas with shallow groundwater table. It happens only when soil moisture is less than field capacity from Eq. (2.18) and has a greater impact during the summer than the winter, giving the effect of a steeper recession during dry period. A simple linear equation is used in the model relating deep evapotranspiration with PET and groundwater storage as

$$EG_i(t) = c_d [c_v EP - EI_i(t) - ED_i(t) - ES_i(t)] \quad (2.23)$$

where  $EG_i(t)$  is average evapotranspiration from groundwater storage (mm), EP is PET (mm), and  $c_d$  (-) is a variable, calculated by  $SG_i(t)/SG_{s,0}$ , in which  $SG_i(t)$  is the groundwater storage of the subwatershed at time t (mm), and  $SG_{s,0}$  is the groundwater storage capacity of the subwatershed (mm). Using the method of groundwater reservoir, there are only two groundwater parameters, the groundwater recession coefficient and the storage capacity, which can be determined by calibration against baseflow separated from the observed hydrograph.

## 2.10 OVERLAND FLOW AND CHANNEL FLOW ROUTING

### 2.10.1 Flow response at a cell level

The routing of overland flow and channel flow in WetSpa Extension is implemented by the method of a linear diffusive wave approximation. This method is suitable for simulating sheet flow and channel flow at a certain degree, and one of the important advantages is that it can be solved analytically, avoiding numerical calculation and identification of the exact boundary conditions. Assuming the cell as a reach with 1-D unsteady flow and neglecting the inertial terms in the St. Venant momentum equation, the flow process in the cell can be modelled by the diffusive wave equation as (Miller and Cunge, 1975)

$$\frac{\partial Q}{\partial t} + c_i \frac{\partial Q}{\partial x} - d_i \frac{\partial^2 Q}{\partial x^2} = 0 \quad (2.24)$$

where Q ( $m^3/s$ ) is the flow discharge at time t (s) and location x (m),  $c_i$  is the kinematic wave celerity at cell i (m/s),  $d_i$  is the dispersion coefficient at cell i ( $m^2/s$ ). Considering a

system bounded by a transmitting barrier upstream and an adsorbing barrier downstream, the solution to Eq. (2.24) at the cell outlet, when the flow velocity and diffusion coefficient are constant, can be obtained by the first passage time density distribution of a Brownian motion and expressed as (Eagleson, 1970)

$$u_i(t) = \frac{l_i}{2\sqrt{\pi d_i t^3}} \exp\left[-\frac{(c_i t - l_i)^2}{4d_i t}\right] \quad (2.25)$$

where  $u_i(t)$  is the cell impulse response function (1/s), and  $l_i$  is cell size (m). Two parameters  $c_i$  and  $d_i$  are needed to define the cell response function, which can be estimated using the relation of Manning as (Henderson, 1966)

$$c_i = \frac{5}{3} v_i \quad (2.26)$$

and

$$d_i = \frac{v_i R_i}{2S_i} \quad (2.27)$$

where  $R_i$  is the average hydraulic radius of cell  $i$  (m),  $S_i$  is the cell slope (m/m), and  $v_i$  is the flow velocity of the cell  $i$  (m/s). The hydraulic radius is determined by a power law relationship with an exceeding probability (Molnar and Ramirez, 1998), which relates hydraulic radius to the controlling area and is seen as a representation of the average behaviour of the cell and the channel geometry

$$R_i = a_p (A_i)^{b_p} \quad (2.28)$$

where  $A_i$  is the drained area upstream of the cell (km<sup>2</sup>), which can be easily determined by the flow accumulation routine in ArcView GIS,  $a_p$  (-) is a network constant and  $b_p$  (-) a geometry scaling exponent, both depending on the discharge frequency. The flow velocity is calculated by the Manning's equation as

$$v_i = \frac{1}{n_i} R_i^{\frac{2}{3}} S_i^{\frac{1}{2}} \quad (2.29)$$

where  $n_i$  is the Manning's roughness coefficient (m<sup>-1/3</sup>s), which depends upon land use categories and the channel characteristics. Default Manning's roughness coefficients can be collected from literature (Table 3.2). The velocity calculated by Eq. (2.29) may be very large or even zero due to variations in land surface slope. Therefore it is bounded between

predetermined limits  $v_{\min}$  and  $v_{\max}$  during model calculation. Flow velocity is a time-dependent, discharge-related and location-related hydrological variable. But to be applicable of the diffusive wave approximation method for hydrological analysis, the flow must be only location-related. In reality, water depth usually increases as water goes downstream. As water deepens, the effective resistance of the streambed and banks on the flow diminishes because the hydraulic radius increases. To reflect this property, the channel roughness coefficient is set between predetermined limits  $n_{\max}$  and  $n_{\min}$ , depending upon the GIS derived stream orders in the WetSpa Extension. Thus, with the supporting Equations (2.26) to (2.29), the cell impulse unit response function  $u_i(t)$  can be calculated for each grid cell over the entire watershed, which reflects the redistribution tendency in the flow element serving as a flow redistribution function.

### 2.10.2 Flow response at a flow path level

Under the assumption of linear routing system, the flow response at the end of a flow path, resulting from a unit impulse input to a single cell, can be calculated without the interference of the inputs to the other cells. Determining the flow-path response consists in routing the impulse through the corresponding sequence of cells down to the system outlet. Along the flow-path, the impulse travels through many cells, each of them having a different unit-impulse response function. In this routing process, the output of any cell becomes the input to the receiving cell, and the original input distribution is continuously modified by the flow dynamics in the cells, which are described by their impulse response functions. The flow path response is found by successively applying the convolution integral, giving

$$U_i(t) = \prod_{j=1}^N u_j(t) \quad (2.30)$$

where  $U(t)$  is flow path response function (1/s), the subscript  $i$  refers to the cell in which the input occurs,  $j$  is the cell sequence number, and  $N$  is the total number of cells along the flow path. The diffusion equation model satisfies Eq. (2.30) within the cells, which means that it allows for longitudinal decomposability. Since the cell unit impulse response functions are time-invariant, the result of the convolutions of Eq. (2.30) is also time-invariant, and therefore, there is a linear relation between the flow path response and the impulse input.

Assuming that the flow path response  $U_i(t)$  is also a first passage time distribution, De Smedt F. et al. (2000) proposed an approximate numerical solution to Eq. (2.30), relating the discharge at the end of a flow path to the available runoff at the start of the flow path

$$U_i(t) = \frac{1}{\sqrt{2\pi\sigma_i^2 t^3 / t_i^3}} \exp\left[-\frac{(t-t_i)^2}{2\sigma_i^2 t / t_i}\right] \quad (2.31)$$

where  $t_i$  is the mean flow time from the input cell to the flow path end (s), and  $\sigma_i^2$  is the variation of the flow time (s<sup>2</sup>). The parameters  $t_i$  and  $\sigma_i^2$  are spatially distributed, and can be obtained by convolution integral along the topographic determined flow paths as a function of flow celerity and dispersion coefficient

$$t_i = \sum_{j=1}^N \left( \frac{1}{c_j} \right) l_j \quad (2.32)$$

and

$$\sigma_i^2 = \sum_{j=1}^N \left( \frac{2d_j}{c_j^3} \right) l_j \quad (2.33)$$

The summations presented in Eq. (2.32) and (2.33) can be calculated for each grid cell as a weighted flow length to the water outlet or any downstream converging point with the routine FLOWLENGTH involved in the standard GIS tools. Examples of such flow path impulse response function are presented in Figure 2.10 for different mean flow time and its variation. It is seen that the response function is asymmetric with respect to time caused by the wave attenuation.

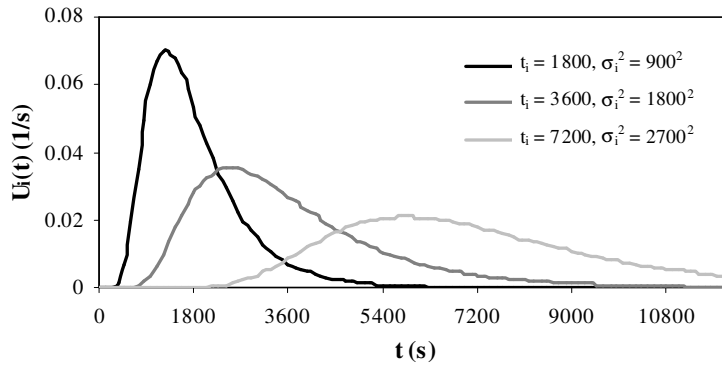


**Fig. 2.10.** Flow path response functions with different  $t_i$  and  $\sigma_i^2$

The flow response at the end of a flow path, to an arbitrary input at the start cell, can be calculated by convolving the input runoff volume by the flow path unit impulse response function. From a physical point of view, this is equivalent to decomposing the input into infinite impulses and adding all the responses into a single response. Thus, the outflow hydrograph to an arbitrary input can be determined as

$$Q_i(t) = \sum_{\tau=0}^{t-\tau} V_i(\tau) U_i(t-\tau) \quad (2.34)$$

where  $Q_i(t)$  is the outflow at the end of a flow path produced by an arbitrary input in cell  $i$  ( $\text{m}^3/\text{s}$ );  $U_i(t-\tau)$  is the flow path response function ( $1/\text{s}$ ), being equivalent to the instantaneous unit hydrograph (IUH) used in the conventional hydrology, and  $\tau$  is the time delay ( $\text{s}$ );  $V_i(\tau)$  is the input runoff volume at cell  $i$  and at time  $\tau$  ( $\text{m}^3$ ), including surface runoff and interflow, as well as groundwater runoff if cell  $i$  is located at the subcatchment outlet.

### 2.10.3 Flow response of the catchment

Considering the areal decomposability in a linear routing system, the catchment flow response can be determined as the sum of its elements responses from all contributing cells. Thus, the catchment flow response can be calculated as

$$Q(t) = \sum_{i=1}^{N_w} Q_i(t) \quad (2.35)$$

where  $Q(t)$  is the total flow at the catchment outlet ( $\text{m}^3/\text{s}$ ),  $N_w$  is the number of cells over the entire catchment. Hence, the flow routing consists of tracking runoff along its topographic determined flow path, and evaluating groundwater flow out of the subcatchment. The total discharge is the sum of the overland flow, interflow and groundwater flow, and is obtained by convolution of the flow response from all grid cells. The advantage of this approach is that it allows the spatially distributed runoff and hydrological parameters of the terrain to be used as inputs to the model, and can route runoff from a certain land use area to the catchment outlet or any downstream converging point.

## 2.11 SUBWATERSHED INTEGRATION

In case of watershed modelling on medium or large scale, model parameterisation and computation on small grid size are tedious, costly and time consuming. On the other hand, working with coarse spatial resolution may introduce errors by aggregation of spatial input data and misrepresentation of the true watershed characteristics. To cope with this problem, WetSpa Extension provides a simplified semi-distributed option working on the scale of a small hydrological unit, so as to allow adequate simulation and mapping of the areal distribution of the hydrological processes. These units correspond to very small subcatchments, built up from high resolution DEM data, rather than to large grid cells with approximately the same area as the subwatersheds. This has the advantage of allowing for the internal drainage structure of the units, which would be impossible by using large grid cells. Model parameters, meteorological data input, and state variables for each simulation unit are obtained by integration of the values from all cells of that subcatchment. Meanwhile, the water and energy balance, as well as the process state variables, are computed on each unit during model simulation at each time step.

The subwatershed parameters calculated by WetSpa Extension include area, slope, potential rainfall excess coefficient, interception capacity, depression capacity, soil physical properties, etc. Flow hydrographs are first calculated at the outlet of each subcatchment using the subcatchment response function, and thereafter, the flow is routed to the catchment outlet along the river channel by means of channel flow response function. Considering the effect of cell characteristics on the subwatershed IUH, the subcatchment response function is computed by integration of the flow path response functions for all cells in the subcatchment weighted by their potential rainfall excess coefficient. The equation can be written as

$$U_s(t) = \frac{\sum_{i=1}^{N_s} [C_i U_i(t)]}{\sum_{i=1}^{N_s} C_i} \quad (2.36)$$

where  $U_s(t)$  is the response function or IUH of the subcatchment (1/s),  $C_i$  is the potential rainfall excess coefficient at cell  $i$  (-),  $U_i(t)$  is the flow path response function at the subcatchment outlet with runoff input at cell  $i$  (1/s), and  $N_s$  is the number of cells in the

subcatchment. The flow hydrograph at subcatchment outlet is obtained by summation of its surface runoff, interflow and groundwater flow, and can be expressed as

$$Q_s(t) = \sum_{\tau=0}^{t-\tau} V_s(\tau) U_s(t-\tau) + QG_s(t) \quad (2.37)$$

where  $Q_s(t)$  is the flow hydrograph at the subcatchment outlet ( $m^3/s$ ),  $V_s(\tau)$  is volume of readily available runoff of the subcatchment including surface runoff and interflow ( $m^3$ ),  $\tau$  is the time delay (s), and  $QG_s(t)$  is the groundwater flow at the subcatchment outlet ( $m^3/s$ ). The total hydrograph at the watershed outlet is obtained by integration of the flow hydrographs produced from each subwatershed, and can be expressed as

$$Q(t) = \sum_{s=1}^{N_r} Q_s(\tau) U_r(t-\tau) \Delta t \quad (2.38)$$

where  $Q(t)$  is the flow hydrograph at the catchment outlet ( $m^3/s$ ),  $U_r(t)$  is the channel response function from the subcatchment outlet to the catchment outlet calculated by Eq. (2.31) ( $1/s$ ),  $\Delta t$  is the time interval (s), and  $N_r$  is the number of subcatchment or the number of stream links in the catchment. With the unit response functions defined for each simulation unit and the corresponding river channel, water can be routed accumulatively downstream up to the catchment outlet. However, the process of flow routing within each subcatchment can be omitted in case of highly intensive watershed discretization, since the water may flow out of the subwatershed within the first time step. In practice, division of the watershed should be performed according to the project purpose and the complexity of the terrain. A few simulations are necessary to decide the watershed discretization to meet various objectives of the project.

## 2.12 CATCHMENT WATER BALANCE

Water balance for the entire catchment is used to keep track of water changes in the hydrological system, and also a measure of model performance by comparing the simulation results with the field observations. Among the constituents in the system, soil

water content is an important state variable that influence fluxes into and out of the root zone (infiltration, evapotranspiration, percolation and interflow) and the energy balance on the land surface. The stores of interception, depression, soil moisture and groundwater are treated as separate control volume, but related subsequently. Precipitation is the input to the system, while direct runoff, interflow, groundwater flow, and evapotranspiration are losses from the hydrological system.

When modelling for a relatively long time period, changes in the storage of interception, depression and channel can be neglected, and the general watershed water balance can be expressed as

$$P = RT + ET + \Delta SS + \Delta SG \quad (2.39)$$

where P is the total precipitation in the watershed over the simulation period (mm), RT and ET are total runoff and total evapotranspiration (mm),  $\Delta SS$  is the change in soil moisture storage for the watershed between the start and the end of the simulation period (mm), and  $\Delta SG$  is the change in groundwater storage of the watershed (mm). For a given simulation period T (s) and initial moisture and groundwater storage condition, these components can be expressed as

$$P = \sum_{t=0}^T \sum_{i=1}^{N_w} P_i(t) \quad (2.40)$$

$$RT = \sum_{t=0}^T \sum_{i=1}^{N_w} [RS_i(t) + RI_i(t)] + \sum_{t=0}^T \sum_{s=1}^{N_r} \left[ \frac{QG_s(t)}{A_s} \Delta t \right] \quad (2.41)$$

$$ET = \sum_{t=0}^T \sum_{i=1}^{N_w} [EI_i(t) + ED_i(t) + ES_i(t)] + \sum_{t=0}^T \sum_{s=1}^{N_r} [EG_i(t)] \quad (2.42)$$

$$\Delta SS = \sum_{i=1}^{N_w} D_i [\theta_i(T) - \theta_i(0)] \quad (2.43)$$

$$\Delta SG = \sum_{s=1}^{N_r} [SG_s(T) - SG_s(0)] \quad (2.44)$$

where  $\theta_i(T)$  and  $\theta_i(0)$  are cell soil moisture content at the end and the start of the simulation period ( $m^3/m^3$ ),  $SG_s(T)$  and  $SG_s(0)$  are subcatchment groundwater storage at the end and the start of the simulation period (mm), and the others have been described in above

sections. All of these components vary over time. A change in any one component of the watershed water balance can result in changes in the other components in the system. This is particularly useful for analysing the impact of land use changes on the watershed hydrological processes. For instance, deforestation results in more surface runoff and less infiltration, thus, decreasing the change in soil moisture storage and groundwater storage for a storm event, and the evapotranspiration is limited by the moisture content as well. When the model performs on a very long time series, the changes in soil moisture and groundwater storage will be less important, and the total precipitation is more or less equal to the sum of the runoff and the evapotranspiration.

### **3. PARAMETER IDENTIFICATION AND MODEL EVALUATION**

#### **3.1 DEFAULT PARAMETERS**

##### **3.1.1 Default parameters characterizing soil texture classes**

Soil textural classes are used to provide information concerning soil physical properties, such as porosity, hydraulic conductivity, pore size distribution index, etc. Although other descriptors such as horizon and structural size certainly influence the hydraulic parameters of soils, Cosby et al. (1984) perform a two-way analysis of variance of nine descriptors to conclude that soil texture alone can account for most of the discernible patterns. Over the last two decades, a great deal of efforts has been made to the estimation of soil hydraulic properties from the information on soil textures in the literature (McCuen et al., 1981; Rawls et al., 1982; Cosby et al., 1984; Rawls & Brakensiek, 1985; Carsel & Parrish, 1988). In WetSpa Extension, soil textures are classified into 12 USDA (U.S. Department of Agriculture) classes ranging from 1 to 12 based on the percentage of sand, silt and clay in the soil sample. Fine textured soils have a high percentage of clay and are very sticky when wet and hard when dry, while coarse textured soils have a high percentage of sand and are loose and friable. A lookup table is then established as presented in Table 3.1 to estimate hydraulic properties as a function of soil texture classes using mean values obtained from the literature.

**Table 3.1.** Default parameters characterizing soil textural classes

Texture classes	Hydraulic conductivity <sup>1</sup> (mm/h)	Porosity <sup>1</sup> (m <sup>3</sup> /m <sup>3</sup> )	Field capacity <sup>1</sup> (m <sup>3</sup> /m <sup>3</sup> )	Wilting point <sup>1</sup> (m <sup>3</sup> /m <sup>3</sup> )	Residual moisture <sup>1</sup> (m <sup>3</sup> /m <sup>3</sup> )	Pore size distribution index <sup>2</sup> (-)
Sand	208.80	0.437	0.062	0.024	0.020	3.39
Loamy sand	61.20	0.437	0.105	0.047	0.035	3.86
Sandy loam	25.92	0.453	0.190	0.085	0.041	4.50
Silt loam	13.32	0.501	0.284	0.135	0.015	4.98
Silt	6.84	0.482	0.258	0.126	0.015	3.71
Loam	5.58	0.463	0.232	0.116	0.027	5.77
Sandy clay loam	4.32	0.398	0.244	0.136	0.068	7.20
Silt clay loam	2.30	0.471	0.342	0.210	0.040	8.32
Clay loam	1.51	0.464	0.310	0.187	0.075	8.32
Sandy clay	1.19	0.430	0.321	0.221	0.109	9.59
Silt clay	0.90	0.479	0.371	0.251	0.056	10.38
Clay	0.60	0.475	0.378	0.251	0.090	12.13

<sup>1</sup>Obtained by analysis of data presented in Rawls et al. (1982) <sup>2</sup>Obtained from Cosby et al. (1984)

Soil texture is a key variable in the coupled relationship between climate, soil, and vegetation. Under given climatic and vegetation conditions the above soil-texture-dependent physical properties, through their influence on soil water movement and the energy state of the water in the soil column, determine the soil wetness values which in turn establish the water condition of the vegetation (Fernandez-Illescas et al., 2001). One advantage in favour of using texture as the only distinguishing factor among components is that this approach significantly simplifies model data management. When only a single distinguishing factor is used, components with a common texture can be lumped together and the spatial soils information passed from the GIS to the hydrology model is set at 12 different specifications. Among the soil properties listed in Table 3.1, hydraulic conductivity has by far the largest coefficient of variation based on the analysis of Carsel & Parrish (1988), and is more sensitive than other soil related parameters. These parameters allow to be revised during model calibration for refining better fit as described in Chapter 4.

### 3.1.2 Default parameters characterizing land use classes

Land use or land cover is an important boundary condition, which directly or indirectly influence many hydrological processes. The most obvious influence of land use on the

water balance of a catchment is on the evapotranspiration process. Different land use types have different evapotranspiration rates, due to their different vegetation cover, leaf area indices, root depths and albedo. During storms, interception and depression rates are different for different land use types. Land use also influences the infiltration and soil water redistribution process, because especially the saturated hydraulic conductivity is influenced by plant roots and pores resulting from soil fauna (Ragab & Cooper, 1993). An extreme example is the influence of build up areas and roads on overland flow. Moreover, land use influences surface roughness, which controls overland flow velocity and floodplain flow rates. Therefore, the effect of land use should be taken into account as much as possible in the simulation calculations.

In WetSpa, the vegetation type definition is based on IGBP (International Geosphere-Biosphere Program) classification system. The following table shows the exact definition:

IGBP vegetation type definition

- ```

=====
Category 1 - Evergreen Needleleaf Forest
Category 2 - Evergreen Broadleaf Forest
Category 3 - Deciduous Needleleaf Forest
Category 4 - Deciduous Broadleaf Forest
Category 5 - Mixed Forest
Category 6 - Closed Shrublands
Category 7 - Open Shrublands
Category 8 - Woody Savannah
Category 9 - Savannahs
Category 10 - Grasslands
Category 11 - Permanent Wetlands
Category 12 - Croplands
Category 13 - Urban and Built-Up
Category 14 - Cropland / Natural Vegetation Mosaic
Category 15 - Snow and Ice
Category 16 - Barren or Sparsely Vegetated
Category 17 - Water Bodies
=====

```

Reference:

Eidenshink, J.C., Faundeen, J.L., 1994, The 1-km AVHRR global land data set: first stages in implementation, international Journal of Remote Sensing, 15:3443:3462

Therefore, 17 basic land use classes are specified in the WetSpa Extension, based on the observed physical and biophysical cover of the land surface, as well as the function and the actual purpose for which the land is currently being used. Such information is obtained

from ground surveys or remote sensing images. For each land use type, several vegetation parameters are defined taking the reference of previous studies as shown in Table 3.2. In order to more correctly simulate the effect of vegetation on interception and evapotranspiration, a range of leaf area index and interception capacity is given in the table corresponding to the minimum and maximum values in a year for each vegetation class. Calculation of the temporal variation is described in Chapter 2. Moreover, some of the parameters, such as root depth, roughness coefficient, etc., should be determined as functions of both soil type and land use. However, for the present implementation, these parameters remain a function of land use type only.

Values of Manning's roughness coefficient shown in Table 3.2 are typical values obtained from experiments reported in the literature. These values are generally representatives of very small areas when correspondence exists between reality and the mathematical model of one-dimensional flow over a plane. Therefore, if a larger grid size, e.g. larger than 100 m, is used in the model, these values should be adjusted downward to reflect the greater number of rills on long slopes (Wu et al., 1982; Hairsine & Parlange, 1986; Vieux & Farajalla, 1994).

**Table 3.2.** Default parameters characterizing land use classes

| Category | Cover                         | Interception capacity(mm) |         | Root depth(m) | Manning's Coefficient | Vegetated fraction(%) | Leaf area index(-) |         |
|----------|-------------------------------|---------------------------|---------|---------------|-----------------------|-----------------------|--------------------|---------|
|          |                               | Maximum                   | Minimum |               |                       |                       | Maximum            | Minimum |
| 1        | Evergreen Needleleaf Forest   | 2                         | 0.5     | 1.0           | 0.40                  | 80                    | 60                 | 50      |
| 2        | Evergreen Broadleaf Forest    | 3                         | 0.5     | 1.0           | 0.60                  | 90                    | 60                 | 50      |
| 3        | Deciduous Needleleaf Forest   | 2                         | 0.5     | 1.0           | 0.40                  | 80                    | 60                 | 10      |
| 4        | Deciduous Broadleaf Forest    | 3                         | 0.5     | 1.0           | 0.80                  | 80                    | 60                 | 10      |
| 5        | Mixed Forest                  | 3                         | 0.5     | 1.0           | 0.55                  | 83                    | 60                 | 30      |
| 6        | Closed Shrublands             | 3                         | 0.5     | 0.8           | 0.40                  | 80                    | 60                 | 10      |
| 7        | Open Shrublands               | 2                         | 0.5     | 0.8           | 0.40                  | 80                    | 60                 | 10      |
| 8        | Woody Savannah                | 3                         | 0.5     | 1.0           | 0.50                  | 80                    | 60                 | 8       |
| 9        | Savannahs                     | 2                         | 0.5     | 0.8           | 0.40                  | 80                    | 60                 | 5       |
| 10       | Grasslands                    | 2                         | 0.5     | 0.8           | 0.30                  | 80                    | 20                 | 5       |
| 11       | Permanent Wetlands            | 1                         | 0.2     | 0.5           | 0.50                  | 80                    | 60                 | 5       |
| 12       | Croplands                     | 2                         | 0.5     | 0.8           | 0.35                  | 85                    | 60                 | 5       |
| 13       | Urban and Built-Up            | 0                         | 0.0     | 0.5           | 0.05                  | 0                     | 0                  | 0       |
| 14       | Cropland / Natural Vegetation | 2                         | 0.5     | 0.8           | 0.35                  | 83                    | 40                 | 5       |
| 15       | Snow and Ice                  | 0                         | 0.0     | 0.1           | 0.05                  | 0                     | 0                  | 0       |
| 16       | Barren or Sparsely Vegetation | 1                         | 0.2     | 0.5           | 0.10                  | 5                     | 20                 | 5       |
| 17       | Water Bodies                  | 0                         | 0.0     | 0.1           | 0.05                  | 0                     | 0                  | 0       |

Obtained and Adapted from Dickinson et al. (1993), Lull (1964), Zinke (1967), Rowe (1983), Chow (1964), Haan (1982), Yen (1992) and Ferguson (1998).

In case the model is applied to a medium or large watershed, the parameter of channel roughness coefficient, which is governed mainly by bed material and channel cross section, will have a great influence to the predicted hydrograph. In natural rivers without overbank flow, the roughness coefficient is generally small for downstream channels due to their fine bed materials, and is large for upstream channels in contrast. To account for these effects, a linear relationship is assumed in the model relating Manning's roughness coefficient to the stream order described as

$$n_r = n_{r,\max} - \left( \frac{O - O_{\min}}{O_{\max} - O_{\min}} \right) (n_{r,\max} - n_{r,\min}) \quad (3.1)$$

where  $n_r$  is the Manning's coefficient ( $m^{-1/3}s$ ) for stream order  $O$ ,  $O_{\max}$  and  $O_{\min}$  are maximum and minimum stream order derived from ArcView GIS, and  $n_{r,\max}$  and  $n_{r,\min}$  are maximum and minimum Manning's coefficients corresponding to  $O_{\max}$  and  $O_{\min}$  ( $m^{-1/3}s$ ). Clearly, the Manning's coefficient has largest value for the channel with minimum order and smallest value for the channel with maximum order with Equation 3.1. The value of  $n_{r,\max}$  and  $n_{r,\min}$  can be defined in the script according to the channel characteristics.

### 3.1.3 Potential runoff coefficient

The runoff coefficient of a grid or catchment is the ratio of runoff volume to rainfall volume. A simple and practical technique is developed in WetSpa Extension to estimate the runoff coefficient under varying land use, soil type, slope, rainfall intensity and antecedent soil moisture condition as described in Chapter 2. Undoubtedly, these variables act independently but also interact in their effect on the runoff coefficient. A table of potential runoff coefficient is built for deferent land use, slope and soil type combinations and under the condition of near saturated soil moisture. Water lost from the soil surface is considered to infiltrate into the soil used for further vertical percolation, evapotranspiration and lateral interflow. To simply the table, the original land use classes are reclassified into 5 classes as forest, grass, crop, bare soil and impervious area.

**Table 3.3.** Potential runoff coefficient for different land use, soil type and slope

| Land use  | Slope (%) | Sand | Loamy sand | Sandy loam | Loam | Silt loam | Silt | Sandy clay loam | Clay loam | Silty clay loam | Sandy clay | Silty clay | Clay |
|-----------|-----------|------|------------|------------|------|-----------|------|-----------------|-----------|-----------------|------------|------------|------|
| Forest    | <0,5      | 0.03 | 0.07       | 0.10       | 0.13 | 0.17      | 0.20 | 0.23            | 0.27      | 0.30            | 0.33       | 0.37       | 0.40 |
|           | 0,5-5     | 0.07 | 0.11       | 0.14       | 0.17 | 0.21      | 0.24 | 0.27            | 0.31      | 0.34            | 0.37       | 0.41       | 0.44 |
|           | 5-10      | 0.13 | 0.17       | 0.20       | 0.23 | 0.27      | 0.30 | 0.33            | 0.37      | 0.40            | 0.43       | 0.47       | 0.50 |
|           | >10       | 0.25 | 0.29       | 0.32       | 0.35 | 0.39      | 0.42 | 0.45            | 0.49      | 0.52            | 0.55       | 0.59       | 0.62 |
| Grass     | <0,5      | 0.13 | 0.17       | 0.20       | 0.23 | 0.27      | 0.30 | 0.33            | 0.37      | 0.40            | 0.43       | 0.47       | 0.50 |
|           | 0,5-5     | 0.17 | 0.21       | 0.24       | 0.27 | 0.31      | 0.34 | 0.37            | 0.41      | 0.44            | 0.47       | 0.51       | 0.54 |
|           | 5-10      | 0.23 | 0.27       | 0.30       | 0.33 | 0.37      | 0.40 | 0.43            | 0.47      | 0.50            | 0.53       | 0.57       | 0.60 |
|           | >10       | 0.35 | 0.39       | 0.42       | 0.45 | 0.49      | 0.52 | 0.55            | 0.59      | 0.62            | 0.65       | 0.69       | 0.72 |
| Crop      | <0,5      | 0.23 | 0.27       | 0.30       | 0.33 | 0.37      | 0.40 | 0.43            | 0.47      | 0.50            | 0.53       | 0.57       | 0.60 |
|           | 0,5-5     | 0.27 | 0.31       | 0.34       | 0.37 | 0.41      | 0.44 | 0.47            | 0.51      | 0.54            | 0.57       | 0.61       | 0.64 |
|           | 5-10      | 0.33 | 0.37       | 0.40       | 0.43 | 0.47      | 0.50 | 0.53            | 0.57      | 0.60            | 0.63       | 0.67       | 0.70 |
|           | >10       | 0.45 | 0.49       | 0.52       | 0.55 | 0.59      | 0.62 | 0.65            | 0.69      | 0.72            | 0.75       | 0.79       | 0.82 |
| Bare soil | <0,5      | 0.33 | 0.37       | 0.40       | 0.43 | 0.47      | 0.50 | 0.53            | 0.57      | 0.60            | 0.63       | 0.67       | 0.70 |
|           | 0,5-5     | 0.37 | 0.41       | 0.44       | 0.47 | 0.51      | 0.54 | 0.57            | 0.61      | 0.64            | 0.67       | 0.71       | 0.74 |
|           | 5-10      | 0.43 | 0.47       | 0.50       | 0.53 | 0.57      | 0.60 | 0.63            | 0.67      | 0.70            | 0.73       | 0.77       | 0.80 |
|           | >10       | 0.55 | 0.59       | 0.62       | 0.65 | 0.69      | 0.72 | 0.75            | 0.79      | 0.82            | 0.85       | 0.89       | 0.92 |
| IMP       |           | 1.00 | 1.00       | 1.00       | 1.00 | 1.00      | 1.00 | 1.00            | 1.00      | 1.00            | 1.00       | 1.00       | 1.00 |

The potential runoff coefficients for impervious (including open water surface) are set to 1. In addition, surface slope is discretized into 4 classes as shown in Table 3.3. Values in the table are taking the reference from literature (Kirkby 1978, Chow et al. 1988, Browne 1990, & Fetter 1980) and adjusted after Mallants and Feyen (1990).

In order to estimate the potential runoff coefficient on the basis of a continuous slope, a simple linear relationship between potential runoff coefficient and surface slope is used, which can be described as

$$C = C_0 + (1 - C_0) \frac{S}{S + S_0} \quad (3.2)$$

where C is the potential runoff coefficient for a surface slope S (%), C<sub>0</sub> is the potential runoff coefficient for a near zero slope corresponding to the values listed on the first row of each land use class in Table 3.4, and S<sub>0</sub> (%) is a slope constant for different land use and soil type combinations, as listed in Table 3.4, which is calibrated using the data in Table 3.4. Figure 3.1 gives a graphical presentation of the grid potential runoff coefficient for a forest cover as a function of slope and different soil types.

**Table 3.4.** Slope constant  $S_0$  for determining potential runoff coefficient

| Land use  | Sand  | Loamy sand | Sandy loam | Loam  | Silt loam | Silt  | Sandy clay loam | Clay loam | Silty clay loam | Sandy clay | Silty clay | Clay  |
|-----------|-------|------------|------------|-------|-----------|-------|-----------------|-----------|-----------------|------------|------------|-------|
| Forest    | 0.680 | 0.650      | 0.620      | 0.590 | 0.560     | 0.530 | 0.500           | 0.470     | 0.440           | 0.410      | 0.380      | 0.350 |
| Grass     | 0.580 | 0.551      | 0.522      | 0.493 | 0.464     | 0.435 | 0.405           | 0.376     | 0.347           | 0.318      | 0.289      | 0.260 |
| Crop      | 0.500 | 0.471      | 0.442      | 0.413 | 0.384     | 0.355 | 0.325           | 0.296     | 0.267           | 0.238      | 0.209      | 0.180 |
| Bare soil | 0.420 | 0.393      | 0.365      | 0.338 | 0.311     | 0.284 | 0.256           | 0.229     | 0.202           | 0.175      | 0.147      | 0.120 |

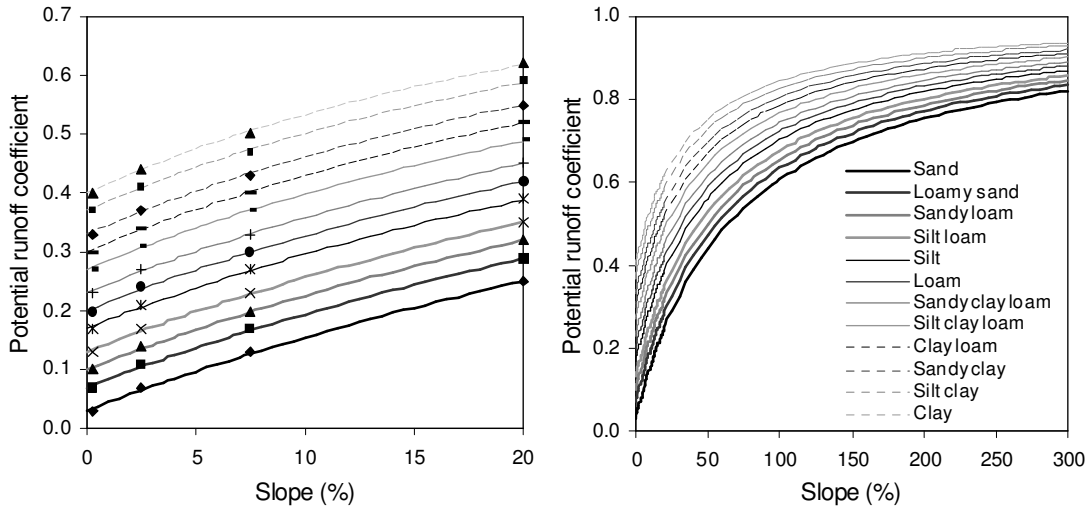


**Fig. 3.1.** Potential runoff coefficient vs. slope for forest and different soil types

The left figure of Figure 3.1 shows the potential runoff coefficient for a slope ranging from 0 to 20% and the supporting points, and the right one shows the potential runoff coefficient for a slope ranging from 0 to 300%. Clearly, the potential runoff coefficient approaches to  $C_0$  when slope is very small, and 1 when slope is infinite. The figure also shows that the changing magnitude of potential runoff coefficient is decreasing along with the increasing of surface slope. This conforms that the runoff volume for a certain amount of rainfall is less or even not affected by slope beyond a critical slope (Sharma, 1986).

The influence of urban areas to the storm runoff is self-evident. Due to the grid size, cells may not be 100% impervious in reality. In WetSpa Extension, the remaining area is assumed to be pervious and covered by grass, and therefore, the potential runoff coefficient for urban areas is calculated as

$$C_u = IMP + (1 - IMP)C_{grass} \quad (3.3)$$

where  $C_u$  and  $C_{grass}$  are potential runoff coefficient for urban and grass grid, and IMP is the proportion of impervious area. Table 3.5 is developed to associate an impervious cover percent with several of the specified land use categories. Impervious percent for residential area, commercial and industrial is estimated based on the information in Chow et al. (1988). Other estimates are considered reasonable guesses. Zero impervious percent is assumed for land use categories not listed (i.e. agriculture, grass land, and forest land).

**Table 3.5.** Impervious percentages associated with selected land use classes

| No. | Land use description                       | Impervious percent (%) |
|-----|--------------------------------------------|------------------------|
| 1   | Residential area                           | 30                     |
| 2   | Commercial and industrial area             | 70                     |
| 3   | Mixed urban or built-up land               | 50                     |
| 4   | Transportation and communication utilities | 100                    |
| 5   | Streams, Canals, lakes and reservoirs      | 100                    |
| 6   | Forest wetland                             | 100                    |
| 7   | Bare exposed rock                          | 100                    |

In case the model is applied to a medium or large watershed, direct flow generated from the flow surface becomes an essential part of the storm runoff. Due to the effect of grid size, upstream channel cells may not be fully occupied by flow. Equation 3.4 is then used to calculate the potential runoff coefficient for these channel cells.

$$C_r = RP + (1 - RP)C \quad (3.4)$$

where  $C_r$  is the potential runoff coefficient for a channel grid,  $C$  is the potential runoff coefficient without considering the channel effect, and  $RP$  is the percentage of channel area of the grid calculated by the estimated flow width divided by the grid size. The flow width is determined by a power law relationship with an exceeding probability (Molnar & Ramirez, 1998), which relates flow width to the controlling area and is seen as a representation of the average behaviour of the cell and the channel geometry.

$$W_i = a_w (A_i)^{b_w} \quad (3.5)$$

where  $A_i$  is the drained area upstream of the cell ( $\text{km}^2$ ),  $a_w$  (-) is a network constant and  $b_w$  (-) a geometry scaling exponent both depending on the flood frequency.

Researches have shown that the runoff efficiency (volume of runoff per unit of area) increases with the decreasing catchment area, i.e. the larger the catchment area the smaller the runoff efficiency (Boers & Ben-Asher, 1982; Brown et al., 1999). Analogously, The potential runoff coefficient is affected by the grid size, in which more surface runoff is produced when modelling with a small grid size, and vice versa. This can be explained by that spatial variability in climatic inputs such as rainfall and hydrometeorological variables, in soil characteristics such as hydraulic conductivity and porosity, in topography, and land use, increase with spatial scale (Vijay & Woolhiser, 2002). For instance, the average saturated hydraulic conductivity and the surface retention capacity are higher when modelling in a coarser resolution, causing more infiltration and less surface runoff. These have been addressed in many of the literatures (Loague, 1988; Mazon & Yen, 1994; Saghafian et al., 1995). Therefore, the grid size should be chosen properly in order to adequately represent the spatial heterogeneity of a watershed, and the values of potential runoff coefficient are allowed to readjust during calibration.

#### **3.1.4 Depression storage capacity**

Depression storage capacity is a value that is land use dependent and represents the total amount of water that can be stored in small surface depressions. Moreover, the soil type and the slope steepness also affect the depression storage capacity for ponding water and thereby the conditions for surface runoff. Generally rougher surfaces store more surface water than smoother surfaces and steeper slopes store less surface water than gentle slopes (Moore and Larson, 1979; Ullah and Dickinson, 1979a, b; Onstad, 1984). After the depression storage amount is met, runoff within a cell begins. A table of depression storage capacity, as shown in Table 3.6, is built in WetSpa Extension for different land use, soil type and slope combinations, based on the analysis of data in ASCE (1969), SINCE (1972), Sheaffer et al., (1982), and Geiger et al. (1987). The depression storage capacity for impervious areas is considered as wetting loss, and set to 0.5 mm (Fronteau & Bauwens, 1995).

In order to obtain a depression storage capacity as a function of a continuous slope used in the WetSpa Extension, a simple regression equation as in Hansen et al. (1999) is applied, in which the depression storage capacity is controlled by land use and soil type, and

decreases with slope exponentially.

$$Sd = Sd_0 \exp(-bS) \quad (3.5)$$

where  $Sd$  is the depression storage capacity (mm),  $S$  is the slope (%),  $Sd_0$  is the depression storage capacity for a near zero slope and different soil types (mm), corresponding to the values listed on the first row of each land use class in Table 3.6, and  $b = -9.5$ , calibrated using the data in Table 3.6. Figure 3.2 shows the depression storage capacity for a grass cover as a function of slope and different soil types.

**Table 3.6.** Depression storage capacity for different land use, soil type and slope

| Land use  | Slope (%) | Sand | Loamy sand | Sandy loam | Loam | Silt loam | Silt | Sandy clay loam | Clay loam | Silty clay loam | Sandy clay | Silty clay | Clay |
|-----------|-----------|------|------------|------------|------|-----------|------|-----------------|-----------|-----------------|------------|------------|------|
| Forest    | <0,5      | 8.00 | 7.50       | 7.00       | 6.50 | 6.00      | 5.50 | 5.00            | 4.50      | 4.00            | 3.50       | 3.00       | 2.50 |
|           | 0,5-5     | 6.31 | 5.91       | 5.52       | 5.13 | 4.73      | 4.34 | 3.94            | 3.55      | 3.15            | 2.76       | 2.37       | 1.97 |
|           | 5-10      | 3.92 | 3.68       | 3.43       | 3.19 | 2.94      | 2.70 | 2.45            | 2.21      | 1.96            | 1.72       | 1.47       | 1.23 |
|           | >10       | 1.92 | 1.80       | 1.68       | 1.56 | 1.44      | 1.32 | 1.20            | 1.08      | 0.96            | 0.84       | 0.72       | 0.60 |
| Grass     | <0,5      | 5.00 | 4.73       | 4.45       | 4.18 | 3.91      | 3.64 | 3.36            | 3.09      | 2.82            | 2.55       | 2.27       | 2.00 |
|           | 0,5-5     | 3.94 | 3.73       | 3.51       | 3.30 | 3.08      | 2.87 | 2.65            | 2.44      | 2.22            | 2.01       | 1.79       | 1.58 |
|           | 5-10      | 2.45 | 2.32       | 2.18       | 2.05 | 1.92      | 1.78 | 1.65            | 1.52      | 1.38            | 1.25       | 1.11       | 0.98 |
|           | >10       | 1.20 | 1.14       | 1.07       | 1.01 | 0.94      | 0.87 | 0.81            | 0.74      | 0.68            | 0.61       | 0.55       | 0.48 |
| Crop      | <0,5      | 3.00 | 2.86       | 2.73       | 2.59 | 2.45      | 2.32 | 2.18            | 2.05      | 1.91            | 1.77       | 1.64       | 1.50 |
|           | 0,5-5     | 2.37 | 2.26       | 2.15       | 2.04 | 1.94      | 1.83 | 1.72            | 1.61      | 1.51            | 1.40       | 1.29       | 1.18 |
|           | 5-10      | 1.47 | 1.40       | 1.34       | 1.27 | 1.20      | 1.14 | 1.07            | 1.00      | 0.94            | 0.87       | 0.80       | 0.74 |
|           | >10       | 0.72 | 0.69       | 0.66       | 0.62 | 0.59      | 0.56 | 0.52            | 0.49      | 0.46            | 0.43       | 0.39       | 0.36 |
| Bare soil | <0,5      | 1.50 | 1.45       | 1.41       | 1.36 | 1.32      | 1.27 | 1.23            | 1.18      | 1.14            | 1.09       | 1.05       | 1.00 |
|           | 0,5-5     | 1.12 | 1.09       | 1.05       | 1.02 | 0.99      | 0.95 | 0.92            | 0.88      | 0.85            | 0.81       | 0.78       | 0.75 |
|           | 5-10      | 0.74 | 0.72       | 0.70       | 0.67 | 0.65      | 0.63 | 0.61            | 0.58      | 0.56            | 0.54       | 0.52       | 0.49 |
|           | >10       | 0.36 | 0.35       | 0.34       | 0.33 | 0.32      | 0.31 | 0.30            | 0.28      | 0.27            | 0.26       | 0.25       | 0.24 |
| IMP       |           | 0.50 | 0.50       | 0.50       | 0.50 | 0.50      | 0.50 | 0.50            | 0.50      | 0.50            | 0.50       | 0.50       | 0.50 |

The left figure of Figure 3.2 shows the depression storage capacity for a slope ranging from 0 to 20% and the supporting points, and the right one shows the depression storage capacity for a slope ranging from 0 to 100%. Clearly, the depression storage capacity approaches to  $Sd_0$  for a very small slope, and 0 for a steep slope. This conforms that the effect of depression storage is not important for a steep slope in controlling overland flow generation (Hansen et al., 1999).

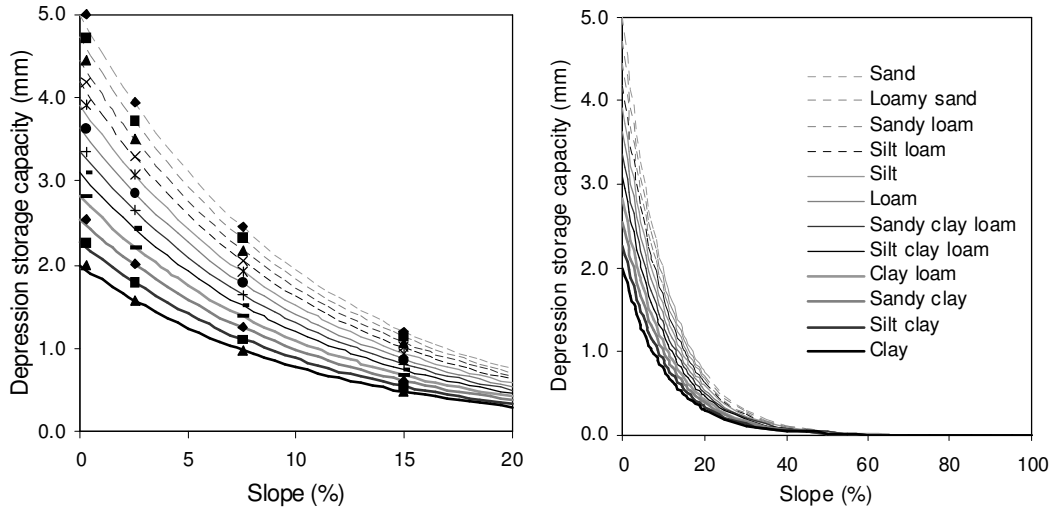


**Fig. 3.2.** Depression storage capacities vs. slope for grass and different soil types

The computation of depression storage capacity for urban areas is the same like the process in calculating potential runoff coefficient, which is the weighted mean of the depression storage capacity for impervious area and grassland. The equation can be expressed as

$$Sd_u = 0.5IMP + (1 - IMP)Sd_{grass} \quad (3.6)$$

where  $Sd_u$  and  $Sd_{grass}$  are the depression storage capacity for an urban and grass grid respectively (mm). As there is no depression loss on water surface, the depression storage capacity for a channel cell can be calculated as

$$Sd_r = (1 - RP)Sd \quad (3.7)$$

where  $Sd_r$  (mm) is the depression storage capacity for a channel grid, and  $Sd$  (mm) is the depression storage capacity without considering the channel effect.

The values of depression storage capacity are also affected by the grid size as discussed in section 3.1.3. Therefore, cautions should be made with regards to use these values for a large grid. These parameters are allowed to modify during the GIS preprocessing in order to get a better fit.

## 3.2 GLOBAL PARAMETERS

For simplifying the process of parameter calibration, 12 global parameters are used in the WetSpa Extension, i.e. the correction factor of PET, interflow scaling factor, groundwater recession coefficient, initial soil moisture, initial groundwater storage, base temperature for snowmelt, temperature degree-day coefficient, rainfall degree-day coefficient, surface runoff exponent, and the rainfall intensity corresponding surface runoff exponent of 1. These parameters have physical interpretations and are important in controlling runoff production and hydrographs at basin outlet, but difficult to assign properly on a grid scale. Therefore, calibration of these global parameters against observed runoff data is preferable in addition to the adjustment of distributed model parameters.

### 1) Correction factor for potential evapotranspiration

The PET data used in the model are obtained from pan measurement or calculated by Penman-Monteith or other equations using available weather data. These reference evapotranspiration rates refer to water surface or a grass cover in large fields. Actual reference or PET rates, however, may depend on local factors that are not addressed by these methods. For instance, the land use, elevation, as well as the micro-meteorological conditions for the grid to be simulated may be different from those prevailing at the site of the meteorological station whose data are being used. To account for these effects, a correction factor is required in the computed PET. The correction factor is normally close to 1, and can be calibrated by the model through a long-term water balance simulation. Specifically, when modelling in a mountainous catchment, the evapotranspiration stations are usually very sparse and are located in the river valley. To account for the effect of elevation, the correction factor for PET may be much lower in this case.

### 2) Scaling factor for interflow computation

Interflow or subsurface runoff is an essential runoff component for the humid temperate region especially for the areas with sloping landscapes and well-vegetated cover. In WetSpa Extension, interflow is assumed to occur when soil moisture exceeds the field capacity and there is sufficient hydraulic gradient to move the water. Darcy's law is then used for the simulation of interflow. Dingman (1994) pointed out that due to

the anisotropy of water content dependent hydraulic conductivity, soil water preferentially flows laterally given greater lateral hydraulic conductivity than vertical. Even though a uniform soil matrix is considered in the model, but in fact, the porosity and permeability of soil tend to decrease with depth given the weight of overlying soil and the translocation of material in percolating water to lateral subsurface flow. Moreover, soil water passing quickly to a stream through root canals, animal tunnels, or pipes produced by subsurface erosion may become a critical component of peak flow. To account for these effects, a scaling factor for lateral hydraulic conductivity in computing interflow is used in the model. This scaling factor is generally greater than 1, and can be calibrated by comparing the recession part of computed flood hydrographs with the observed hydrographs.

### 3) Groundwater recession coefficient

Groundwater flows are estimated on subcatchment scale in WetSpa Extension as described in Chapter 2. The groundwater recession coefficient reflects the storage characteristics of the subwatershed and, therefore, is the same for all hydrographs at a given location. In accordance with Equation (2.21), the groundwater recession coefficient will remain constant if storage and discharge volumes are divided by area and expressed as depth in mm (Wittenberg, 1999). This is under the condition that groundwater flow for each subcatchment has the same recession constant, and total groundwater at the outlet of the river is only a time-shifted superposition of partial groundwater flow from each subcatchment.

In real river basins, baseflow recession coefficient for each subcatchment may not be the same, and may have a considerable deviation from the theoretical constant. A great portion of the deviation is associated with variability of subcatchment characteristics. Others may be attributed to aquifer heterogeneity and divergence from the Dupuit-Forchheimer assumption of essentially horizontal groundwater flow. For model simplification, a general value of groundwater flow recession coefficient is determined at the basin outlet in the input file. A linear correction is then performed for each subcatchment based on its drainage area and the average slope, for which higher values are assigned for the subcatchments with large drainage area and steep slope, and lower values for the subcatchments with small area and gentle slope. The shape and

stream density of the subcatchment is not accounted for in the current version. The equation can be expressed as

$$c_{g,s} = c_g \frac{S_s}{S} W_s \quad (3.8)$$

where  $c_{g,s}$  and  $c_g$  ( $m^2/s$ ) are groundwater recession coefficient of the subcatchment and the entire basin,  $S_s$  and  $S$  are average slope of the subcatchment and the entire basin, and  $W_s$  is the areal weight of the subcatchment.  $c_g$  can be derived by the analysis of flow records as described in Martin (1973) and Wittenberg (1999). Calibration of this parameter is necessary by comparing the computed and observed low flow hydrographs.

#### 4) Initial soil moisture

Soil moisture content is a key element in the model controlling the hydrological processes of surface runoff production, evapotranspiration, percolation and interflow. A proper initial soil moisture condition may provide a much more realistic starting point for predictions. However, for a long-term flow simulation in a watershed, the initial soil moisture condition is less important, as it affects the hydrological processes only in the initial part of the simulation. An assumption of uniform initial moisture distribution can be made in this case with modelling purpose of flood prediction under present condition. A ratio against field capacity is then defined in the input parameter file for setting up the initial soil moisture conditions. This value can be adjusted during calibration by analysis of water balance output and comparison between the computed and observed hydrographs for the initial phase.

If the model is used for short-term flow simulation or event-based flood prediction, the antecedent moisture condition becomes one of the most important factors in runoff production as well as its distribution. The concept of topographic wetness index (TWI) adapted from Moore et al. (1993) can be introduced in the model to evaluate antecedent moisture condition of a watershed with  $TWI = \ln(A/S)$ , where  $\ln(.)$  is the natural logarithm,  $A$  is the upslope drainage area ( $m^2$ ), and  $S$  is the local slope (-). The TWI distribution can be easily obtained from a high resolution DEM. Those cells with high TWI values have larger upslope contributing areas or smaller cell slopes or a combination of the two properties that lead to accumulation of soil moisture. While an

assumption is made for maximum and minimum moisture content within the watershed, the antecedent moisture distribution can be obtained by simply relating moisture content to the TWI values. Cells with very high TWI values may consider to be saturated with runoff coefficient of one. These cells are normally distributed along the main river or in the depression areas in a watershed.

5) Initial groundwater storage

In WetSpa Extension, groundwater balance is maintained on subcatchment scale and for the active groundwater storage, which is that part of storage in perched or shallow aquifers that contribute to the surface stream flow. Water percolating from the root zone storage may flow to active groundwater storage or may be lost by deep percolation. Active groundwater eventually reappears as baseflow, but deep percolation is considered lost from the simulated system. A value of initial groundwater storage in depth (mm) is set up in the input parameter file for all subcatchment. This value can be adjusted during calibration by comparing the computed and observed low flows for the initial phase.

6) Base temperature for snowmelt

The precipitation is assumed to fall as snow if the temperature is below the base temperature. Snowmelt starts when the temperature is above the base temperature. The base temperature is typically a value near 0°C, particularly for short computation period using average temperature as input. The user may specify this value during model calibration.

7) Temperature degree-day coefficient

The range of the temperature degree-day coefficient is typically 1.8 – 3.7 mm/°C/day for rain-free conditions (Anderson, 1973; Male and Gray, 1981). This value can be determined by comparison between computed and observed spring flood hydrographs during calibration. In general, the temperature degree-day coefficient is varied both in time and space. For instance, the albedo is very high for new, cold snow falling in the beginning of the accumulation season and decreases with the age of the snow, which results in an increase of the degree-day coefficient. Moreover, the temperature degree-day coefficient is also land use dependent, for which forest cover leads to a higher value, while bare soil leads to a smaller value. For simplicity purpose, these

influencing factors are not accounted for in the current model, and recommended to be coupled in the future version.

8) Rainfall degree-day coefficient

The rainfall degree-day coefficient determines the rate of snow melting caused by condensation of humid air on the snow surface and the advective heat transferred to the snow pack by precipitation, and is used for calculation of an additional snowmelt due to rainfall. The value of rainfall degree-day coefficient is generally very small, typically around 0.01 (mm/mm/°C/day), and can be determined during model calibration. If zero value is given, the effect of rainfall on snowmelt will not be considered.

9) Surface runoff exponent for a near zero rainfall intensity

Rainfall intensity has a big influence in controlling the proportion of surface runoff and infiltration. As pointed by Dunne (1991), infiltration rate increases with rainfall intensity for two reasons: (1) Higher rainfall intensity tends to exceed the saturated hydraulic conductivity of larger proportions of the soil surface, and thereby to raise the spatially averaged hydraulic conductivity, and (2) Higher rainfall intensity gives more surface runoff rate and the inundated flow depth. To account for this effect on the production of surface runoff, an empirical exponent is introduced in the model as described in Eq. (2.7). The concept is that the proportion of surface runoff is very small, or even nil, under the condition of very small rainfall intensity, and the proportion increases along with the increase of rainfall intensity up to a stage for which a potential runoff coefficient is achieved. In WetSpa Extension, this exponent is assumed to be a variable starting from a higher value for a near zero rainfall intensity, and changing linearly up to 1 along with the rainfall intensity, when the predetermined maximum rainfall intensity is reached. This value is generally less than 3 according to the previous applications. If an exponent value 1 is given, the actual runoff coefficient is then a linear function of the relative soil moisture content, and the effect of rainfall intensity on the runoff coefficient is not taken into account.

10) Rainfall intensity corresponding to a surface runoff exponent of 1

This parameter corresponds to threshold rainfall intensity in unit of mm/h or mm/d depending upon the temporal resolution of the model simulation, over which the surface runoff exponent equals 1, and the actual runoff coefficient becomes a linear

function of the relative soil moisture content. Calibration of this parameter can be performed by comparison of the observed and computed surface runoff volume and the peak discharge for high floods. This parameter is in fact spatially distributed, depending upon the cell characteristics, such as soil type, land use, and slope, etc. A constant value is assumed in the current model for simplification.

### 3.3 MODEL EVALUATION

In order to evaluate how well WetSpa Extension reproduces an observed hydrograph, a series of statistics are used. In addition to the evaluation based on a visual comparison and an evaluation of peak flow rate and time to the peak, the bias, model confidence, and the model efficiency are also taken into account. These statistical measures provide quantitative estimates for the goodness of fit between observed and predicted values, and are used as indicators of the extent at which model predictions match observation. Based on the results of these tests, model predictive capabilities are assessed. The goodness of fit in the peak discharge and time to the peak can be evaluated by their relative and absolute errors respectively, while other evaluation criteria are described as following:

#### 1) Model bias

Model bias can be expressed as the relative mean difference between predicted and observed stream flows for a sufficiently large simulation sample, reflecting the ability of reproducing water balance, and perhaps the most important criterion for comparing whether a model is working well in practice. The criterion is given by the equation

$$CR1 = \frac{\sum_{i=1}^N (Qs_i - Qo_i)}{\sum_{i=1}^N Qo_i} \quad (3.9)$$

where CR1 is the model bias,  $Qs_i$  and  $Qo_i$  are the simulated and observed stream flows at time step  $i$  ( $m^3/s$ ), and  $N$  is the number of time steps over the simulation period. Model bias measures the systematic under or over prediction for a set of predictions. A lower CR1 value indicates a better fit, and the value 0.0 represents the perfect simulation of observed flow volume.

## 2) Model confidence

Model confidence is one of the important criteria in assessment of continuous model simulation, and can be expressed by its determination coefficient, which is calculated as the portion of the sum of the squares of the deviations of the simulated and observed discharges from the average observed discharge.

$$CR2 = \frac{\sum_{i=1}^N (Q_{s_i} - \overline{Q_o})^2}{\sum_{i=1}^N (Q_{o_i} - \overline{Q_o})^2} \quad (3.10)$$

where CR2 is the model determination coefficient,  $\overline{Q_o}$  is the mean observed stream flow over the simulation period. CR2 represents the proportion of the variance in the observed discharges that are explained by the simulated discharges. It varies between 0 and 1, with a value close to 1 indicating a high level of model confidence.

## 3) Nash-Sutcliffe efficiency

The Nash-Sutcliffe coefficient (Nash and Sutcliffe, 1970) describes how well the stream flows are simulated by the model. As pointed out by Kachroo and Natale (1992), this efficiency criterion is commonly used for model evaluation, because it involves standardization of the residual variance, and its expected value does not change with the length of the record or the scale of runoff. The equation can be described as

$$CR3 = 1 - \frac{\sum_{i=1}^N (Q_{s_i} - Q_{o_i})^2}{\sum_{i=1}^N (Q_{o_i} - \overline{Q_o})^2} \quad (3.11)$$

where CR3 is the Nash-Sutcliffe efficiency used for evaluating the ability of reproducing the time evolution of stream flows. The CR3 value can range from a negative value to 1, with 1 indicating a perfect fit between the simulated and observed hydrographs. CR3 below zero indicates that average measured stream flow would have been as good a predictor as the modelled stream flow. A perfect model prediction has CR3 score equal to 1.

## 4) Logarithmic version of Nash-Sutcliffe efficiency for low flow evaluation

A logarithmic transformed Nash-Sutcliffe criterion is presented in Equation 3.11, which gives emphasize for evaluating the quality of low flow simulations (Smakhtin et

al., 1998).

$$CR4 = 1 - \frac{\sum_{i=1}^N [\ln(Q_{s_i} + \varepsilon) - \ln(Q_{o_i} + \varepsilon)]^2}{\sum_{i=1}^N [\ln(Q_{o_i} + \varepsilon) - \ln(\overline{Q_o} + \varepsilon)]^2} \quad (3.12)$$

where CR4 is a logarithmic Nash-Sutcliffe efficiency for evaluating the ability of reproducing the time evolution of low flows, and  $\varepsilon$  is an arbitrary chosen small value introduced to avoid problems with nil observed or simulated discharges. The value of  $\varepsilon$  should be sufficiently low, and those observed discharges lower than  $\varepsilon$  value are negligible. Otherwise the CR3 criterion would present a bias. Similar as CR3, a perfect value of CR4 is 1.

5) Adapted version of Nash-Sutcliffe efficiency for high flow evaluation

An adapted version of the Nash-Sutcliffe criterion is proposed as in Equation 3.12. It is in fact a combination between the calibration criteria used by Guex (2001) for the hydrological study on the Alzette river basin and the HEC-1 objective function (USACE, 1998).

$$CR5 = 1 - \frac{\sum_{i=1}^N (Q_{o_i} + \overline{Q_o})(Q_{s_i} - Q_{o_i})^2}{\sum_{i=1}^N (Q_{o_i} + \overline{Q_o})(Q_{o_i} - \overline{Q_o})^2} \quad (3.13)$$

where CR5 is an adapted version of Nash-Sutcliffe criterion for evaluating the ability of reproducing the time evolution of high flows. As can be seen in the formula, more weight is given on high discharges than low ones. A perfect value of CR5 is 1.

Other model performance indices are described as follows:

- Modified Correlation Coefficient  $r_{\text{mod}}$ , which reflects differences both in hydrograph size and in hydrograph shape (McCuen and Snyder, 1975):

$$r_{\text{mod}} = r \times \left[ \frac{\min\{\sigma_o, \sigma_s\}}{\max\{\sigma_o, \sigma_s\}} \right]$$

where,  $\sigma_o$  and  $\sigma_s$  are the standard deviations of observed and simulated discharges respectively,  $r$  is the correlation coefficient between observed and simulated hydrographs. The perfect value for this criterion is 1.

- The mean squared error (*MSE*) is:

$$MSE = \frac{1}{n} \sum_{i=1}^n \varepsilon_i^2$$

where  $\varepsilon_i$  is the residuals, or estimated errors, are the differences between the observed data and fitted model:

$$\varepsilon_i = (Qs_i - Qo_i)$$

- Mean absolute error

the mean absolute error is a quantity used to measure how close forecasts or predictions are to the eventual outcomes. The mean absolute error (MAE) is given by

$$MAE = \frac{1}{n} \sum_{i=1}^n |\varepsilon_i|$$

- Root Mean Squared Error

The root mean squared error (*RMSE*) is evaluated by the equation:

$$RMSE = \sqrt{MSE}$$

where *MSE* is the mean squared error. For a perfect fit, *RMSE* = 0. so, the *RMSE* index ranges from 0 to infinity, with 0 corresponding to the ideal.

- Model Volumetric efficiency (*MVE*)

The volumetric efficiency ranges from 0 to 1 and represents the fraction of water delivered at the proper time; its compliment represents the fractional volumetric mismatch. The *MVE* is most accurate when detailed discharge time series are available. The *MVE* would be particularly helpful in comparing the performance of similarly scaled, rainfall-runoff transfer functions. A major advantage of the *MVE* its physical significance as it treats every cubic meter of water the same as any other cubic meter, whether it be delivered during low recession or during peak flows (Criss and Winston, 2008):

$$MVE = 1 - \frac{\sum_{i=1}^N |(Qs_i - Qo_i)|}{\sum_{i=1}^N Qo_i}$$

where *MVE* is the volumetric efficiency. A perfect value of *MVE* is 1.

## 4. MODEL OPERATION

### 4.1 PROGRAM INSTALLATION

Installation of WetSpa requires a Windows 98/ME/2000/XP or Windows NT 4.0 operating system. Also required are licensed versions of ESRI's ArcView 3.2 GIS Application and Spatial Analyst v2.0 Extension. In addition, the software of Visual FORTRAN 6.1 or other FORTRAN compilers are required if the user wants to edit and modify the program source code. The minimum drive space required is 100MB. Additional space may be necessary depending on the spatial and temporal scale of the project. By simple copy and paste operation, the model can be installed and run on any computer drives and under any existing directories. Specific folders are referenced from that drive location throughout the modelling process. Figure 4.1 gives a schematic view of the model's project folders.

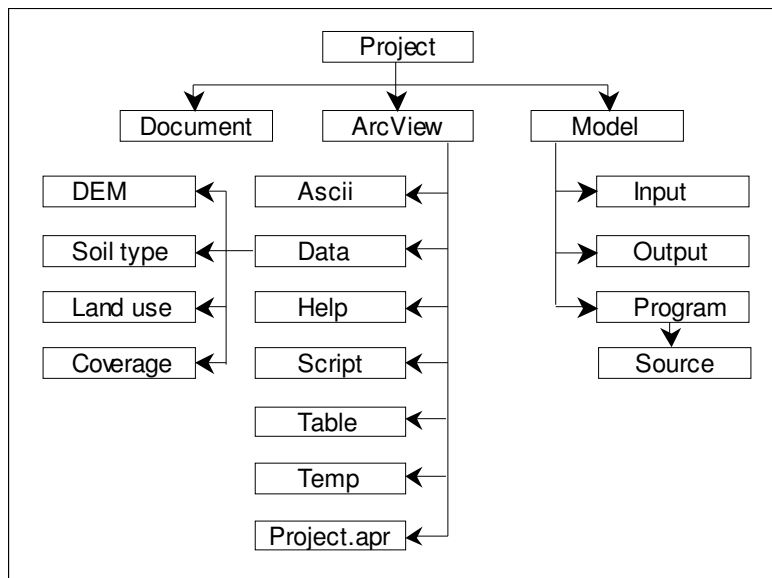


**Fig. 4.1.** Schematic view of the model's project folders

Where Project is the general folder of the modelling project, and the others are:

- 1) Document: for storing model documents
- 2) ArcView: for storing ArcView GIS components
- 3) ASCII: for storing spatial parameter maps in ASCII format
- 4) Data: for storing spatial data of base maps

- 5) Help: for storing model help files
- 6) Script: for storing ArcView Avenue scripts
- 7) Table: for storing model lookup tables.
- 8) Temp: project working directory for storing intermediate and temporary files
- 9) Project.apr: ArcView project of the model
- 10) DEM: digital elevation model
- 11) Soil type: digital soil type map in grid format
- 12) Land use: digital land use map in grid format
- 13) Coverage: for storing coverage data including stations, streams, boundaries, etc.
- 14) Model: for storing model inputs, outputs and programs
- 15) Input: for storing model input files
- 16) Output: for storing model output files
- 17) Program: for storing model executive programs
- 18) Source: for storing program source codes

## **4.2 PROGRAM DESCRIPTION**

### **4.2.1 Avenue scripts and their tasks**

- 1) conductivity: creates a grid of saturated hydraulic conductivity
- 2) delta\_h: calculates standard deviation of flow time from cells to the basin outlet
- 3) delta\_s: calculates standard deviation of flow time from cells to the main river
- 4) depression: calculates depression storage capacity for each cell
- 5) fieldcapacity: creates a moisture grid at soil field capacity
- 6) fillsink: fill sinks to remove small imperfections from DEM
- 7) flowacc: creates an accumulated flow grid at each cell
- 8) flowdir: creates a flow direction grid from each cell to its steepest downslope neighbour
- 9) flowlen: calculates a downstream distance grid along its flow path
- 10) interception: calculates minimum and maximum interception storage capacity
- 11) lai: creates a grid of leaf area index

- 12) manning: calculates Manning's roughness coefficient for each cell
- 13) mask: creates a mask grid of the watershed
- 14) moisture: creates an initial soil moisture grid based on the topographic index
- 15) poreindex: creates a grid of soil pore size distribution index
- 16) porosity: creates a moisture grid at soil porosity
- 17) radius: calculates hydraulic radius for each cell according to flood frequency
- 18) residual: creates a moisture grid at residual soil moisture content
- 19) rootdepth: creates a grid of root depth
- 20) runoffco: creates a grid of potential runoff coefficient
- 21) slope: creates a slope grid for both land surface and river channel
- 22) streamlink: assigns unique values to sections of stream network
- 23) streamnet: creates a grid of stream network
- 24) streamorder: assigns a numeric order to branches of a river network
- 25) streamtoline: converts stream grid to a line coverage
- 26) t0\_h: calculates flow time from each cell to the basin outlet
- 27) t0\_s: calculates flow time from each cell to the main river
- 28) thiessen: creates a grid of Thiessen polygons
- 29) velocity: creates a velocity grid for both overland flow and channel flow
- 30) v\_fraction: creates a grid of maximum fractional vegetation cover
- 31) watershed: determines subwatersheds based on stream links
- 32) wiltingpoint: creates a moisture grid at permanent wilting point

#### **4.2.2 Lookup tables**

- 1) depression.dbf: default values of depression storage capacity for different land use, soil texture, and near zero slopes
- 2) landuse\_reclass.dbf: land use reclassification table for deriving potential runoff coefficient and depression storage capacity of the 5 main land use classes
- 3) landuse\_remap.dbf: default model parameters based on land use classes, including root depth, manning's roughness coefficient, interception capacity, vegetated fraction and leaf area index
- 4) radius: default parameters governing average hydraulic radius for a certain flood

frequency

- 5) runoff\_coefficient.dbf: default potential runoff coefficient for different land use, soil texture, and near zero slopes
- 6) soil\_remap: default parameters based on soil texture categories, including hydraulic conductivity, porosity, field capacity, wilting point, residual moisture, pore size distribution index, etc.

### **4.2.3 Fortran programs and their tasks**

- 1) mean: calculates mean parameters of each subcatchment
- 2) iuh: calculates the unit response function of each cell to the catchment and subcatchment outlet, the unit hydrograph of each subcatchment to the catchment and subcatchment outlet, and the unit hydrographs of main rivers.
- 3) model1: semi-distributed model on subcatchment scale
- 4) model2: fully distributed model on cell scale
- 5) water\_balance: calculates water balance on grid scale without flow routing
- 6) evaluation: statistics of simulation results and model evaluation

## **4.3 GIS PRE-PROCESSING**

The purpose of GIS pre-processing is to create all necessary spatial parameter maps used in the WetSpa Extension. Open a new ArcView project 'project' (or other name) under the subdirectory \project\arcview. Set the project's working directory to \project\arcview\temp, in which the intermediate and temporary GIS files are stored, and all other input and output files are transferred from or to their subdirectory referencing to this path. Before performing GIS pre-processing, be sure that the ArcView Extensions: Spatial Analyst, GeoProcessing, WetSpa and Create Thiessen Polygons, are added to the ArcView project. Next, Load grid themes of elevation, landuse and soiltype from the subdirectory \project\arcvie\data to the View 'Topography', 'Landuse' and 'Soiltype' separately. Set the theme names as 'Elevation', 'Landuse' and 'Soil'. Note that the extent of these three base maps must be the same in order to perform the model simulation properly.

### 4.3.1 Surface grid preparation

Surface parameter grids based on a DEM are prepared in the view Topography of the ArcView project. The preparation of a proper DEM employs many geo-processing schemes, and can be implemented independently from the project using more powerful GIS software, such as ArcInfo etc. From the available DEM, its hydrological potential is calculated in ArcView by performing the following functions: filling sinks, determining flow direction and flow accumulation, assigning stream network, stream link and stream order, calculating slope and hydraulic radius, and delineating subcatchments, etc. Figure 4.2 gives a screenshot of the surface grid menu.

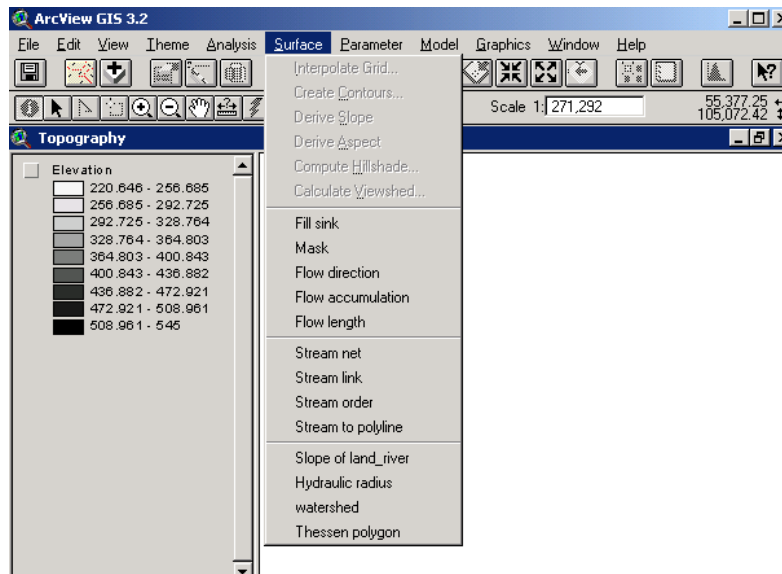


Fig. 4.2. Screenshot of surface menu

#### 1) Fill Sinks

A sink is a cell or set of spatially connected cells whose flow direction cannot be assigned one of the eight valid values in a flow direction Grid. This can occur when all neighbouring cells are higher than the processing cell. In ArcView GIS, sinks are considered to have undefined flow directions and are assigned a value that is the sum of their possible directions. To create an accurate representation of flow direction and therefore accumulated flow, it is required to use a data set that is free of sinks. The fill

sinks request in the surface menu takes a grid theme 'Elevation' and fills all sinks and areas of internal drainage contained within it. The process of filling sinks can create new sinks, so a looping process is used until all sinks are filled (ESRI, 1999). The output theme is named as 'Filled Elevation' displayed in the same view, and the corresponding ASCII file 'elevation.asc' is saved in the subdirectory /project/arcview/ascii used for estimation of altitude-distributed temperature.

2) Mask

A mask grid defines the study region in the grid domain, which can be used to extract catchment boundary, determine the extent of other grids, etc. The request takes the grid theme 'Filled Elevation' and assigns a unique value 1 for the cells within the study catchment with output theme 'Mask' displayed in the same view.

3) Flow direction

The flow direction request calculates the direction of flow out of each cell into one of its eight neighbours. The direction of flow is determined by finding the direction of steepest descent from each cell. If a cell is lower than its 8 neighbours that cell is given the value of its lowest neighbour and flow is defined towards this cell. If the descent to all adjacent cells is the same, the neighbourhood is enlarged until the steepest descent is found (ESRI, 1999). The request takes the grid theme 'Filled Elevation' and calculates flow direction for each cell with output theme 'Flow Direction' displayed in the same view.

4) Flow accumulation

The flow accumulation request creates a grid of accumulated flow to each cell by accumulating the weight for all cells that flow into each downslope cell. Cells of undefined flow direction can only receive flow; they will not contribute to any downstream flow. The accumulated flow is based upon the number of cells flowing into each cell in the output grid. Output cells with a high flow accumulation are areas of concentrated flow, and therefore can be used to identify stream channels. Output cells with a flow accumulation of zero are local topographic highs and can be used to identify ridges. The request takes the grid theme 'Flow Direction' and calculates flow accumulation for each cell with output 'Flow Accumulation' displayed in the same view.

5) Stream network

The results of the flow accumulation are used to create a vector stream network by applying a threshold value to subset cells with a high-accumulated flow. All cells that have more than a user-defined number of cells flowing into them are assigned a value of one; all other cells are assigned no data. The resulting stream network can be used as a predicted hydrography (ESRI, 1999). The stream network request takes the grid theme 'Flow Accumulation' and delineates a stream network grid 'Stream Network' displayed in the same view.

6) Stream link

Links are the sections of a stream channel connecting two successive junctions, a junction and the outlet, or a junction and the drainage divide (ESRI, 1999). The stream link request takes the grid themes 'Flow Direction' and 'Stream Network', and assigns unique values to sections of a stream network between intersections. The output theme is named as 'Stream Link' displayed in the same view, which can be used as the source grid to create drainage basins that correspond the branches of a stream network. Meanwhile, the output grid data is written to an ASCII file 'link.asc' used to calculate IUH of stream channels.

7) Stream order

The stream order request takes the grid themes 'Flow Direction' and 'Stream Network', and assigns a numeric order to segments of the stream network. The Shreve method is used in the model, in which all links with no tributaries are assigned an order of 1 and the orders are additive downslope. When two links intersect, their magnitudes are added and assigned to the downslope link. The output theme is named as 'Stream Order' displayed in the same view, and used as a source grid in assigning Manning's n for stream channels.

8) Slope

The process of slope derivation calculates the rate of maximum change for locations on the elevation grid theme and creates a new grid theme 'Slope' as output. Each cell in the output theme contains a continuous slope value represented as a percentage. Considering that the stream network is in a vector style, and its slope is determined by the elevation difference and distance between the up and down cells along the

streamline, the channel slope is calculated separately from the general slope using DEM and the stream network information. This avoids the disturbance in channel slopes for a river, especially for stream channels with asymmetric side slopes of the riverbank. The final slope grid is then obtained using the general slope grid overlaid by the grid of channel slope. An ASCII file 'slope.asc' is saved in the subdirectory /project/arcview/ascii for use in calculating interflow from each cell.

#### 9) Hydraulic radius

The hydraulic radius request takes the grid theme 'Flow accumulation, and calculates hydraulic radius for each grid cell. The hydraulic radius is determined by a power law relationship with an exceeding probability, which relates hydraulic radius to the controlling area and is seen as a representation of the average behaviour of the cell and the channel geometry. Generally, a flood frequency with 2-year return period is chosen for normal floods. The two controlling parameters can be adjusted in the lookup table 'radius.dbf' to meet the specific characteristics of catchment. The output grid theme is named as 'Radius (m)', and is used for calculation of flow velocity at each cell.

#### 10) Watershed

The watershed request takes the grid themes 'Flow Direction' and 'Stream Link', and determines the subcatchment for each stream link. The output grid theme is named as 'Watershed' displayed in the same view, and is saved as an ASCII file for semi-distributed modelling and the simulation of groundwater balance. If the subcatchment does not delineate as expected, delete the grid themes 'Stream Network', 'Stream Link' and 'Watershed' by invoking the delete theme command in the edit dropdown menu, and rebuild the three grid themes by setting a new threshold value. Often it is necessary to closely zoom into the area of interest to ensure the outlet point's location is positioned correctly.

### **4.3.2 Soil based grid preparation**

To calculate the soil hydraulic properties, activate the view 'Soiltype', select the 'Parameter' dropdown menu, and the commands related to soil types are highlighted (Fig. 4.3), including 'Conductivity', 'Porosity', 'Field capacity', 'Residual moisture', 'Pore distribution index', and 'wilting point', etc. The commands 'Maximum saturation',

‘Arithmetic mean of G’ and ‘Geometric mean of G’ are designed for future model improvement, where G is the capillary drive (mm). By clicking each of the command, the grid files are created to redefine and display the soil units with respect to their hydrological properties, and the corresponding ASCII files are saved in the subdirectory /project/arcview/ascii.

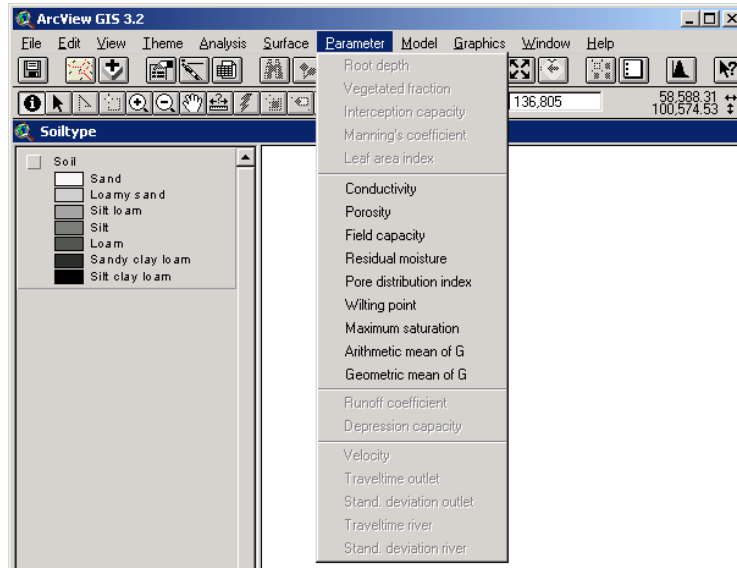


**Fig. 4.3.** Screenshot of parameter menu

Another activated function under the dropdown menu is the ‘Initial moisture’. This function creates an initial relative saturation grid of the soil using the method of the Topographical Wetness Index. A minimum ratio reflecting the moisture condition of the driest cells is asked in a pop up window, which can be selected from the provided list. The output theme is named as ‘Initial Moisture’ displayed in the same view, and the ASCII file ‘moisture.asc’ is saved in the subdirectory /project/arcview/ascii. Note that this operation is optional and designed for event based flood modelling, for which the initial soil moisture condition is rather important.

### 4.3.3 Land use based grid preparation

To calculate the land use dependent model parameters, activate the view ‘Landuse’, select the ‘Parameter’ dropdown menu, and the commands related to land use grid are highlighted, including ‘Root depth’, ‘Vegetated fraction’, ‘Interception capacity’,

‘Manning’s coefficient’, and ‘Leaf area index’. There are two interception capacity themes created by the command ‘Interception capacity’, e.g. maximum interception capacity and minimum interception capacity, corresponding to the summer and winter situation. The command ‘Manning’s coefficient’ creates a map of Manning’s roughness coefficient for both overland flow and channel flow. Therefore, the theme ‘Stream order’ needs to be created firstly in the view ‘Topography’. A selection list is shown in the window asking for a Manning’s n interpolation method for the stream channels.

- 1) Interpolation among different stream orders, for which the channel Manning’s n is defined based on the stream orders with lower values downstream and higher value upstream. A maximum and a minimum Manning’s n value are asked to determine corresponding to the lowest and highest stream order.
- 2) Remain the default constant as in the lookup table, for which a constant Manning’s n is defined for the river channels using the value assigned in the lookup table.
- 3) Change to another constant, for which a modified constant Manning’s n is defined for the river channels.

The command ‘Leaf area index’ is designed for future model improvement. By clicking each of the commands, the grid files are created to redefine and display the land use units with respect to their hydrological properties based on the predefined lookup table, and the corresponding ASCII parameter files are saved in the subdirectory /project/arcview/ascii.

#### **4.3.4 Potential runoff coefficient and depression storage capacity**

Next, the parameter maps of potential runoff coefficient and depression storage capacity are generated in the view ‘Runoff coefficient & depression’. Since both parameter maps are functions of slope, soil type and land use, these three base maps need to be created firstly in their views. The program can load these three grid themes directly from their views, and the parameter grids are created and displayed in a separate view ‘Runoff coefficient & depression’ in order to give a clear view of them. By activating the view ‘Runoff coefficient & depression’, selecting the ‘Parameter’ dropdown menu, the commands ‘Runoff coefficient’ and ‘Depression capacity’ will be highlighted. An impervious percentage for urban cells is asked when calculating the grid of potential runoff

coefficient. A default value 30% is given for a grid with cell size 100X100 m. By clicking each of the commands, the resulting grid files are created and displayed in the view, and the corresponding ASCII parameter files are saved in the subdirectory /project/arcview/ascii.

#### **4.3.5 Flow routing parameters**

The flow routing parameter grids are calculated in the view 'Routing Parameter', including flow velocity, mean flow times to the basin outlet and to the main river from each cell, and the standard deviations of the flow times. These parameter maps are used for calculating flow response functions from each cell to the basin outlet as well as to the main river. By activating the view 'Routing Parameter', selecting the 'Parameter' dropdown menu, the commands 'Velocity', 'T0\_h', 'Delta\_h', 'T0\_s' and 'Delta\_s' will be highlighted. By clicking each of the commands, the resulting grid files are created and displayed in the view, and the corresponding ASCII parameter files are saved in the subdirectory /project/arcview/ascii.

- 1) Run the script 'Velocity' from the menu 'Parameter'. This function creates a flow velocity grid based on the Manning's n, hydraulic radius and slope grid. A popup window shows and asks you if a flow velocity limit is necessary. The flow velocity is set to the upper limit when the calculated velocity is higher than the upper limit, and to the lower limit vice versa. The upper and lower limits 3.0 m/s and 0.005 m/s are given by default.
- 2) Run the script 'T0\_h' from the menu 'Parameter'. This function creates a flow travel time grid in hours from each cell to the catchment outlet using the weighted FLOWLENGTH routine. The ASCII file 't0\_h.asc' is saved in the subdirectory /project/arcview/ascii.
- 3) Run the script 'Delta\_h' from the menu 'Parameter'. This function creates a standard deviation grid of flow times in hours from each cell to the catchment outlet using the weighted FLOWLENGTH routine. The ASCII file 'delta\_h.asc' is saved in the subdirectory /project/arcview/ascii.
- 4) Run the script 'T0\_s' from the menu 'Parameter'. This function creates a flow travel time grid in hours from each cell to its subcatchment outlet. The ASCII file 't0\_s.asc' is saved in the subdirectory /project/arcview/ascii.

- 5) Run the script 'Delta\_s' from the menu 'Parameter'. This function creates a standard deviation grid of flow times in hours from each cell to its subcatchment outlet. The ASCII file 'delta\_s.asc' is saved in the subdirectory /project/arcview/ascii.

#### **4.3.6 Thiessen polygon**

Rainfall and PET data used in WetSpa Extension are tabular data gathered from point measuring stations inside or surrounding the catchment. In order to obtain a more accurate estimate of rainfall and PET values for a grid or a working unit, the Thiessen Polygon extension in ArcView is executed together with the themes of weather stations and the catchment boundary. This involves creating a Thiessen polygon theme in ArcView for all stations, then identifying each grid with the covering station identity number. The steps for creation of Thiessen polygon of rainfall data as well as its grid and ASCII file are:

- 1) To begin this process, three themes, rainfall stations, catchment boundary and a mask grid, need to be loaded into the View 'Thiessen Polygon', from which all others themes can be created. The rainfall station theme is obtained from a point shape file named as 'stations', which contains the fields of latitude, longitude, station name and station ID. The boundary shape file is obtained by conversion of a mask grid map to a polygon shape file.
- 2) Activate the theme 'Stations' by clicking on the name in the View's theme list. Then, run the avenue script by clicking the command 'Thiessen polygon' in the dropdown menu 'Surface'. Select 'ID' when prompted to "Select point field for polygon link ID", and select 'Boundary' when prompted to 'Select polygon theme for boundary'. Define the name of the output file as 'thiessen.shp' in the subdirectory /project/arcview/data. The Thiessen polygon coverage theme is then displayed in the view after the execution.
- 3) If it is wanted to convert the Thiessen polygon from coverage to grid, click 'Yes' when asked 'Covert the Thiessen.shp to grid Thiessen?'. Define the grid name as 'thiessen' in the subdirectory /project/arcview/data. Set the output grid cell size, number of rows and number of columns the same as the mask map, and pick the field 'ID' for cell values. A grid named 'Thiessen' will be displayed in the view, after clicking 'Yes' when promoted to 'Add grid as theme to the view'.
- 4) Click 'Yes' when promoted to 'Save the Thiessen polygon grid as Ascii file', the

ASCII file 'Thiessen\_p.asc' is stored in the subdirectory /project/arcview/ascii.

Following the same procedures, the Thiessen polygon grid for PET and temperature can be created using the point theme of PET and temperature stations instead of rainfall stations. The corresponding ASCII fill is named as 'Thiessen\_e.asc' and 'Thiessen\_t.asc' stored in the subdirectory /project/arcview/ascii. Note that there must be at least 2 stations in the point theme for performing the 'Thiessen polygon' command. If only one station exists, the Thiessen polygon grid is just the same as the musk grid with cell values of station ID number.

#### **4.3.7 Drainage systems for a complex terrain**

In case the WetSpa Extension is used for modelling a complex terrain, e.g. an urban or suburban watershed, on a small catchment scale, the sewer systems, communication lines, and artificial canals, lakes, reservoirs, etc., are important elements in drainage structure configuration, and govern flow direction more strongly than the derived aspect at local scale. Surface flow on these areas should thus be described with more detailed methodology, which allows a correct physical representation of the flow regime. Since most of these barriers are not sufficient to be represented in a DEM, additional procedures in term of deriving more realistic flow direction map are performed using GIS overlaying technique in the model. The procedures are:

- 1) Compute a general flow direction grid using the elevation grid alone without considering the effect of artificial areas, from which a stream network grid is generated.
- 2) Compute flow direction maps independently for sewer areas, main communication lines, artificial canals, and the stream network derived from the general flow direction grid, etc., based on the DEM and the available line and polygon themes.
- 3) Overlay the general flow direction map by the flow direction maps of sewer areas, communication lines, artificial canals, and the stream network subsequently, which allowing water to drain from the sewer areas at their outlets and water to cross communication lines and canals at their concave points to join the river.
- 4) The drainage paths delineated from the DEM are compared with existing hardcopy maps. Make any necessary corrections to the generated flow direction map in order to have the river reaches flow where they should and to be able to estimate a flow length

closer to reality, particularly for the areas close to the catchment boundary, lakes, reservoirs and the meandering channel reaches.

As an option, the above procedures can be integrated by modifying the elevation grid using ArcView GIS tools, in which the elevation of sewer areas, communication lines, and stream networks are lowered subsequently, e.g. 0.2, 0.4, 0.6 m. Similar flow direction grid can be obtained based on the modified elevation grid, but cautions should be made when performs this method to an even more complex terrain. The derived flow direction map is then used for further drainage structure delineation. The above procedures can be omitted, if the effects of human infrastructures are not remarkable to the flow regime in the catchment.

## **4.4 CREATION OF INPUT FILES**

### **4.4.1 Input files of time series**

WetSpa Extension reads input data from four input files. The names of these files are fixed during data preparation, namely p.txt, pet.txt, t.txt and q.txt. All files are in a text format and stored in the subdirectory /project/model/input. All data are of unformatted statements, so that the exact position of each entry is not crucial. However, there must be at least one space or a comma between entries and data must be entered for each item.

#### 1) Precipitation series

The input precipitation series are in the format of year, month, day, hour, and followed by the precipitation values in mm at each gauging station. The first row of the file is year, month, day and hour, followed by the elevations of each precipitation station (m) for use in potential topographic precipitation interpolation. The precipitation series must be in an ascending order corresponding to the ID number in the precipitation Thiessen polygons. If the model runs on a daily scale, set the hour value zero. Table 4.1 gives a sample file of precipitation series on hourly scale.

#### 2) Potential evapotranspiration series

The file pet.txt contains PET data in mm for all evaporation stations used in the model simulation. This input file is omitted if other PET calculation method is selected

instead of using measured data. The format of pet.txt file is the same as the precipitation series. The first row of the file is year, month, day and hour, followed by the elevations of each evaporation station (m) for use in potential topographic evapotranspiration interpolation. The data series must be in an ascending order corresponding to the ID number in the evapotranspiration Thiessen polygons. If the model runs on a daily scale, put a zero value in the hour's column. Table 4.2 gives a sample file of PET series on hourly scale.

**Table 4.1.** Sample file of precipitation series p.txt

| year | Month | day | hour | 904   | 570   | 473  | 312  |
|------|-------|-----|------|-------|-------|------|------|
| 1998 | 10    | 23  | 16   | 1.406 | 1.4   | 1.38 | 1.36 |
| 1998 | 10    | 23  | 17   | 2.018 | 2.01  | 1.98 | 1.92 |
| 1998 | 10    | 23  | 18   | 0.966 | 0.963 | 0.95 | 0.93 |
| 1998 | 10    | 23  | 19   | 1.054 | 1.05  | 1.03 | 1.01 |
| 1998 | 10    | 23  | 20   | 0.352 | 0.35  | 0.34 | 0.33 |
| 1998 | 10    | 23  | 21   | 9.656 | 9.618 | 9.48 | 9.51 |
| 1998 | 10    | 23  | 22   | 0.264 | 0.263 | 0.26 | 0.25 |
| 1998 | 10    | 23  | 23   | 0.528 | 0.525 | 0.52 | 0.51 |

**Table 4.2.** Sample file of PET series pet.txt

| Year | Month | Day | hour | 901   | 380   | 270   |
|------|-------|-----|------|-------|-------|-------|
| 1998 | 10    | 23  | 16   | 0.05  | 0.05  | 0.048 |
| 1998 | 10    | 23  | 17   | 0.048 | 0.047 | 0.043 |
| 1998 | 10    | 23  | 18   | 0.048 | 0.047 | 0.043 |
| 1998 | 10    | 23  | 19   | 0.05  | 0.05  | 0.048 |
| 1998 | 10    | 23  | 20   | 0.05  | 0.05  | 0.048 |
| 1998 | 10    | 23  | 21   | 0.05  | 0.05  | 0.048 |
| 1998 | 10    | 23  | 22   | 0.04  | 0.038 | 0.036 |
| 1998 | 10    | 23  | 23   | 0.04  | 0.038 | 0.036 |

### 3) Temperature series

Temperature data is optional, used only when snow accumulation and snowmelt occur in the study catchment. The first row of the file is year, month, day and hour, followed by the elevations of each temperature station (m). The format of the rest of the file is the same as that in the precipitation series with temperature unit of °C. If the model runs on a daily scale, set the hour value zero as shown in Table 4.3. Note that the temperature

stations should be listed in a continuously ascending order and corresponding to the station numbers in the temperature Thiessen polygons.

**Table 4.3.** Sample file of temperature series t.txt

| Year | month | Day | hour | 295  | 141  | 702  |
|------|-------|-----|------|------|------|------|
| 1991 | 1     | 10  | 0    | 2.5  | 4    | 4.4  |
| 1991 | 1     | 11  | 0    | 4.7  | 5.9  | 2    |
| 1991 | 1     | 12  | 0    | 3.5  | 4.8  | 2.9  |
| 1991 | 1     | 13  | 0    | 2    | 4.2  | -0.3 |
| 1991 | 1     | 14  | 0    | -3.5 | -1.7 | -6.2 |
| 1991 | 1     | 15  | 0    | -4   | -2.7 | -7.6 |
| 1991 | 1     | 16  | 0    | -3.4 | -3.6 | -7.5 |
| 1991 | 1     | 17  | 0    | -5.3 | -5.1 | -6.7 |
| 1991 | 1     | 18  | 0    | -1.8 | -3.1 | -3.8 |

#### 4) Discharge series

The observed discharge series are optional, used only for graphical comparison of the model outputs and statistical analysis for model evaluation. The format of the discharge file is the same as the precipitation file with values in m<sup>3</sup>/s. Set the hour value zero if the model runs on a daily scale. Table 4.4 gives a sample file of discharge series on hourly scale.

**Table 4.4** Sample file of discharge series q.txt

| Year | month | Day | hour | q1    | q2    | q3    |
|------|-------|-----|------|-------|-------|-------|
| 1998 | 10    | 23  | 16   | 1.664 | 1.784 | 0.946 |
| 1998 | 10    | 23  | 17   | 1.664 | 1.829 | 1.015 |
| 1998 | 10    | 23  | 18   | 1.664 | 1.93  | 1.056 |
| 1998 | 10    | 23  | 19   | 1.719 | 2.031 | 1.132 |
| 1998 | 10    | 23  | 20   | 1.794 | 2.069 | 1.225 |
| 1998 | 10    | 23  | 21   | 2.255 | 2.713 | 1.529 |
| 1998 | 10    | 23  | 22   | 2.558 | 3.092 | 2.481 |
| 1998 | 10    | 23  | 23   | 3.026 | 3.905 | 4.39  |

### 4.4.2 Global parameters and spatial output specifications

#### 1) Global model parameters

Before running WetSpa model, several global model parameters must be prepared, which are applied to each grid cell or each subcatchment. The file is named as input.txt

and stored in the subdirectory /project/model/input. Table 4.5 illustrates a template of global parameters in the input file input.txt.

**Table 4.5.** Template of global model parameters

|        |      |                 |                 |       |                  |     |                   |                   |                  |                  |  |
|--------|------|-----------------|-----------------|-------|------------------|-----|-------------------|-------------------|------------------|------------------|--|
| dt (h) |      |                 |                 |       |                  |     |                   |                   |                  |                  |  |
| 24     |      |                 |                 |       |                  |     |                   |                   |                  |                  |  |
| Ci     | Cg   | K <sub>ss</sub> | K <sub>ep</sub> | G0    | G <sub>max</sub> | T0  | K <sub>snow</sub> | K <sub>rain</sub> | K <sub>run</sub> | P <sub>max</sub> |  |
| 2.0    | 15.0 | 0.95            | 1.00            | 250.0 | 300.0            | 0.0 | 2.0               | 0.00              | 3.0              | 50.0             |  |

Where dt is the time interval (h), for which the value in the second row of the table can be any hours, e.g. 1 for hourly scale and 24 for daily scale. Ci is an interflow scaling factor reflecting the effect of organic material and root systems in the topsoil layer on horizontal hydraulic conductivity. Cg is a groundwater flow recession coefficient reflecting the groundwater recession regime for entire catchment. K<sub>ss</sub> is a soil moisture ration relative to the field capacity for setting up the initial soil moisture content. This gives a uniform distribution of initial relative moisture condition and can be used for model simulation with a long time series. For performing an event based flood simulation, the initial moisture grid by the method of TWI can be applied. To do so, a negative value of K<sub>ss</sub> should be given in the file, for instance, -1.0. K<sub>ep</sub> is a correction factor for PET. G0 is the initial groundwater storage in depth (mm). G<sub>max</sub> is the maximum groundwater storage in depth (mm). T0 is a base temperature (°C) for estimating snowmelt, in which the precipitation shifts from rain to snow at T0. K<sub>snow</sub> is a temperature degree-day coefficient (mm/°C/day) for calculating snowmelt. K<sub>rain</sub> is a rainfall degree-day coefficient (mm/mm/°C/day) determining the rate of snowmelt caused by rainfall. Note that if there is no snow accumulation occurred in the study catchment, the parameters T0, K<sub>snow</sub> and K<sub>rain</sub> are set to negative values, e.g. -1.0, and the temperature input dataset 't.txt' is not necessary. K<sub>run</sub> is an exponent reflecting the effect of rainfall intensity on the actual surface runoff coefficient when the rainfall intensity is very small. P<sub>max</sub> is a threshold of rainfall intensity in mm/day or mm/hour depending on the modelling time step, over which the value of K<sub>run</sub> is set to 1.

2) Location and time specifications for spatial output

In order to obtain flow hydrographs at some specified subcatchment outlets, as well as

the spatial distribution of hydrological processes, such as surface runoff, interflow, groundwater recharge, soil moisture and actual evapotranspiration, for a certain period, a station and time list must be prepared before running the model. The list is attached in the same file input.txt stored in the subdirectory /project/model/input, following the part of global model parameters. Table 4.6 shows a template of spatial output specifications.

**Table 4.6.** Template of spatial output specifications

|                      |   |   |    |    |    |      |    |    |   |
|----------------------|---|---|----|----|----|------|----|----|---|
| Q_sub                | 6 |   |    |    |    |      |    |    |   |
| 3                    | 5 | 8 | 12 | 25 | 36 |      |    |    |   |
| Surface runoff       |   |   |    |    |    |      |    |    |   |
| 2                    |   |   |    |    |    |      |    |    |   |
| 1997                 | 8 | 9 | 0  |    |    | 1997 | 8  | 10 | 0 |
| 1997                 | 1 | 1 | 0  |    |    | 1997 | 12 | 31 | 0 |
| Interflow            |   |   |    |    |    |      |    |    |   |
| 1                    |   |   |    |    |    |      |    |    |   |
| 1997                 | 1 | 1 | 0  |    |    | 1997 | 12 | 31 | 0 |
| Groundwater-recharge |   |   |    |    |    |      |    |    |   |
| 1                    |   |   |    |    |    |      |    |    |   |
| 1997                 | 1 | 1 | 0  |    |    | 1997 | 12 | 31 | 0 |
| Soil moisture        |   |   |    |    |    |      |    |    |   |
| 3                    |   |   |    |    |    |      |    |    |   |
| 1997                 | 8 | 9 | 0  |    |    | 1997 | 8  | 10 | 0 |
| 1997                 | 8 | 1 | 0  |    |    | 1997 | 8  | 31 | 0 |
| 1997                 | 1 | 1 | 0  |    |    | 1997 | 12 | 31 | 0 |
| Evapotranspiration   |   |   |    |    |    |      |    |    |   |
| 0                    |   |   |    |    |    |      |    |    |   |

a) Flow hydrograph at subcatchment outlet

The number of the interested subcatchments is given after the mark ‘q\_sub’, and the sequence number of each subcatchment is listed in the following line. This option is useful for simulating flow hydrographs simultaneously both at catchment outlet and at some gauging stations inside the catchment. The identification of specified subcatchments can be realized by modifying the stream link theme by using ArcView edit tools and making the discretization of the catchment.

b) Spatial distribution of surface runoff

This option gives a series of accumulative surface runoff distribution files after

running the fully distributed model. The number of expected spatial outputs is given under the mark 'Surface runoff', and the wanted time periods are listed in the following lines. The input time period is in the format of start year, month, day, hour, and end year, month, day, hour as shown in the Table. If the model runs on a daily scale, set the hour value to be zero. If no spatial outputs are wanted, put zero value under the mark 'Surface runoff'.

c) Spatial distribution of interflow

This option gives a series of accumulative interflow distribution files after running the fully distributed model. The format of the input values is the same as for the surface runoff list.

d) Spatial distribution of groundwater recharge

This option gives a series of accumulative groundwater recharge distribution files after running the fully distributed model. The format of the input values is the same as for the surface runoff list.

e) Spatial distribution of relative soil saturation

This option gives a series of average moisture distribution files after running the fully distributed model. The format of the input values is the same as for the surface runoff list.

f) Spatial distribution of actual evapotranspiration

This option gives a series of accumulative actual evapotranspiration distribution files after running the fully distributed model. The format of the input values is the same as for the surface runoff list.

## **4.5 MODEL CALIBRATION AND VERIFICATION**

### **4.5.1 CALIBRATION AND VERIFICATION PROCESSES**

The purpose of calibration is to derive characteristics, equation constants, weighting factors, and other parameters that serve to define the model for a particular watershed. In distributed and continuous simulation, the calibration process is greatly rigorous and complex than that in model calibration for lumped model and discrete storm analysis, in that more parameters are involved in a distributed continuous model, a much greater amount of hydro-meteorological data is employed, and the fitting of the model requires a greater number of hydrological factors and more rigorous statistical procedures. To overcome these problems, calibration of WetSpa is not carried out for all model parameters, but for the most important parameters only, for instance, the channel roughness coefficient, plant coefficient, interflow scaling factor, and groundwater flow recession coefficient. Other parameters, such as hydraulic conductivity, root depth, interception and depression storage capacity, and so on, are set to values interpolated from the literature representing average conditions, and not calibrated but fixed to the selected values.

Once the preparation of input data and model parameters are accomplished, the user can start to run the model for parameter calibration and model prediction. Programs can be run within the Arcview project interface, or directly executed in the subdirectory /project/model/program. Since the running of fully distributed model costs large memory space and computing time depending upon the catchment area, grid size, the length of time series and interval, it is preferable to run the semi-distributed model firstly, adjust roughly the global and distributed model parameters, and then go to the fully distributed model, in order to save computing time for model calibration. The following is an outline of the steps for model calibration within ArcView interface.

#### 1) Calculating mean parameters for each subcatchment

From the menu 'Model' of the ArcView project or any view of the project, run the program 'Mean'. This program computes mean model parameters of each subcatchment for use in the semi-distributed modelling and adjusting global model parameters preliminarily during model calibration. This operation can also be implemented independently by clicking the program 'mean' in the subdirectory

/project/model/program. The output file 'mean.txt' is saved in the subdirectory /project/model/output.

## 2) Calculating unit hydrographs

Run program 'IUH' from the dropdown menu. This program calculates unit response function from each grid cell to the main rivers and basin outlet for use in fully distributed model, from each subcatchment to the main rivers and basin outlet for use in semi-distributed model, the unit response function for main rivers for use in both distributed and semi-distributed models, and unit response function for the entire catchment used for general parameter analysis. This operation can also be implemented independently by clicking the program 'IUH' in the subdirectory /project/model/program. The output text files 'uh\_cell\_h.txt', 'uh\_cell\_s.txt', 'uh\_sub\_h.txt', 'uh\_sub\_s.txt', 'uh\_river.txt' and 'uh\_watershed.txt' are in the same format and saved in the subdirectory /project/model/output.

## 3) Modelling with a semi-distributed approach

From the menu 'Model' of the ArcView project or any view of the project, run the program 'Model1'. Two options are available in the program: Predict outflow at catchment outlet and predict outflow both at catchment outlet and subcatchment outlets. Both options simulate flow hydrograph and water balance on a subcatchment scale, with output files q\_tot.txt and balance.txt saved in the subdirectory /project/model/output. Additionally, option two routes water firstly to the subcatchment outlet, and then to the catchment outlet using channel response functions. Therefore, the produced hydrographs at the catchment outlet may be slightly different from the result of option one due to truncation errors in computing IUH. It also gives another output file q\_sub.txt, which are the predicted discharges at selected subcatchment outlet saved in the subdirectory /project/model/output. Since both options give the same output file name q\_tot.txt and balance.txt, the modeller needs to rename the file name if it is expected to keep the previous modelling results.

## 4) Model evaluation

Run program 'Model Evaluation' from the dropdown menu. This program gives a detailed description the observed data, simulation results, as well as the assessment of the current model parameters. The output file 'evaluation.txt' is saved in the

subdirectory /project/model/output.

5) Calibration of global parameters

Based on the evaluation results and the visual comparison between observed and calculated hydrographs, readjust global parameters in the input file 'input.txt', repeat step 3 and 4, until a good match is reached. If obvious errors exist and can not be overcome by adjusting global parameters, users may return to the GIS pre-processing phase, adjust values in the lookup table and recalculate the spatial parameter grids so as to make the input parameters more reliable.

6) Modelling with a fully distributed approach

Keep the input files as in Model1, run program 'Model2' from the dropdown menu 'Model'. This program simulates hydrological processes on cell scale, and predicts hydrograph at basin outlet, water balance on catchment scale, as well as spatial distribution of surface runoff, interflow, groundwater recharge, soil moisture and actual evapotranspiration at selected time periods. Output files 'q\_tot.txt', 'q\_sub.txt', 'balance.txt' and other spatial distribution outputs are saved in the subdirectory '/project/model/output'.

- a) The output files 'q\_tot.txt', 'q\_sub.txt' and 'balance.txt' are in the same format as the outputs of Model1. If users want to keep the flow and water balance results of Model1, those files must be renamed to avoid being replaced by the outputs of Model2.
- b) The output spatial runoff distribution files are named in the order listed in the 'input.txt', for instance, 'runoff1.asc', 'runoff2.asc', etc. Other spatial outputs are given similarly, such as 'interflow1.asc', 'recharge1.asc', 'moisture1.asc', 'evaporation1.asc', and so on. All these output files are saved in the subdirectory /project/model/output.
- c) The computation time becomes much longer if too many spatial outputs are asked in the input file while running the fully distributed model. Therefore, it is suggested to generate less spatial outputs during model calibration. All expected spatial outputs can be given at the final run after model calibration, or using the program 'Water balance' as described below.
- d) Run program 'Model Evaluation' again to see the performance of the fully

distributed model. Users are allowed to readjust global and spatial distributed input parameters in order to make a better match between calculated and observed hydrographs.

7) Simulation of water balance without flow routing

This program is designed to compute water balance for each grid cell within the simulation period. Since the program does not cover the parts of flow routing, it can run more quickly and gives exactly the same water balance and spatial distribution outputs as Model2.

- a) Keep the input files as in Model1 or Model2, run program 'Water balance' from the dropdown menu 'Model'.
- b) The output file 'balance.txt' and other spatial output file are saved in the
- c) The output file 'balance.txt' and other spatial output file are saved in the subdirectory 'project/model/output'. The previous output files need to be renamed if the user wants to keep them.
- d) The spatial input parameters can be reviewed based on the analysis of these spatial outputs, and some of the input parameter maps may need to be recalculated accordingly.

8) Model verification

Model verification is being used to validate the calibrated model parameters by running the model for an independent period of record and comparing the results with observed data after calibration of the model is complete. This procedure will help to ensure that the calibration is not unique and limited to the data set employed for calibration.

#### **4.5.2 Parameter adjustment**

In WetSpa Extension, calibration runs are made with trial simulation. Model output is compared with observed stream flow both at the catchment outlet and the internal discharge monitoring stations, and evaluated by the 5 assessment criteria described in section 3.3. Based upon those comparisons and evaluations, parameter adjustments are made to improve the performance of the model. The initial choice of model parameters is not a critical concern since adjustments will be made during calibration. However, those parameters that have physical relevance should be determined to reduce the possibilities

for future adjustment during model calibration.

Model parameters that are typically encountered in a continuous simulation of WetSpa Extension are listed in Table 4.6, in which the parameters that can be determined by independent analysis are indicated. For other parameters that need to be empirically determined, the initial value might be determined based upon known values in previous simulation studies, characteristic values of similar catchment, or default values collected from the literature. A desirable part of the calibration process is to make an independent estimate of the basin's water balance. This calculation would yield the whole, annual or perhaps monthly estimates of basin precipitation, evapotranspiration, runoff, soil moisture and groundwater storage that can be helpful in calibrating the model parameters. Adjustments are made firstly to those parameters, which have the greatest impact on the model output, then proceeding to variables with lesser sensitivity. The process may be expressed as five basic steps with each having several trials.

- 1) Achieve fit of runoff volumes throughout the simulation period. This process preliminary involves adjustment of precipitation weighting factors, potential runoff coefficient, evapotranspiration factors, as well as interflow and groundwater flow production factors. Calibration fit is usually judged by comparing monthly, annual and the total runoff volumes.
- 2) Achieve fit of peak discharge and the time to peak. This step involves working with runoff distribution and routing factors, particularly for the components in controlling high flow hydrographs, such as hydraulic radius, channel roughness coefficient, etc.
- 3) Achieve fit of hydrograph shape. This step mainly involves adjustment of model parameters in controlling low flow hydrographs, such as the interflow and groundwater flow factors, as well as evapotranspiration factors during dry period.
- 4) Achieve fit of snow melting floods if snow accumulation and snowmelt occurs in the study catchment. This step involves adjustment of model parameters in controlling snowmelt processes, including base temperature, temperature degree-day coefficient, rainfall degree-day coefficient, and temperature lapse rate.
- 5) Refine hydrograph fit. This final step involves working with different initial conditions and other distributed runoff production and flow routing parameters to refine a better hydrograph shape.

### **4.5.3 Parameter sensitivity**

Parameter sensitivity comprises the determination of changes in the individual parameters, in order to get an insight into the required precision of the model parameters relative to the precision of the model output. Table 4.7 describes the order of parameter priority in more detail and gives relative sensitivity of the variables, which are used in the WetSpa Extension. ‘Relative sensitivity’ indicates the degree to which parameter affects model output. ‘Major effects’ indicates which aspect of the output is primarily affected. ‘Calibration priority’ suggests the order in which parameters are typically adjusted. And ‘Independent evaluation’ indicates those parameters that are typically determined independent of the calibration process, because they are more physically based. All parameters in WetSpa Extension represent a physical process. It is essential that parameter values remain physically reasonable throughout the calibration process to keep the fit from being a local optimization that will not work when extrapolated to new data. Therefore, a verification step is desirable to ensure that the fit is a general solution, not one unique only to the calibration data used.

**Table 4.7. Parameter sensitivity for model calibration**

| Parameter                               | Relative sensitivity | Major Effects           | Calibration priority | Independent evaluation |
|-----------------------------------------|----------------------|-------------------------|----------------------|------------------------|
| <b>Precipitation/Evapotranspiration</b> |                      |                         |                      |                        |
| Station weight                          | High                 | Runoff volume           | 1                    | √                      |
| Correction factor                       | High                 | Runoff volume           | 1                    |                        |
| Vegetation fraction                     | High                 | Runoff volume           | 2                    |                        |
| Vertical precipitation gradient         | Medium               | Runoff volume           | 2                    | √                      |
| Vertical PET gradient                   | Medium               | Runoff volume           | 2                    | √                      |
| Maximum groundwater storage             | Medium               | Low flow shape          | 2                    |                        |
| <b>Snowmelt</b>                         |                      |                         |                      |                        |
| Base temperature                        | High                 | Snowmelt                | 1                    | √                      |
| Temperature degree-day factor           | High                 | Snowmelt                | 1                    | √                      |
| Rainfall degree-day factor              | High                 | Snowmelt                | 2                    | √                      |
| Temperature lapse rate                  | High                 | Snowmelt                | 2                    | √                      |
| <b>Runoff distribution</b>              |                      |                         |                      |                        |
| Potential runoff coefficient            | High                 | Volume, high flow shape | 1                    |                        |
| Surface runoff exponent                 | High                 | Volume, peak discharge  | 1                    |                        |
| Threshold rainfall intensity            | High                 | Volume, peak discharge  | 1                    |                        |
| Impervious fraction                     | High                 | Volume, high flow shape | 1                    | √                      |
| Interception capacity                   | Medium               | Runoff volume           | 2                    | √                      |
| Depression capacity                     | Medium               | Runoff volume           | 2                    | √                      |
| <b>Flow routing</b>                     |                      |                         |                      |                        |
| Surface roughness coefficient           | Medium               | High flow shape         | 2                    | √                      |
| Channel roughness coefficient           | High                 | High flow shape         | 2                    | √                      |
| Hydraulic radius                        | High                 | High flow shape         | 2                    |                        |
| Threshold of minimum slope              | Medium               | High flow shape         | 3                    |                        |
| Threshold of stream network             | Medium               | High flow shape         | 3                    |                        |
| Interflow scaling factor                | High                 | Volume, flow shape      | 1                    |                        |
| Baseflow recession coefficient          | High                 | Low flow shape          | 1                    |                        |
| Number of subcatchments                 | Medium               | Low flow shape          | 3                    |                        |
| <b>Soil properties</b>                  |                      |                         |                      |                        |
| Hydraulic conductivity                  | Medium               | Runoff volume           | 3                    | √                      |
| Porosity                                | Low                  | Runoff volume           | 3                    | √                      |
| Field capacity                          | Low                  | Runoff volume           | 3                    | √                      |
| Wilting point                           | Low                  | Runoff volume           | 3                    | √                      |
| Residual moisture content               | Low                  | Runoff volume           | 3                    | √                      |
| Pore size distribution index            | Low                  | Runoff volume           | 3                    | √                      |
| Root depth                              | Medium               | Runoff volume           | 3                    | √                      |
| <b>Initial conditions</b>               |                      |                         |                      |                        |
| Soil moisture                           | Low                  | Flow shape              | 3                    | √                      |
| Groundwater storage                     | Low                  | Flow shape              | 3                    | √                      |
| Interception storage                    | Low                  | Flow shape              | 3                    | √                      |
| Depression storage                      | Low                  | Flow shape              | 3                    | √                      |
| Initial baseflow                        | Low                  | Flow shape              | 3                    | √                      |

## 4.6 MODEL OUTPUT

### 4.6.1 Intermediate output

WetSpa Extension produces the mean parameters for each subcatchment and the unit response functions for each grid cell, subcatchment and the main river channels separately, in order to avoid repeatable computations during model calibration. These intermediate outputs are further used as inputs in the distributed and semi-distributed models. Since WetSpa Extension simulates hydrological processes continuously, it uses and creates an immense amount of data, particularly if a long period of record is involved. Judging the fit of the final stream flow output along is difficult for model calibration. Reviewing these intermediate outputs therefore provides a possibility for efficiently parameter adjustments.

#### 1) Mean parameters of each subcatchment

Taking the Bissen subcatchment in the Alzette river basin, the Grand-duchy of Luxembourg, as a testing area, a sample intermediate output file mean.txt is shown in Table 4.8.

**Table 4.8.** Sample output file of mean.txt

| No | C    | S    | Kc   | PS   | FC   | PI   | WP   | RM   | IX   | IN   | DP   | RD | TP | TE | TT | IMP  | A    |
|----|------|------|------|------|------|------|------|------|------|------|------|----|----|----|----|------|------|
| 1  | 0.41 | 9.42 | 10.9 | 0.49 | 0.29 | 11.1 | 0.12 | 0.05 | 1.14 | 0.48 | 1.85 | 1  | 3  | 3  | 3  | 0    | 11.3 |
| 2  | 0.40 | 11.9 | 11.9 | 0.48 | 0.28 | 11.0 | 0.12 | 0.05 | 1.18 | 0.48 | 1.71 | 1  | 4  | 3  | 3  | 0.01 | 25.6 |
| 3  | 0.37 | 13.3 | 12.1 | 0.47 | 0.25 | 11.0 | 0.11 | 0.07 | 1.25 | 0.49 | 1.87 | 1  | 4  | 3  | 3  | 0.02 | 20.9 |
| 4  | 0.45 | 9.64 | 17.6 | 0.49 | 0.29 | 10.4 | 0.12 | 0.04 | 0.99 | 0.46 | 1.56 | 1  | 3  | 3  | 3  | 0    | 8.28 |
| 5  | 0.36 | 8.16 | 25.7 | 0.48 | 0.26 | 9.7  | 0.11 | 0.05 | 1.12 | 0.48 | 2.31 | 1  | 2  | 2  | 2  | 0    | 14.3 |
| 6  | 0.40 | 12.6 | 9.2  | 0.48 | 0.29 | 11.2 | 0.12 | 0.05 | 1.21 | 0.48 | 1.72 | 1  | 4  | 3  | 3  | 0.01 | 24.4 |
| 7  | 0.33 | 7.88 | 21.4 | 0.47 | 0.26 | 9.8  | 0.12 | 0.07 | 1.26 | 0.48 | 2.8  | 1  | 1  | 1  | 1  | 0    | 5.31 |
| 8  | 0.44 | 8.98 | 8.6  | 0.49 | 0.31 | 11.3 | 0.13 | 0.04 | 1.06 | 0.48 | 1.58 | 1  | 4  | 3  | 3  | 0    | 13   |
| 9  | 0.40 | 7.85 | 26.2 | 0.48 | 0.26 | 9.7  | 0.11 | 0.05 | 1.05 | 0.46 | 2.33 | 1  | 2  | 2  | 2  | 0    | 2.03 |
| 10 | 0.42 | 8.15 | 13.4 | 0.49 | 0.3  | 10.8 | 0.12 | 0.04 | 1.04 | 0.47 | 1.83 | 1  | 4  | 3  | 3  | 0    | 6.95 |
| 11 | 0.38 | 6.39 | 24.0 | 0.48 | 0.26 | 9.9  | 0.11 | 0.05 | 1.03 | 0.47 | 2.19 | 1  | 3  | 2  | 2  | 0    | 9.39 |
| 12 | 0.40 | 5.88 | 18.5 | 0.48 | 0.28 | 10.2 | 0.12 | 0.05 | 1.00 | 0.47 | 2.14 | 1  | 2  | 2  | 2  | 0    | 6.69 |
| 13 | 0.45 | 9.20 | 12.3 | 0.44 | 0.26 | 10.0 | 0.15 | 0.14 | 1.05 | 0.47 | 1.69 | 1  | 2  | 2  | 2  | 0.01 | 14.5 |

Where No is the number of the subcatchment, C is the potential runoff coefficient (-), S is the mean subcatchment slope (%), Kc is the mean hydraulic conductivity (mm/h), PS is the mean soil porosity (m<sup>3</sup>/m<sup>3</sup>), FC is the mean field capacity (m<sup>3</sup>/m<sup>3</sup>), PI is the mean pore size distribution index (-), WP is the mean wilting point (m<sup>3</sup>/m<sup>3</sup>), RM is the mean residual soil moisture (m<sup>3</sup>/m<sup>3</sup>), IX is the maximum interception capacity (mm), IN is the minimum interception capacity (mm), DP is the mean depression storage capacity (mm), RD is the mean root depth (m), TP is the Thiessen polygon number for precipitation (-), TE is the Thiessen polygon number for PET (-), TT is the Thiessen polygon number for temperature (-), IMP is the percentage of urban areas (%), and A is the subcatchment area (km<sup>2</sup>).

2) Instantaneous unit hydrographs (IUH)

The files of instantaneous unit hydrograph (IUH) or the unit impulse response function include uh\_cell\_h.txt for routing water from cell to the basin outlet, uh\_cell\_s.txt for routing water from cell to the main river, uh\_sub\_h.txt for routing water from subcatchment to the basin outlet, uh\_sub\_s.txt for routing water from subcatchment to its outlet, uh\_river.txt for routing water from subcatchment outlet to basin outlet, and uh\_watershed.txt which is the IUH for the entire catchment.

**Table 4.9.** Parts of output file uh\_cell\_h.txt

|   |    |       |       |       |       |       |       |       |       |       |       |       |       |       |
|---|----|-------|-------|-------|-------|-------|-------|-------|-------|-------|-------|-------|-------|-------|
| 1 | 21 | 0.027 | 0.147 | 0.180 | 0.158 | 0.125 | 0.094 | 0.070 | 0.052 | 0.038 | 0.028 | 0.021 | 0.016 | ..... |
| 1 | 22 | 0.018 | 0.112 | 0.155 | 0.150 | 0.128 | 0.103 | 0.080 | 0.062 | 0.047 | 0.036 | 0.027 | 0.021 | ..... |
| 3 | 35 | 0.007 | 0.022 | 0.040 | 0.057 | 0.069 | 0.077 | 0.080 | 0.078 | 0.074 | 0.069 | 0.062 | 0.055 | ..... |
| 1 | 20 | 0.109 | 0.214 | 0.184 | 0.137 | 0.098 | 0.070 | 0.050 | 0.036 | 0.027 | 0.020 | 0.014 | 0.011 | ..... |
| 1 | 13 | 0.478 | 0.218 | 0.116 | 0.068 | 0.042 | 0.027 | 0.018 | 0.012 | 0.008 | 0.006 | 0.004 | 0.002 | ..... |
| 3 | 36 | 0.005 | 0.018 | 0.035 | 0.052 | 0.065 | 0.074 | 0.077 | 0.077 | 0.074 | 0.069 | 0.063 | 0.057 | ..... |
| 0 | 6  | 0.882 | 0.075 | 0.022 | 0.010 | 0.005 | 0.003 | 0.002 |       |       |       |       |       |       |
| 1 | 26 | 0.001 | 0.043 | 0.100 | 0.126 | 0.126 | 0.113 | 0.097 | 0.080 | 0.065 | 0.052 | 0.042 | 0.033 | ..... |
| 0 | 10 | 0.004 | 0.596 | 0.192 | 0.089 | 0.048 | 0.029 | 0.018 | 0.012 | 0.008 | 0.004 | 0.001 |       |       |
| 1 | 20 | 0.133 | 0.220 | 0.179 | 0.130 | 0.092 | 0.066 | 0.047 | 0.034 | 0.025 | 0.019 | 0.014 | 0.010 | ..... |
| 1 | 17 | 0.321 | 0.236 | 0.147 | 0.093 | 0.061 | 0.041 | 0.029 | 0.020 | 0.014 | 0.011 | 0.008 | 0.006 | ..... |
| 1 | 12 | 0.520 | 0.210 | 0.105 | 0.060 | 0.036 | 0.023 | 0.016 | 0.011 | 0.007 | 0.005 | 0.004 | 0.002 |       |
| 1 | 15 | 0.389 | 0.228 | 0.135 | 0.083 | 0.053 | 0.035 | 0.024 | 0.017 | 0.012 | 0.008 | 0.006 | 0.004 | ..... |

All IUH files are in the same format. The total rows in the file `uh_cell_h.txt` and `uh_cell_s.txt` are the count of effective cells over the catchment. The total rows in `uh_sub_h.txt`, `uh_sub_s.txt` and `uh_river.txt` are equal to the number of subcatchments. And there is only one row in the file `uh_watershed.txt`. An example of the file `uh_cell_h.txt` is shown in Table 4.9, where the first column is the start non-zero time step of the IUH, the second column is the end non-zero time step of the IUH, and the values from the third column till the end are IUH non-zero values at each time step.

#### 4.6.2 Final output

WetSpa Extension produces a variety of output files, depending on the selected options during the simulation run. The basic output files are the time series including predicted hydrographs at the catchment outlet or the selected subcatchment outlets, and water balance for the entire catchment over the simulation period. Other output files contain information about the spatial distributions of simulated hydrological processes at a predetermined time period. The program writes output into ASCII files, for which the file names are fixed in the program, or identified in the input file. All output files are stored in the subdirectory `/project/model/output`.

##### 1) Discharge at the catchment outlet

A sample output file `q_tot.txt` for the Bissen catchment is shown in Table 4.10, where the first 4 columns are year, month, day and hour. If the model runs on a daily scale, the values in the Hour's column are zero.  $P$  is the hourly rainfall (mm),  $Q_s$  is the calculated surface runoff ( $\text{m}^3/\text{s}$ ),  $Q_i$  is the calculated interflow ( $\text{m}^3/\text{s}$ ),  $Q_g$  is the calculated groundwater flow ( $\text{m}^3/\text{s}$ ), and  $Q$  is the total runoff at the catchment outlet calculated by the summation of surface runoff, interflow and groundwater flow ( $\text{m}^3/\text{s}$ ). This file is the most useful output providing the simulated rainfall and runoff plot, in which the time increment for the output hydrograph is equal to the parameter  $dt$  given in the input file.

**Table 4.10.** Sample output file of q\_tot.txt

| year | month | day | Hour | P    | Qs     | Qi    | Qg    | Q      |
|------|-------|-----|------|------|--------|-------|-------|--------|
| 1998 | 10    | 23  | 16   | 1.38 | 0.274  | 0.539 | 0.947 | 1.760  |
| 1998 | 10    | 23  | 17   | 1.99 | 0.569  | 0.542 | 0.948 | 2.059  |
| 1998 | 10    | 23  | 18   | 0.95 | 1.535  | 0.544 | 0.949 | 3.029  |
| 1998 | 10    | 23  | 19   | 1.03 | 2.262  | 0.549 | 0.950 | 3.761  |
| 1998 | 10    | 23  | 20   | 0.34 | 3.033  | 0.554 | 0.951 | 4.538  |
| 1998 | 10    | 23  | 21   | 9.51 | 3.497  | 0.560 | 0.952 | 5.009  |
| 1998 | 10    | 23  | 22   | 0.26 | 9.084  | 0.567 | 0.952 | 10.603 |
| 1998 | 10    | 23  | 23   | 0.52 | 11.122 | 0.585 | 0.953 | 12.659 |
| 1998 | 10    | 24  | 0    | 0    | 12.723 | 0.606 | 0.953 | 14.282 |
| 1998 | 10    | 24  | 1    | 0.43 | 13.545 | 0.628 | 0.953 | 15.126 |
| 1998 | 10    | 24  | 2    | 0    | 13.926 | 0.652 | 0.953 | 15.532 |
| 1998 | 10    | 24  | 3    | 0    | 13.771 | 0.676 | 0.953 | 15.400 |
| 1998 | 10    | 24  | 4    | 0    | 13.331 | 0.698 | 0.954 | 14.983 |

## 2) Discharge at the selected subcatchment outlet

Table 4.11 gives an example of output file q\_sub.txt for the Bissen catchment, where the first 4 columns are year, month, day and hour, and the next 4 columns are calculated discharges at the outlet of subcatchment 1, 5, 10, and 11. This file gives simulated discharge data at a user selected location, which is useful for plotting hydrographs at an interested site, or comparing with observed hydrographs if an internal flow gauge exists at that site.

**Table 4.11.** Sample output file of q\_sub.txt

| year | month | day | Hour | 1     | 5     | 10    | 11    |
|------|-------|-----|------|-------|-------|-------|-------|
| 1998 | 10    | 23  | 16   | 0.645 | 0.809 | 0.410 | 0.516 |
| 1998 | 10    | 23  | 17   | 0.834 | 0.927 | 0.506 | 0.684 |
| 1998 | 10    | 23  | 18   | 1.245 | 1.204 | 0.713 | 0.960 |
| 1998 | 10    | 23  | 19   | 1.214 | 1.227 | 0.681 | 0.785 |
| 1998 | 10    | 23  | 20   | 1.210 | 1.247 | 0.678 | 0.769 |
| 1998 | 10    | 23  | 21   | 1.046 | 1.156 | 0.596 | 0.633 |
| 1998 | 10    | 23  | 22   | 3.808 | 2.853 | 2.027 | 2.975 |

|      |    |    |    |       |       |       |       |
|------|----|----|----|-------|-------|-------|-------|
| 1998 | 10 | 23 | 23 | 2.637 | 2.324 | 1.332 | 1.093 |
| 1998 | 10 | 24 | 0  | 1.983 | 1.937 | 1.012 | 0.772 |
| 1998 | 10 | 24 | 1  | 1.436 | 1.579 | 0.782 | 0.615 |
| 1998 | 10 | 24 | 2  | 1.188 | 1.394 | 0.681 | 0.633 |
| 1998 | 10 | 24 | 3  | 0.963 | 1.205 | 0.580 | 0.560 |
| 1998 | 10 | 24 | 4  | 0.837 | 1.091 | 0.519 | 0.538 |

### 3) Water balance for the entire catchment

Both the semi-distributed and the fully distributed model produce a water balance time series. A sample output file balance.txt for the Bissen catchment is show in Table 4.12, where T is the time step (-), P is the average hourly rainfall (mm), I is the average interception losses (mm), Sm is the average soil moisture in the root zone (mm), F is the average infiltration losses (mm), Et is the average actual evapotranspiration losses (mm), Perc is the average percolation out of root zone (mm), Rs is the average surface runoff (mm), Ri is the average interflow (mm), Rg is the average groundwater flow (mm), R is the total runoff (mm), and GT is the average active groundwater storage at this time step (mm). This file provides information on the simulated water balance for the entire catchment at each time step, which can be used for model calibration and evaluation.

**Table 4.12.** Sample output file of balance.txt

| T  | P     | I     | Sm     | F     | Et    | Perc  | Rs    | Ri    | Rg    | R     | GT     |
|----|-------|-------|--------|-------|-------|-------|-------|-------|-------|-------|--------|
| 1  | 1.384 | 0.594 | 282.46 | 0.616 | 0.048 | 0.017 | 0.121 | 0.007 | 0.012 | 0.14  | 150.17 |
| 2  | 1.986 | 0     | 283.99 | 1.546 | 0.049 | 0.018 | 0.331 | 0.007 | 0.012 | 0.349 | 150.17 |
| 3  | 0.952 | 0.049 | 284.66 | 0.703 | 0.049 | 0.019 | 0.131 | 0.007 | 0.012 | 0.15  | 150.18 |
| 4  | 1.034 | 0.049 | 285.40 | 0.766 | 0.049 | 0.02  | 0.14  | 0.008 | 0.012 | 0.16  | 150.19 |
| 5  | 0.342 | 0.049 | 285.60 | 0.228 | 0.049 | 0.02  | 0.036 | 0.008 | 0.012 | 0.056 | 150.20 |
| 6  | 9.506 | 0.049 | 292.90 | 7.324 | 0.049 | 0.02  | 2.006 | 0.008 | 0.012 | 2.026 | 150.21 |
| 7  | 0.261 | 0.049 | 293.02 | 0.163 | 0.039 | 0.028 | 0.024 | 0.011 | 0.012 | 0.047 | 150.22 |
| 8  | 0.521 | 0.039 | 293.35 | 0.371 | 0.039 | 0.028 | 0.057 | 0.011 | 0.012 | 0.08  | 150.24 |
| 9  | 0     | 0     | 293.73 | 0.42  | 0.039 | 0.028 | 0     | 0.011 | 0.012 | 0.023 | 150.25 |
| 10 | 0.431 | 0.074 | 293.97 | 0.275 | 0.029 | 0.029 | 0.051 | 0.011 | 0.012 | 0.074 | 150.27 |
| 11 | 0     | 0     | 294.05 | 0.12  | 0.029 | 0.029 | 0     | 0.012 | 0.012 | 0.023 | 150.29 |
| 12 | 0     | 0     | 294.03 | 0.028 | 0.029 | 0.029 | 0     | 0.012 | 0.012 | 0.024 | 150.31 |
| 13 | 0     | 0     | 294.00 | 0.006 | 0.029 | 0.029 | 0     | 0.012 | 0.012 | 0.024 | 150.32 |

#### 4) Spatial output

Table 4.13 shows a part of the output file runoff.asc, which is the spatial distribution of surface runoff over the catchment for the time interval 14-15, Oct. 18, 1998, where ncols is the number of columns, nrows is the number of rows, xllcorner is corner coordinate in x direction (m), yllcorner is corner coordinate in y direction (m), cellsize is the cell size (m), and nodata\_value is the no data value.

**Table 4.13.** Parts of output file runoff.asc

|              |        |        |        |        |        |        |        |        |        |       |       |       |
|--------------|--------|--------|--------|--------|--------|--------|--------|--------|--------|-------|-------|-------|
| ncols        | 539    |        |        |        |        |        |        |        |        |       |       |       |
| nrows        | 356    |        |        |        |        |        |        |        |        |       |       |       |
| xllcorner    | 45240  |        |        |        |        |        |        |        |        |       |       |       |
| yllcorner    | 84580  |        |        |        |        |        |        |        |        |       |       |       |
| cellsize     | 50     |        |        |        |        |        |        |        |        |       |       |       |
| nodata_value | -1.000 |        |        |        |        |        |        |        |        |       |       |       |
|              | -1.000 | -1.000 | -1.000 | -1.000 | -1.000 | -1.000 | -1.000 | -1.000 | 1.006  | 2.863 | 2.863 | ..... |
|              | -1.000 | -1.000 | -1.000 | -1.000 | -1.000 | -1.000 | -1.000 | -1.000 | -1.000 | 2.463 | 2.463 | ..... |
|              | -1.000 | -1.000 | -1.000 | -1.000 | -1.000 | -1.000 | -1.000 | -1.000 | -1.000 | 2.463 | 2.463 | ..... |
|              | -1.000 | -1.000 | -1.000 | -1.000 | -1.000 | -1.000 | -1.000 | -1.000 | 2.152  | 2.463 | 2.863 | ..... |
|              | -1.000 | -1.000 | -1.000 | -1.000 | -1.000 | -1.000 | -1.000 | 2.152  | 2.463  | 2.863 | 2.863 | ..... |
|              | -1.000 | -1.000 | -1.000 | -1.000 | -1.000 | -1.000 | 2.463  | 2.463  | 2.863  | 2.863 | 2.863 | ..... |
|              | -1.000 | -1.000 | -1.000 | -1.000 | -1.000 | 2.463  | 0.994  | 1.342  | 1.342  | 2.261 | 2.261 | ..... |
|              | -1.000 | -1.000 | -1.000 | -1.000 | 2.463  | 4.364  | 1.342  | 1.342  | 2.261  | 2.261 | 2.261 | ..... |

This file contains information on simulated surface runoff on each grid cell, and can be imported to ArcView for further analysis. Other spatial distribution files, e.g. interflow, groundwater recharge, soil moisture, and actual evapotranspiration, are in the same format as for the surface runoff. The output file names are defined in the program in an ascending order, e.g. runoff1.asc, runoff2.asc, etc.

#### 5) Evaluation results

Table 4.14 gives a sample evaluation output evaluation.txt for the Bissen catchment after running the fully distributed model for an hourly time series in the year 1997. In this table P, Em and Qm are observed precipitation (mm), PET (mm) and discharge (mm) (m<sup>3</sup>/s) respectively, while the period of missing discharge data is not taken into account. I is the interception losses (mm), DS is the soil moisture difference between the start and the end time step (mm), F is the infiltration losses (mm), Et is the actual evapotranspiration (mm), Perc is the percolation out of root zone (mm), Rs is the surface runoff (mm), Ri is the interflow (mm), Rg is the groundwater flow (mm), R is the total runoff (mm), and DG is

difference in groundwater storage between the start and the end time step (mm). CR1 is model bias. CR2 is model determination coefficient. CR3, CR4 and CR5 are Nash-Sutcliffe model efficiencies as described in section 3.3.

The evaluation results also contain the information on the catchment area, the period of model simulation, as well as the periods of missing discharge data if they exist. Specifically, the change in soil moisture and groundwater storage over the simulation period is given in the evaluation output file, in order to make water balance compatible with other items, but its mean and maximum values are estimated state variables.

**Table 4.14.** Model evaluation result evaluation .txt

```

=====
Watershed: Margecany at Hornad River Basin, Slovakia                      Area= 1130.960 (km^2)
=====
      K1      Kg      Kss      Kep      g0      gmax      T0      ksnow      krain      krun      Pmax
-----
      1.984    0.01381    1.0125    1.1597     24.8     381.3     0.18     1.802     0.0005     2.4229     268.7
=====
Period(s) of missing discharge data

Total time steps: 3653 =====> No missing Data!
Period of simulation is from 1/ 1/1991 : 0 to 31/12/2000 : 0

=====
Measured precipitation, evaporation and discharge
      P(mm)      Em(mm)      Qm(mm)      Qm(m3/s)
Sum      6620.7      5090.3      1989.9      26046.9
% of P
Mean      1.812      1.393      0.545      7.13
Max      53.625     7.000      9.458      123.80
=====
Calculated water balance during the simulation period
      P(mm)      I(mm)      SD(mm)      F(mm)      E(mm)      PERC(mm)      SR(mm)      IR(mm)      GR(mm)      R(mm)      GD(mm)
Sum      6621.2      901.2      7.1      5212.1      4531.5      1699.3      216.1      182.6      1584.4      1983.1      -3.9
% of P
Mean      1.813      0.247      198.848    1.427      1.240      0.465      0.059      0.050      0.434      0.543      33.098
Max      53.63      2.19      254.11     48.01     5.69      14.33     5.25     3.56     1.47     6.71     106.05
=====
<P: total precipitation; I: total interception; SD: soil moisture difference; F: total infiltration
E: total evapotranspiration; Perc: total percolation; SR: total surface runoff; IR: total interflow
GR: total groundwater flow; R: total runoff; GD: groundwater storage difference>

G) Model evaluation (excluding the period of missing discharge)

Mean of the observed stream flow-----> MQo:      7.1303
Mean of the simulated stream flow-----> MQs:      7.0955
Standard deviation of observed data-----> SDo:      7.4074
Standard deviation of simulated data-----> SDs:      6.5391
Mean Absolute Error-----> MAE:      2.4637      < % Relative MAE:      34.55 >
Variance-----> VAR:      15.2530
Forecast Efficiency-----> FE:      -0.0001
Mean Squared Error (Error Variance)-----> MSE:      15.2542

Root Mean Squared Error<if unit is m3/s-->RMSE:      3.9057      < % RMSE:      54.78 >
Root Mean Squared Error<if unit is mm/h-->RMSE:      0.0124
Correlation Co-efficient-----> r:      0.8503
Modified Correlation Co-efficient-----> Rmod:      0.7507
Model bias-----> Bias:      -0.0348      < % Bias:      -0.488 >
Model Determination Coefficient-----> MDC:      0.7793
Nash-Sutcliffe model efficiency-----> NS:      0.7220
Modified Nash-Sutcliffe for low flows-----> NSL:      0.5815
Modified Nash-Sutcliffe for high flows-----> NSH:      0.8175
Model Volumetric Efficiency-----> MVE:      0.6545

*** Model performance results in brief:

      Bias(<%)      RMSE(<%)      NS(<%)      NSL(<%)      NSH(<%)      Rmod(<%)      Runoff_m(<%)      Runoff_c(<%)
-----
      -0.49      54.78      72.20      58.15      81.75      75.07      30.06      29.95

```

### **4.6.3 Post processing of model outputs**

In the current WetSpa Extension, no special effort has been paid in developing programs for the post processing of model output. However, the visual comparison between calculated and observed hydrographs can be carried out using Excel or other available software by loading the data from their text files. Moreover, the simulated hydrological processes for the entire catchment, such as precipitation, runoff, evapotranspiration, soil moisture, etc., can be viewed by plotting the data from the water balance output file. These graphs are helpful in adjusting model parameters more accurately and improving the model to have a better performance. Finally, the spatial output data including surface runoff, interflow, groundwater recharge, etc., can be imported to the ArcView project. Using the GIS tools, e.g. reclass, zoom, etc., a clear view can be obtained at the points of special interest. This information is not only a plot of spatial distribution of hydrological processes, but also a valuable feedback in refining model parameters.

## **5. CASE STUDY: BISSEN CATCHMENT, LUXEMBOURG**

### **5.1 Description of the study area**

The Bissen catchment is located in the Attert River basin covering an area of 294 km<sup>2</sup> in the Grand-duchy of Luxembourg (Figure 5.1). The Attert River is a main tributary of the Alzette River, where high-magnitude floods occurred frequently and have caused important damages since the early 1990's. The study catchment is homogeneous from a lithological point of view with essentially marls (El Idrissi et al., 2000). Using hourly rainfall-runoff series, the main goals are to apply the WetSpa Extension in predicting of flood hydrographs at basin outlet, estimating the spatial distribution and variability of the hydrological processes, and testing the sensitivity of model parameters with respect to catchment characteristics.

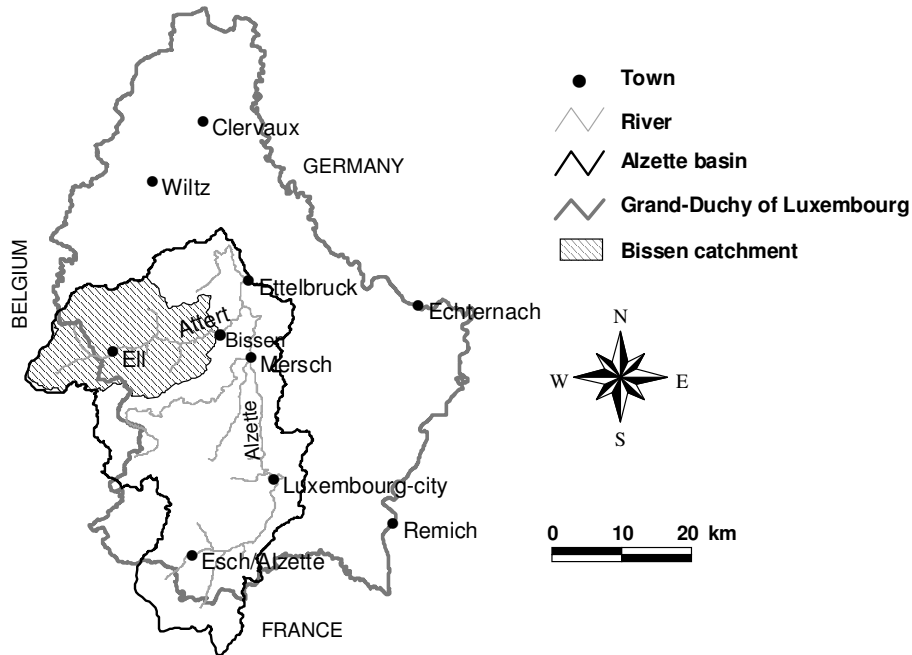


**Figure 5.1.** Location of the Bissen catchment

The climate of the region has a northern humid oceanic regime without extremes. Rainfall is the main source of runoff. The average annual precipitation varies between 800 mm to 1000 mm, which is characterized by distinctive winter and summer seasons. December is the wettest month of the year with average monthly precipitation of 84mm and April is the driest month of the year with average precipitation of 58 mm. The monthly PET values in the basin vary from 13.5 mm in winter to 81.8 mm in mid summer. High runoff occurs in winter and low runoff in summer due to the higher evapotranspiration. Winter storms are strongly influenced by the westerly atmospheric fluxes that bring humid air masses from the Atlantic Ocean (Pfister et al., 2000), and floods happen frequently because of saturated soils and low evapotranspiration. Statistical analysis of the observed data from the Luxembourg airport from 1947-1999 shows a uni-modal distribution of temperature with January being the coldest month of the year with an average temperature of 0.7°C and July is the warmest month of the year with average temperature of 17°C.

The study area has a hilly topography, with elevation ranging from 220.6 to 545.0 m and average basin slope of 8.8% (Figure 5.2). The land-use of the area, as shown in Figure 5.3, is composed of agricultural land (23.7%), grassland (36.8%), forest (34.5%), urban

areas (4.8%) and other land-use types (0.2%). Loam, silt loam, sandy clay loam and loamy sand are main soil types covering 52.0%, 16.0%, 12.5% and 11.6% respectively as shown in Figure 5.4.

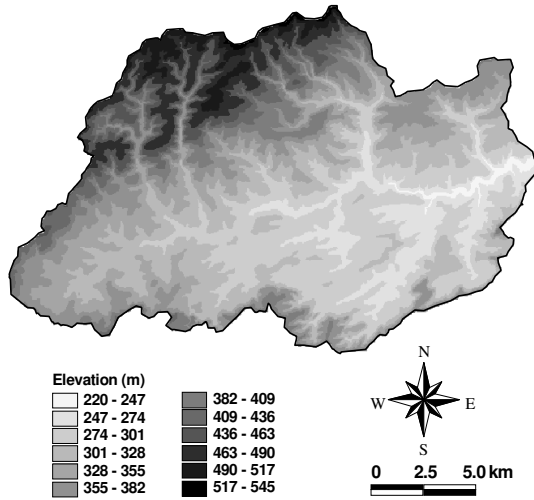


Figure 5.2. Watershed topography of Bissen

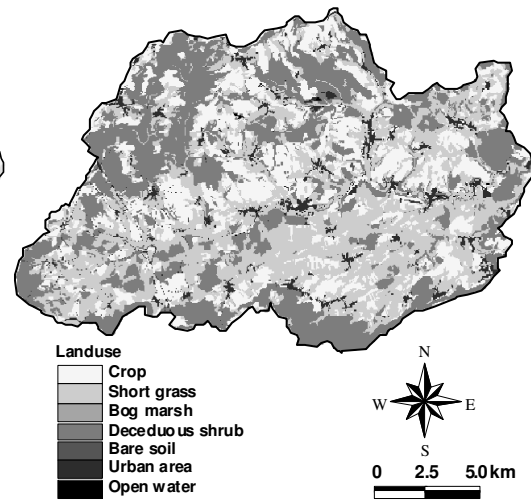


Figure 5.3. Land use map of Bissen

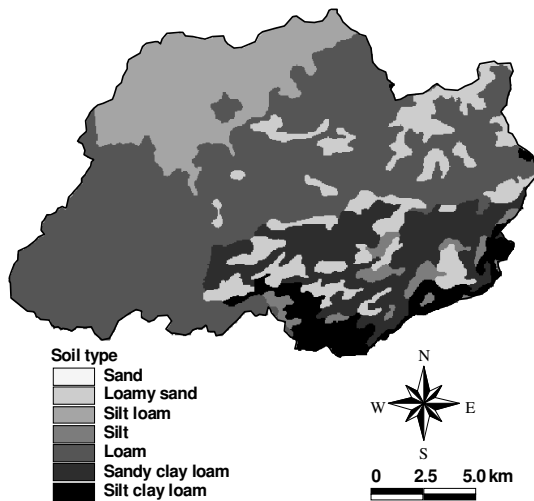


Figure 5.4. Soil type map of Bissen

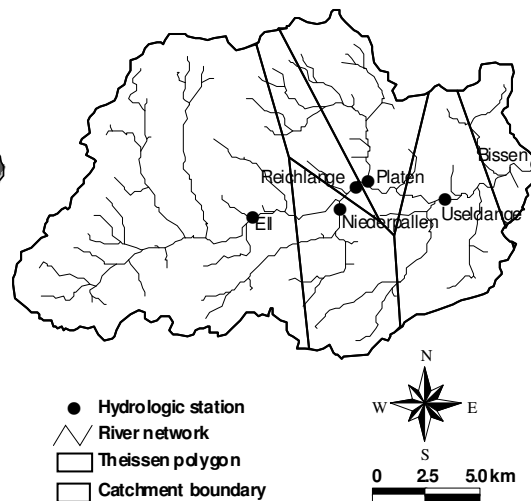


Figure 5.5. River network and Thiessen polygons of Bissen

## 5.2 Data available

### 1) Topographic data

The topographic data is obtained from the numerical elevation data sets of the public ACT (Administration du Cadastre et de la Topographie, Luxembourg). A DEM with 50x50 m grid size for the Bissen catchment is built using 2-meter resolution elevation contour map (Figure 5.1). To check the validity of the data set, flow directions are estimated from the elevation data set and the rivers were generated. Then this is overlain with the actual river network. From this comparison as shown in Figure 5.5, it is seen that the data set has sufficient accuracy to carry out model simulation.

### 2) Land use data

The land use information is taken from CORINE (Co-ordination of Information on the Environment) provided by the Luxembourgian Ministry of Environment, and the cadastral BD-L-TC (La Base de Donnée Topo/Cartographique du Luxembourg) data. Both data sets are based on remote sensing information. These vector data sets are converted firstly to 50x50 m grid according to WetSpa land use classification, as shown in Figure 5.3, and then reclassified to 6 basic land use classes (forest, grass, crop, bare soil, urban and open water) for deriving model parameters of potential runoff coefficient and depression storage capacity.

### 3) Imperviousness and soil data

For model simulation, the pervious and impervious areas in each grid are required. For a grid size of 50 m, the impervious and pervious area ratio for different land use categories was established as described in Chapter 3. Impervious fraction is set to 70% for commercial and industrial area, 30% for residential areas, 100% for water bodies and 0% for other land use categories. Information of soil types is obtained from the digital 1:100,000 Soil Map of the European Communities. The map is reclassified to 12 USDA soil texture classes based on their textural properties, and converted to 50 m grid to match with the base topographic data.

### 4) Rainfall data

6 rainfall stations are available in the Bissen catchment as shown in Figure 5.5. Among them, the Reichlange, located near the catchment centre, is a station recording rainfall at an hourly time step, while others are daily recording raingauges. To obtain an hourly

rainfall series at each raingauge used in the WetSpa Extension, the hourly rainfall measured at Reichlange is taken as a reference, and multiplied by the ratio between the daily rainfall observed at the raingauge and the reference station.

$$P_{hour,i} = \left( \frac{P_{day,i}}{P_{day,r}} \right) P_{hour,r} \quad (5.1)$$

where  $P_{hour,i}$  and  $P_{hour,r}$  are hourly rainfall at gauging site  $i$  and the reference station (mm), and  $P_{day,i}$  and  $P_{day,r}$  are daily rainfall at gauging site  $i$  and the reference station (mm). Based on the raingauge network and the catchment boundary, the Thiessen polygon map is created as shown in Figure 5.5 using ArcView Thiessen Polygon Extension. A unique hourly rainfall structure is then applied for each polygon, i.e. the rainfall series for each grid is set equal to the rainfall series of the nearest raingauge.

#### 4) Potential evapotranspiration

PET is estimated using the Penman-Monteith formula, as described in Chapter 2, with daily meteorological data measured at Luxembourg airport located about 20 km south of the catchment. The same meteorological data series (net radiation, air temperature, relative humidity, and wind speed) are then uniformly applied on the whole study area. The average daily PET series for the Bissen catchment is achieved by applying weighting factor for the daily PET series obtained for the land uses as used in Drogue (2002).

$$EP_d = \%URB. EP_{urb,d} + \%AGR. EP_{agr,d} + \%GRA. EP_{gra,d} + \%FOR. EP_{for,d} \quad (5.2)$$

where  $EP_d$  is the daily PET for the catchment,  $\%URB$ ,  $\%AGR$ ,  $\%GRA$  and  $\%FOR$  are weighting factors (area of land use type / area of catchment) for urban areas, cropland, grassland and forest as listed in Table 5.2, and  $EP_{urb,d}$ ,  $EP_{agr,d}$ ,  $EP_{gra,d}$ , and  $EP_{for,d}$  are daily PET series for each type of land use observed in the catchment. The PET from open water surface is neglected due to its very small percentage in the catchment. The values of canopy resistance, albedo and vegetation height considered in the PET calculation for the different land uses are given in Table 5.1. For cropland, distinction is made between summer and winter where the land use is defined as a bare soil. The parameter values listed in Table 5.1 are in accordance with the values used in scientific publications (Szeicz and Long, 1959; Perrier, 1982; Shuttleworth, 1989; Dickinson et al., 1993). Average values are used except for the canopy resistance, which are chosen

in the range of the common values.

The hourly PET series are finally computed from the daily data in proportion to the hourly temperature distribution (Guex, 2001).

$$EP_{h,i} = EP_d \left( \frac{T_{h,i}}{T_d} \right) \quad (5.3)$$

**Table 5.1.** Default parameter values in the PET formula for different land uses

| Land use                       | Canopy resistance | Albedo (-) | Vegetation height |
|--------------------------------|-------------------|------------|-------------------|
| Grassland                      | 100               | 0.20       | 0.12              |
| Cropland (summer)              | 70                | 0.20       | 1.00              |
| Cropland (winter, = bare soil) | 100               | 0.20       | 0.12              |
| Forest (mainly deciduous)      | 150               | 0.15       | 15.0              |
| Impervious area                | -                 | -          | -                 |

where  $EP_{h,i}$  is the hourly PET value at hour  $i$  (mm),  $T_{h,i}$  is the hourly temperature at hour  $i$  ( $^{\circ}\text{C}$ ), and  $T_d$  is the cumulative hourly temperature within a day ( $^{\circ}\text{C}$ ). In computation of hourly PET with Equation 5.3, the hourly temperature is set to zero if the actual temperature is lower than zero, and the hourly PET is considered to be zero if  $T_d$  is less than or equal to zero.

##### 5) Discharge data

6 stream gauges, namely Ell, Reichlange, Useldange, Bissen, Niederpallen and Platen, as shown in Figure 5.5, exist in the study area recording water levels at a 15-minute time step. The stream gauge Niederpallen and Platen are located at the outlet of two tributaries, while other 4 are located along the main channel with Bissen at the outlet of the catchment. Hourly discharge data are obtained through available rating curves at each gauging site. For Reichlange though, the rating curve has a low reliability, the discharge data could be used for validation purpose on peak flows. A total of 52 months of hourly rainfall, discharge and PET data from December 1996 to March 2001 are available for model calibration, except for Ell and Usldange (29 months from November 1998 to March 2001). The average hourly flow at Bissen during the monitoring period was  $4.38 \text{ m}^3/\text{s}$ , with flows ranging from  $0.86$  to  $86.3 \text{ m}^3/\text{s}$ , and the measured maximum hourly rainfall intensity was  $21.5 \text{ mm/h}$  occurred on July 7, 2000.

Table 5.2 presents the available data, geographical features, as well as the land use composition of each subcatchment. All hydrometeorological data sets used in this study come from the hydroclimatological database built-up and validated by the CRP-GL (Centre de Recherche Public - Gabriel Lippmann of Luxembourg).

**Table 5.2.** Data available and characteristics of the Bissen catchment

| Station                 | Ell      | Reichlang | Useldange | Bissen   | Niederpall | Platen   |
|-------------------------|----------|-----------|-----------|----------|------------|----------|
| River                   | Attert   | Attert    | Attert    | Attert   | Pall       | Roubbach |
| Area (km <sup>2</sup> ) | 107      | 166       | 255       | 294      | 34.6       | 47.1     |
| Perimeter (km)          | 49.9     | 64.4      | 75.3      | 82.1     | 32.6       | 33.0     |
| Average basin slope     | 9.4      | 9.2       | 8.9       | 8.8      | 6.1        | 11.1     |
| Raingauge type          | Daily    | Hourly    | Daily     | Daily    | Daily      | Daily    |
| Start of data series    | 22/10/98 | 01/12/96  | 02/10/98  | 01/12/96 | 01/12/96   | 01/12/96 |
| End of data series      | 01/04/01 | 01/04/01  | 01/04/01  | 01/04/01 | 01/04/01   | 01/04/01 |
| Max. gauged flow        | 25.0     | 13.4      | 51.7      | 86.3     | 22.6       | 11.2     |
| Urban (%)               | 3.5      | 4.0       | 4.1       | 4.8      | 3.9        | 4.8      |
| Crop (%)                | 20.9     | 23.3      | 24.7      | 23.7     | 19.1       | 32.4     |
| Grass (%)               | 33.7     | 37.6      | 37.2      | 36.8     | 51.6       | 25.8     |
| Forest (%)              | 41.8     | 34.9      | 33.9      | 34.5     | 25.0       | 36.7     |
| Water surface (%)       | 0.0      | 0.1       | 0.1       | 0.1      | 0.2        | 0.2      |
| Rest (%)                | 0.0      | 0.0       | 0.0       | 0.1      | 0.0        | 0.0      |

### 5.3 Basin delineation and parameter determination

With the terrain data processing and data acquisition complete, ArcView GIS can be used to estimate the spatial model parameters necessary for WetSpa Extension. The pre-processing starts with a creation of a depression-less DEM ensuring that positive drainage will occur. Next, flow direction and flow accumulation grids are calculated based on the flow path of steepest decent. The stream network is extracted from the master DEM using a threshold cells value of 100, which ensures that a channel is detected when the drainage area is greater than 0.25 km<sup>2</sup>. A grid of stream order used for assigning channel Manning's n is then derived from the stream network grid by the Shreve method. A slope grid is derived from the DEM and the delineated stream network, calculating slopes from each cell to its neighbours as percent rise for both land surface and stream channels. A threshold of minimum slope 0.01% is selected in order to deal with the problem of zero slopes in specific areas. The grid of hydraulic radius (Figure 5.6) is calculated using the

power law relationship described in section 2.10.1 with a network constant  $a = 0.07$  and a geometry scaling exponent  $b = 0.47$ , corresponding a flood frequency of 2-year return period. Finally, a map of subcatchment is extracted from the master DEM with a cells threshold value of 1000. 61 subcatchments are distinguished corresponding to an average subcatchment area of  $4.73 \text{ km}^2$  with minimum subcatchment area of  $0.043 \text{ km}^2$  and maximum subcatchment area of  $14.5 \text{ km}^2$ . The resulting minimum subcatchment area is much smaller than the threshold value  $0.75 \text{ km}^2$  due to the remainder of the extraction. These subcatchments serve as working units in the semi-distributed model, and are also used for simulating groundwater balance in the full-distributed model.

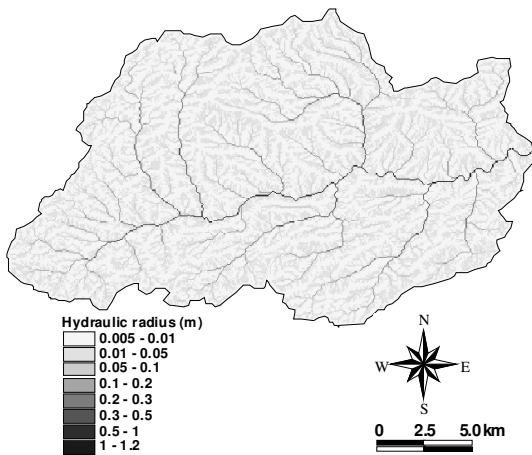


**Figure 5.6.** Hydraulic radius of Bissen

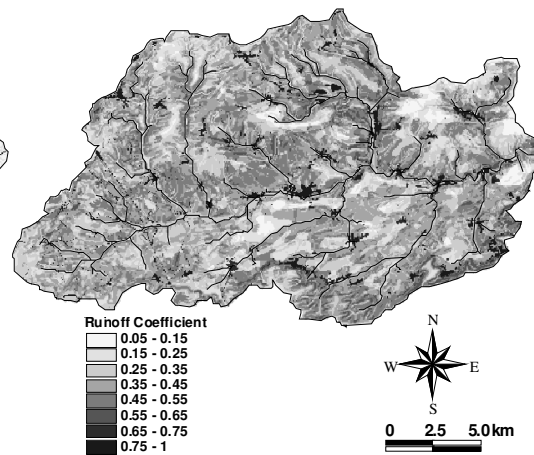


**Figure 5.7.** Runoff coefficient of Bissen

The physical parameters created by ArcView based on the soil type map include the saturated hydraulic conductivity, soil porosity, field capacity, plant wilting point, residual moisture content, and the soil pore size distribution index. The land use based parameters used in the model include root depth, interception capacity, and the Manning's coefficient. The Manning's coefficients for river channels are interpolated based on the GIS derived stream orders, with  $0.03 \text{ m}^{-1/3}\text{s}$  for the highest order and  $0.05 \text{ m}^{-1/3}\text{s}$  for the lowest order. The parameter maps of potential runoff coefficient (Figure 5.7) and depression storage capacity are created based on the combination of the three base maps. The impervious percentage for urban cells is set to be 70%, while the rest are assumed being covered by grass. The flow routing parameters include flow velocity, average travel time and its

standard deviation from cells to the catchment outlet and to the subcatchment outlet. Figure 5.8 and 5.9 shows the calculated mean travel time and its standard deviation from cells to the basin outlet for the Bissen catchment.

Finally, the Thiessen polygons for precipitation and PET (Figure 5.5) are created using the Thiessen polygon extension. Due to the fact that snow accumulation has a very minor effect on the runoff process in this catchment, the snowmelt flow is not accounted during the flow simulation. Therefore the preparation of temperature Thiessen polygon and temperature data series is not necessary in this case study. At this moment, all spatial parameters used in the model simulation are developed. A visual inspection is performed to ensure that the general characteristic of the parameter maps, such as the range, extreme values, etc., are logical and in the right order.

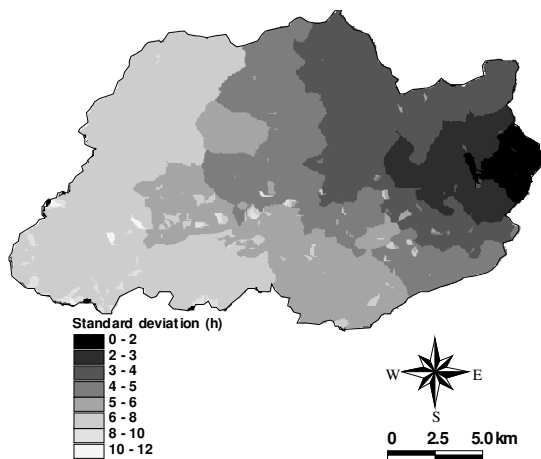


**Figure 5.8.** Mean travel time to the basin Outlet of Bissen

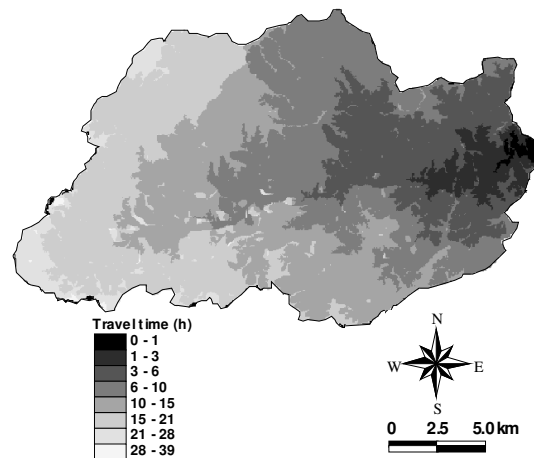


**Figure 5.9.** Standard deviation of flow time to the basin outlet of Bissen

#### 5.4 Model calibration and validation

Model calibration for the study catchment was performed for the time period of Dec. 1996 to Dec. 1999, while the period of Jan. 2000 to Apr. 2001 was used for model validation. Both the visual and statistical comparisons for the observed and simulated flow hydrographs at Bissen station were performed for the calibration and validation periods. Comparisons at other three gauging stations inside the catchment were also implemented as a kind of model validation. The comparisons of simulated and observed values included runoff volumes, hourly time series of flow, and the time to the peak for each individual

flood. In addition to the above comparisons, the water balance components (measured and simulated) were reviewed. This effort involved displaying model results for the whole simulation period for the water balance components of precipitation, infiltration, total runoff, overland flow, interflow, baseflow, PET, actual Evapotranspiration, interception, groundwater recharge, as well as the differences in soil moisture and groundwater storage between the start and end hour. Although observed values were not available for each of the water balance components listed above, the average annual values and its spatial distribution were checked for consistency with expected values for the region to ensure that overall water balance reflected local conditions, as impacted by the catchment hydrological and geographical characteristics. Calibration of the WetSpa Extension was a cyclical process of making parameter changes, running the model, producing the comparisons of simulated and observed values, and interpreting the results.

The calibration process was performed mainly for the global parameters including interflow scaling factor, baseflow recession coefficient, evapotranspiration coefficient, initial soil moisture and groundwater storage, as well as the surface runoff exponent as listed in the input file. Other spatially distributed model parameters were assumed to be reasonable and remained the values as they are. Calibration of the evapotranspiration coefficient could be performed independently by comparing the calculated and observed flow volume for a long time series. The interflow scaling factor was calibrated by matching the computed discharge with the observed discharge for the recession part of the flood hydrograph. Groundwater flow recession coefficient could be obtained by the analysis of recession curves at discharge gauging stations. Refinement of this baseflow recession coefficient was necessary to get a better fit for the low flows. The initial soil moisture and initial groundwater storage were adjusted based on the comparison between the calculated and observed hydrographs for the initial period. And the runoff exponent and the rainfall intensity threshold were adjusted based on the agreement between calculated and observed flows for the small storms with lower rainfall intensity. Since these global model parameters are physically based, the interval of their variation can be predetermined based on the specific characteristics of the study catchment. For instance, the interflow scaling factor is generally within the range of 1 to 10, and the evapotranspiration coefficient should be close to 1. After the adjustment of the input global model parameters and running the

model, the post-processing capabilities of WetSpa Extension (listings, plots, statistics, etc.) were used extensively to evaluate the calibration/verification effort. Figure 5.10 shows a typical calibration result for a flood series occurred in December 1997, corresponding to input global model parameters of  $C_i = 7.5$ ,  $C_g = 9.0 \text{ m}^2/\text{s}$ ,  $K_{ss} = 1.03$ ,  $K_{ep} = 1.02$ ,  $G_0 = 280 \text{ mm}$ ,  $G_{max} = 300 \text{ mm}$ ,  $K_{rain} = 2.0$  and  $P_{max} = 5.0 \text{ mm/h}$ , where the meanings of above denotations can be found in section 3.2.

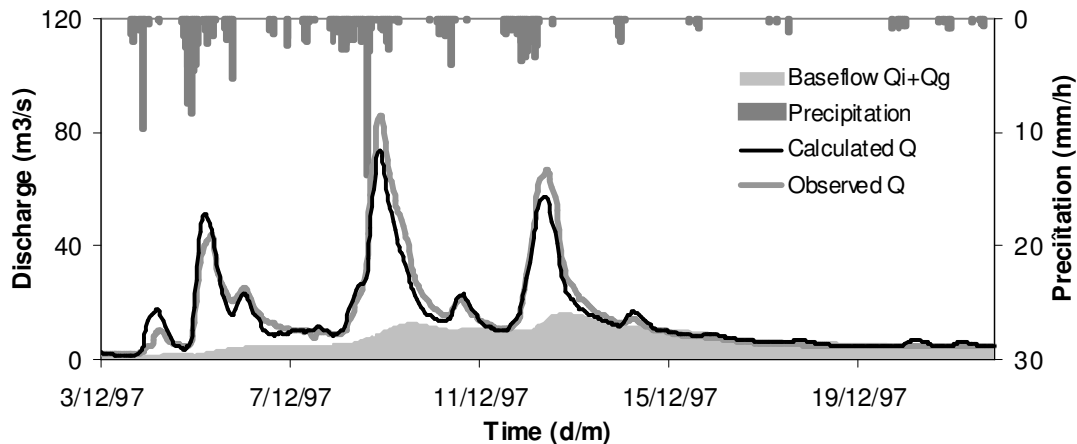


**Figure 5.10.** Observed and calculated flow at Bissen for the floods in Dec. 1999

It can be found from Figure 5.10 that the calculated hydrograph is generally in a good agreement compared with the observed hydrograph. A big storm occurred on the fourth of December, 1997, but did not produce too much runoff due to the lower antecedent soil moisture. Most of the rainfall were therefore infiltrated and used to saturate the soil. Thereafter, another three big storms occurred successively on December 5, 8 and 12, which yielded pick discharges of 44.0, 86.3 and 66.8  $\text{m}^3/\text{s}$  respectively. The calculated pick discharges are 51.1, 73.1 and 58.1  $\text{m}^3/\text{s}$  corresponding to relative errors of 16.1%, -15.3% and -13.0% respectively. The simulated baseflow contribution was not remarkable for the first two floods, but abundant for the third and fourth flood. This can be explained that the soil moisture and the effective groundwater storage were low at beginning, and not sufficient to generate abundant interflow and groundwater flow for the first two floods. Due to the occurrence of following storms, soils were getting saturated and the surplus soil water percolated to the groundwater storage, leading to a higher baseflow for the third and

fourth floods and also the following flow period.

Table 5.3 presents the statistics of observed rainfall, runoff, the flow coefficient (ratio of the outflow water volume at the measuring station to the volume of water precipitated over the drainage area) and the mean flow discharge during the statistical period, as well as the model performance for the calibration/validation period at station Ell, Useldange and Bissen on hourly scale. The model performance is found to be satisfactory as illustrated in the table. Model bias for the simulation period is within the range of -0.025 to 0.035. Model determination coefficient is within the range of 0.765 to 0.815. The flow efficiency coefficient is within the range of 0.614 to 0.798, while the efficiency coefficient ranges from 0.653 to 0.715 for low-flow, and 0.753 to 0.824 for high-flow. These evaluation results indicate that the model has a high confidence and can give a fair representation of both low-flow and high-flow hydrographs for the study catchment.

**Table 5.3.** Statistics and model performance for the calibration/validation period

| Station   | Period            | Total rainfall (m) | Total runoff (m) | Flow coef. (%) | Mean flow (m <sup>3</sup> /s) | CR <sub>1</sub> | CR <sub>2</sub> | CR <sub>3</sub> | CR <sub>4</sub> | CR <sub>5</sub> |
|-----------|-------------------|--------------------|------------------|----------------|-------------------------------|-----------------|-----------------|-----------------|-----------------|-----------------|
| Ell       | 22/10/98-29/01/01 | 2.707              | 1.511            | 55.8           | 2.25                          | 0.035           | 0.765           | 0.772           | 0.653           | 0.786           |
| Useldange | 02/10/98-31/10/00 | 2.818              | 1.455            | 51.6           | 4.68                          | 0.012           | 0.815           | 0.798           | 0.715           | 0.824           |
|           | 12/01/96-31/12/98 | 2.779              | 1.202            | 43.3           | 3.66                          | -0.014          | 0.813           | 0.735           | 0.682           | 0.805           |
| Bissen    | 01/01/99-12/05/00 | 1.726              | 0.798            | 46.2           | 5.47                          | -0.025          | 0.762           | 0.614           | 0.667           | 0.753           |

A graphical comparison between calculated and measured hourly flows at Bissen for the validation year 1999 is presented in Figure 5.11. With the simulated initial hydrological condition at the end of the year 1998, the simulation results for the year 1999 were in fairly good agreement with the measured discharges. Similar simulation results can be obtained for other hydrological years. Figure 5.12 shows the plots of 18 observed peak discharges at Bissen against their calculated peak discharges selected from the whole simulation period for  $Q_{\text{peak}} > 30 \text{ m}^3/\text{s}$ . The correlation coefficient is 0.96, which proves that the flow peak discharges are well reproduced. The errors of the time to the peak for the 18 floods were also examined, in which 12 of them are within the interval of -3 to 3 hours, and the rest are outside this range. The maximum error is 10 hours for the flood on April 1996, as the

precipitation lasted for 3 days with lower rainfall intensity, and long peak flow duration was observed.

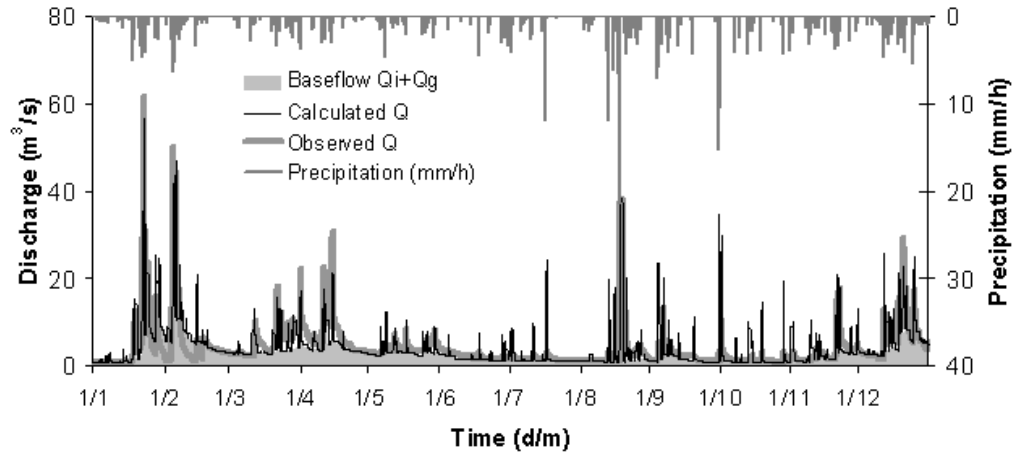


**Figure 5.11.** Observed and calculated hourly flow at Bissen for the year 1999

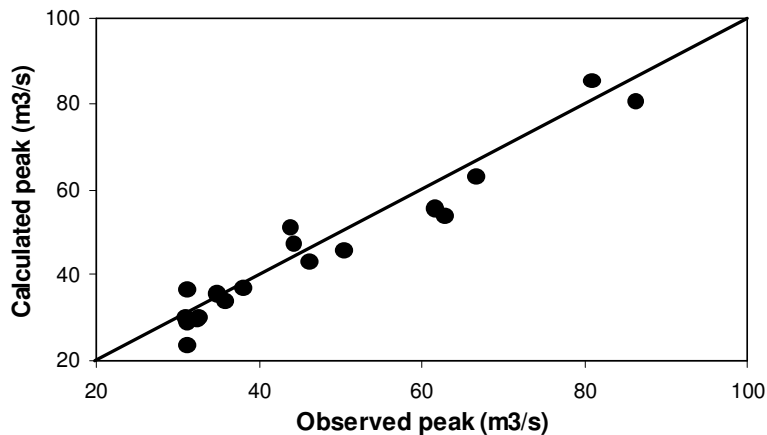


**Figure 5.12.** Peak  $Q_m$  Vs Peak  $Q_c$  selected from the whole simulation period

Figure 5.13 represents the observed and calculated hourly flow frequency curve for the whole simulation period. The flow frequency curve demonstrates consistent patterns between calibration and validation time periods, and in general showed good agreement. However, there are some obvious deviations for small floods, especially for the flow within the discharge interval of 2 to 6  $m^3/s$ , where the calculated flows are over estimated. These deviations may be attributed to the uncertainties inherent in modelling complex processes

such as flood frequency related hydraulic radius, interflow factors, etc.

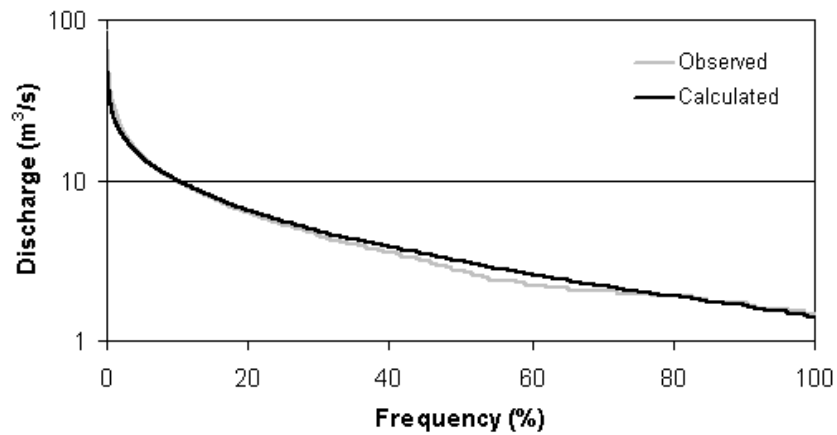


**Figure 5.13.** Observed and calculated hourly flow frequency curves at Bissen

## 5.5 Discussion

The hydrological modelling effort for the comprehensive study of the Bissen catchment is an attempt to apply hydrological modelling from GIS data sets. The modelling approach was developed efficiently and with consistent methodologies. The ability to define spatially distributed model parameters interactively based on topography, land use and soil maps using ArcView GIS allowed users to work quickly, and the ability to compare the intermediate results with existing maps increased the confidence in the validity of the model components. From the viewing and manipulation of the geographical data, to the development of the physical parameters, and to the post processing of the simulation results, it is clear that WetSpa Extension has its ability to calculate basin characteristics directly from terrain models allowed user to complete the comprehensive study in a timely manner.

Based on the hourly hydrograph comparisons at Bissen and other internal stations, it can be concluded that the modelling results have a good to very good agreement with observed hydrographs. Table 5.4 tabulates the measured and calculated water balance for each modelling component over the whole simulation period for the Bissen catchment. The estimated volume of interception, surface runoff and infiltration are 583.9, 688.2 and 3219 mm representing 13.0%, 15.3% and 71.5% of the total precipitation. It can also be calculated from the table that 31.5% of the infiltrated water is percolated out of the root

zone, 19.4% of which becomes lateral interflow, 46.3% of which is evapotranspired into the atmosphere from the root zone (total evapotranspiration – interception – transpiration from the groundwater storage). The transpiration from groundwater storage can be estimated from the percolation amount subtracted by the groundwater volume, which is 249.1 mm in total representing 10.7% of the total evapotranspiration. The rest are remained in the soil moisture and groundwater storage. The estimated surface runoff, interflow and groundwater flow are 688.2, 623.0 and 763.9 mm representing 33.2%, 30.0% and 36.8% respectively of the total runoff. Interflow is an important flow component in this study due to the steep slope and well vegetation over the catchment.

**Table 5.4.** Water balance estimation at Bissen for the whole simulation period

| Component          | Measured<br>(mm) | Calculated<br>(mm) | Percentage<br>(%) | Mean<br>(mm/h) | Max<br>(mm/h) |
|--------------------|------------------|--------------------|-------------------|----------------|---------------|
| Precipitation      | 4505             | 4505               | 100               | 0.119          | 21.49         |
| Interception       |                  | 583.9              | 13.0              | 0.015          | 1.121         |
| Infiltration       |                  | 3219               | 71.5              | 0.085          | 15.84         |
| Evapotranspiration | 2467             | 2323               | 51.6              | 0.061          | 0.732         |
| Percolation        |                  | 1013               | 22.5              | 0.027          | 0.303         |
| Surface runoff     |                  | 688.2              | 15.3              | 0.018          | 5.243         |
| Interflow          |                  | 623.0              | 13.8              | 0.016          | 0.183         |
| Groundwater flow   |                  | 763.9              | 17.0              | 0.020          | 0.037         |
| Total runoff       | 2000             | 2075               | 46.1              | 0.055          | 5.259         |
| SM difference      |                  | 47.11              | 1.05              | 287.2 (mm)     | 372.8 (mm)    |
| GWS difference     |                  | 45.68              | 1.01              | 176.3 (mm)     | 325.7 (mm)    |

SM: soil moisture, GWS: groundwater storage.

Despite the good performance of the model predictions, the model requires the user to provide the necessary elevation, soil and land use data sources that are specific to the study area. The DEM is the starting point for several processes in producing the predicted hydrographs. Moreover, a successful hydrologic model requires information regarding the infiltration potential of the surface where the runoff occurs. The preferred data consists of digital maps containing area soils and land use information with associated potential runoff coefficient and depression storage capacity corresponding to each grid cell with different slope, soil and land use combinations. The functionality of WetSpa Extension was

designed to accommodate both overland flow and channel flow. The routing process is accomplished by the method of linear diffusive approximation without considering the specific channel characteristics for different cross sections, for instance, the channel loss properties, channel width, compound channel roughness, etc. A linear interpolation of Manning's  $n$  was then performed according to the stream orders by setting constant roughness values for the highest and lowest stream order. For the very flat areas (ponds, small lakes, and other zero slope cells), a minimum slope threshold was given, 0.01% for this case study, in order to keep the water moving in a right order on those areas. All these treatments will greatly facilitate the task of data collection and simplify the scheme of model calculation, but may bring errors and uncertainties to the final simulation results.

## **6. CONCLUDING REMARKS**

A GIS-based hydrological model, WetSpa Extension, in its fully and semi-distributed version compatible with remote sensing and GIS has been described in this user manual. The model runs on a microcomputer with a user-friendly interface, and can be applied to a wide range of watersheds for simulating the hydrological behaviour and especially runoff with due account for available topography, soil type, and land use data. The approach consists of the development of a spatially distributed modelling framework that accounts for spatial variability in terrain features to facilitate flood management and the physically realistic spatial integration of the complete water balance at a range of spatial and temporal scales. The model is implemented entirely within ArcView using Avenue scripts along with its Spatial Analyst and a hydrological extension integrated within a GIS environment. Encouraging results have been achieved as illustrated in the two case studies.

The spatial characteristics of input meteorological variables, i.e. temperature, precipitation and PET, are captured by means of Thiessen polygons, on which linear topographic corrections are implemented within each polygon to account for the altitude variation of these meteorological variables. The generation of surface runoff depends upon rainfall intensity and soil moisture status and is calculated as the net precipitation times a runoff coefficient, which depends upon slope, land use and soil type. Snowmelt is estimated from typical temperature variations and a degree-day type of snowmelt model.

The runoff is subsequently routed through the basin along flow paths determined from the high resolution DEM using a diffusive wave transfer model that leads to response functions between any start and end point, depending upon slope, flow velocity and dissipation characteristics along the flow lines. Interflow and percolation is controlled by soil characteristics and modelled by Darcy's law and kinematic approximation. The groundwater flow and its storage are conceptualized as a linear reservoir on small subcatchment scale with recession constant determined at reference gauging stations, and estimated for each subcatchment in relation with its drainage area and average slope.

The spatial variability of model parameters used in river basin simulations is known to affect simulated results. Like other distributed models, WetSpa allows for variability of model parameters in space over a catchment by incorporating information from the spatial variability of soils, land use, and topography, which gives a more accurate representation of natural hydrological processes. However, a high degree of uncertainty exists for many model input parameters including the potential runoff coefficient, soil hydraulic conductivity, roughness coefficient, hydraulic radius, as well as the threshold values for determining stream network, minimum slope and the percentage of impervious areas within an urban cell, etc. Moreover, some global parameters, such as interflow scaling factor, plant coefficient, degree-day coefficient, etc., are used in the model due to their complexity of optimization and for the simplification of model calibration. The large number of uncertainties associated with the input meteorological variables and the model parameters may make the calibration and validation of the model a time intensive undertaking. To deal with this problem, priorities are given to the model parameters with high sensitivity during model calibration as described in chapter 4. Further refinement of other model parameters is recommended in order to improve the model reliability. Additionally, pre-adjustment of model parameters to the channel geometry, boundary conditions, and system connectivity are necessary to achieve the quality of the final model simulation results.

*There are many directions for further research to improve the WetSpa model. One of the most important aspects is to complete a detailed quantitative sensitivity analysis and uncertainty assessment of the model, in order to examine the relative contribution of the model parameters, initial conditions, and input meteorological variables to the model's*

overall predictive uncertainty. In most applications of this type of modelling system, there will be cost restraints on the collection and preparation of necessary geophysical and meteorological input data. It is essential to know which of the inputs are most important and what spatial and temporal resolution are required to the generation of accurate results. Another important area of future research is to study the spatial characteristics of global model parameters used in the model, so as to create all model parameters in a spatial way in relation with terrain features, and enable the model to be used in un-gauged river basins without model optimization. Other possible future researches on the WetSpa model are proposed as follows:

- 1) *Interflow*
- 2) *Automated calibration of the most important model parameters, which has been implemented by coupling WetSpa model with PEST, a model-independent nonlinear parameter estimator provided by S.S. Papadopoulos and Associates (SSP&A). The scheme is to run the model as many times as it needs to adjust selected parameters within their predetermined range until the discrepancies between model outputs and a complementary set of flow observations is reduced to a minimum in the weighted least squares sense.*
- 3) *Development of a practical method to account for the joint effect of altitude, slope, aspect, general circulation of the atmosphere, etc., on the spatial distribution of precipitation, temperature and PET. This will highly increase the reliability of model inputs and decrease the uncertainty of model outputs, especially for modelling in a large mountainous catchment. The technology of using radar information may also be coupled in the WetSpa model to estimate the spatial distribution of rainfall at each time step.*
- 4) *Incorporation of variable travel time effect into flow routing schemes, for which the flow velocity is estimated as time variant variable depending upon the channel geometry and runoff volumes. This may overcome the shortage that flow velocity is assumed time invariant for a flood event in the current modelling approach.*
- 5) *Improvement of the simple snowmelt model used in WetSpa taking account the variability of degree-day constant, the effect of radiation on snowmelt, snow drift and deposition in steep terrain, and so on. This will make the snowmelt model more*

*realistic enabling the simulation of snow cover and melting runoff more accurately over extensive and heterogeneous landscapes*

- 6) Incorporation the influence of lakes and reservoir operation in the WetSpa model by combining efficient hydraulic models for engineering purpose. This will make the modelling system more flexible for flow simulation of large river basins with lakes and reservoirs involved.*
- 7) Update the current WetSpa into a real fully distributed model by combining with a distributed groundwater model. Groundwater balance is then calculated on grid cell basis allowing the estimation of groundwater table fluctuation and the simulation of saturation overland flow once the water table reaches the ground surface or the soil is fully saturated.*
- 8) Application of this model to study the soil erosion and deposition patterns allowing to keep a physically meaningful control on the effects of different land management scenarios on landscape-scale processes, for which the spatial parameters related to soil erosion and sedimentation will be generated.*
- 9) Application of this model to study the contaminant transport in the surface water and ground water system for the point and non-point source contaminations, for which a range of chemical, biological and physical parameters related to water quality control will be generated.*

*In any of the above cases, there will be a significant increase of model parameters to be estimated and consequently more complex model identifications have to be performed. This will make the model more and more complicated and difficult to be accomplished by untrained users. However, parallel extensions can be built according to the purpose of the project and focusing on specific directions. Generally, this research has laid a foundation for a GIS-based distributed hydrological modelling system for the prediction of flood and the simulation of water balance on catchment scale. Although the simulation results from the model indicate that additional work is necessary to improve model structure and model parameters, the existing model provides a substantial framework on which further researches can be conducted.*

## REFERENCE

- Allen, R.G., Using the FAO-56 dual crop coefficient method over an irrigated region as part of an evapotranspiration intercomparison study, *J. Hydrol.*, 229, 27-41, 2000.
- Anderson, E.A., National Weather Service River Forecast System - Snow Accumulation and Ablation Model, NOAA Technical Memorandum NWS HYDRO-17, U.S. Dept. Commerce, Silver Spring, MD., 1973.
- ASCE, American Society of Civil Engineers, Design and Construction of Sanitary and Storm Sewers, Manuals and Reports of Engineering Practice, No. 37, New York, 1969.
- Batelaan, O., Wang, Z.M. & De Smedt, F., An adaptive GIS toolbox for hydrological modelling, 3-9, eds., Kovar, K. & Nachtnebel, H.P., Application of geographic information systems in hydrology and water resources management, IAHS Publ., 1996.
- Bauwens W., Vanrolleghem P. & Smeets M., An evaluation of the efficiency of the combined sewer-waste-water treatment system under transient conditions, *Water Sci. Technol.*, 33, 199-208, 1996.
- Boers, T.M. & Ben-Asher, J., A review of rainwater harvesting, *Agric. Water Manage.*, 5, 145-158, 1982.
- Brooks, R.H. & Corey, A.T., Properties of porous media affecting fluid flow, *J. Irrig. Drain. Amer. Soc. Civil Eng.*, IR2, 61-88, 1966.
- Brown, V.A., McDonnell, J.J., Burns, D.A. & Kendall, C., The role of event water, a rapid shallow flow component, and catchment size in summer stormflow, *J. Hydrol.*, 217, 171-190, 1999.
- Browne, F.X., Stormwater management, *Standard Handbook of Environmental Engineering*, ed., R.A. Corbitt, 7.1-7.135, McGraw-Hill, New York, 1990.
- Carsel, R.F. & R.S. Parrish, Developing Joint Probability Distributions of Soil Water Retention Characteristics, *Water Resour. Res.*, 24, 755-769, 1988.
- Clark, O.R., Interception of rainfall by prairie grasses, weeds and certain crop plants, *Ecol. Monogr.*, 10, 243-277, 1940.
- Chow, V.T., Maidment, D.R. & Mays, L.W., *Applied Hydrology*, 498, McGraw-Hill Inc., New York, 1988.

- Chow, V.T., Handbook of Applied Hydrology, 7-25, McGraw-Hill, Book Company, New York, 1964.
- Cosby, B.J., Hornberger, G.M., Clapp, R.B. & Ginn, T.R., A statistical exploration of the relationships of soil moisture characteristics to the physical properties of soils, *Water Resour. Res.*, 20, 682–690, 1984.
- Criss, R.E. and Winston W.E., Do Nash values have value? Discussion and alternate proposals, *Hydrol. Process.*, 22, 2723-2725, 2008.
- De Smedt, D., Development of a continuous model for sewer system using MATLAB, MSc. Thesis, Laboratory of Hydrology, Vrije Universiteit Brussel, Belgium, 1997.
- De Smedt, F., Liu, Y.B. & Gebremeskel, S., Hydrological modelling on a catchment scale using GIS and remote sensed land use information, ed., Brebbia, C.A., 295-304, *Risk Analyses II*, WIT press, Southampton, Boston, 2000.
- Dickinson, R.E., Henderson-Sellers, A. & Kennedy, P.J., Biosphere Atmosphere Transfer Scheme (BATS), Version 1e as Coupled to the NCAR Community Climate Model, NCAR Technical Note, NCAR, Boulder, Colorado, 1993.
- Dingman, S.L., *Physical Hydrology*, Prentice-Hall, New Jersey, 1994.
- Dingman, S.L., Barry, R.G. & Reynolds, R.C., Application of kriging to estimating mean annual precipitation in a region of orographic influence, *Water Resour. Bull.*, 24, 329-339, 1988.
- Drogue G., A. El Idrissi, L. Pfister, T. Leviandier, J.F. Iffly & L. Hoffmann, Calibration of a parsimonious rainfall-runoff model: a sensitivity analysis from local to regional scale, eds., Rizzoli A.E. & Jakeman A.J., 464-469, *Integrated assessment and decision support, Proceedings of the First biennial meeting of the International Environmental Modelling and Software Society, Lugano (Switzerland), Vol. 1.*, 2002.
- Dunne, T., Stochastic aspects of the relations between climate, hydrology and landform evolution, *Trans. Jpn. Geomorphol. Union*, 12, 1–24, 1991.
- Eagleson, P.S., *Dynamic Hydrology*, 364, McGraw-Hill Pub., 1970.
- El Idrissi A., G. Drogue, L. Pfister, J.F. Iffly, L. Hoffmann, B. Hingray & F. Guex, Estimation of high floods by three rainfall-runoff models with short rainfall-runoff series (Alzette river basin, Luxembourg), eds., Rizzoli A.E. & Jakeman A.J., 470-475, *Integrated assessment and decision support, Lugano (Switzerland), Vol. 1*, 2002.

- Environmental Systems Research Institute (ESRI), ArcView GIS Version 3.2 Online Help Documentation, 1999.
- Famiglietti, J.S. & Wood, E.F., Multiscale modelling of spatially variable water and energy balance processes, *Water Resour. Res.*, 30, 3061-3078, 1994.
- Ferguson, B.K., *Introduction to Stormwater, Concept, Purpose and Design*, 111, John Wiley & Sons, Inc. USA, 1998.
- Fernandez-Illescas, C.P., Porporato, A., Laio, F. & Rodriguez-Iturbe, I., The ecohydrological role of soil texture in a water-limited ecosystem, *Water Resour. Res.*, 37(12), 2863-2872, 2001.
- Fetter, C.W., *Applied Hydrogeology*, 6, Charles E. Merrill Pub. Co., Columbus, Ohio, 1980.
- Fronteau, C. & Bauwens, W., Een evaluatie van de efficiëntie van het rioolstelsel, RWZI, rivier systeem onder dynamische omstandigheden, *Water*, 84, 203-210, 1995.
- Geiger, W.F., Marsalek, J., Rawls, W.J. & Zuidema, F.C., *Manual on drainage in urbanized areas, Vol. 1, Planning and design of drainage systems, Studies and Reports in Hydrology*, UNESCO, 1987.
- Guex, F., Modélisation hydrologique dans le bassin versant de l'Alzette (Luxembourg), régionalisation des paramètres d'un modèle global, *Travail pratique de Diplôme, Ecole Polytechnique Fédérale de Lausanne*, 67, 2001.
- Haan, C.T., *Hydrological Modelling of Small Watersheds*, 211, Published by American Society of Agricultural Engineers, USA, 1982.
- Hairsine, S.Y. & Parlange, J.Y., Kinematic shock waves on curved surfaces and application to the cascade approximation, *J. Hydrol.*, 87, 187–200, 1986.
- Hansen, B., Schjoning, P. & Sibbesen, E., Roughness indices for estimation of depression storage capacity of tilled soil surfaces, *Soil Till. Res.*, 52, 103-111, 1999.
- Henderson, F.M., *Open Channel Flow*, 522, McMillan, New York, 1966.
- Horton, R.E., Rainfall interception, *Monthly Weather Review*, 47, 603-623, 1919.
- Kachroo, R.K. & Natale, L., Non-linear modelling of rainfall–runoff transformation, *J. Hydrol.* 135, 341–369, 1992.
- Kastelec1, D. & Košmelj, K., Spatial interpolation of mean yearly precipitation using universal kriging, eds., Mrvar, A. & Ferligoj, A., *Developments in Statistics*,

- Metodološki zvezki, 17, Ljubljana, 2002.
- Kirkby, M.J., Hill Slope Hydrology, 235, John Wiley & Sons, Ltd., 1978.
- Kite, G.W. & Kauwen, N., Watershed modelling using land classification, *Water Resour. Res.*, 28, 3193-3200, 1992.
- Linsley, R.K., Kohler, J., Max A. & Paulhus, J.L.H., *Hydrology for Engineers*, 237, 3rd Ed., McGraw-Hill, New York, 1982.
- Liu, Y.B., Gebremeskel, S., De Smedt, F., Hoffmann, L. & Pfister, L., A diffusive transport approach for flow routing in GIS-based flood modelling, *J. Hydrol.*, 283, 91-106, 2003.
- Liu, Y.B., Gebremeskel, S., De Smedt, F. & Pfister, L., Flood prediction with the WetSpa model on catchment scale, eds., Wu et al., 499-507, *Flood Defence '2002*, Science Press, New York Ltd., 2002.
- Loague, K.M., Impact of rainfall and soil hydraulic property information on runoff predictions at the hillslope scale, *Water Resour. Res.*, 24(9), 1501–1510, 1988.
- Lull, H.W., Ecological and silvicultural aspects, *Handbook of applied hydrology*, ed., Ven Te Chow, 6.1-6.30, McGraw-Hill, New York, 1964.
- Male, D.H. & Gray, D.M., Snowcover Ablation and Runoff, In *Handbook of Snow: Principles, Processes, Management and Use*, 360-436, eds., D.M. Gray and D.H. Male, Pergamon Press, 1981.
- Mallants D. & Feyen J., Kwantitatieve en kwalitatieve aspecten van oppervlakte en grondwaterstroming (in Dutch), 76, Vol. 2, KUL, 1990.
- Martin, G.N., Characterization of simple exponential baseflow recessions, *J. Hydrol.* 12, 57-62, 1973.
- Martinez, J., Rango, A. & Major, E., *The Snowmelt-Runoff Model (SRM) User's Manual*. NASA Reference Publ. 1100, Washington, D.C., USA, 1983.
- Mazion, E. & Yen, B.C., Computational discretization effect on rainfall-runoff simulation, *J. Water Resour. Plan. Manage.*, 120(5), 715–734, 1994.
- McCuen, R.H., W.J. Rawls & D.L. Brakensiek, Statistical Analysis of the Brooks-Corey and the Green-Ampt Parameters Across Soil Textures, *Water Resour. Res.*, 17(4), 1005-1013, 1981.
- Miller, W.A. & J.A. Cunge, Simplified equations of unsteady flow, eds., K. Mahmood & V. Yevjevich, *Unsteady flow in open channels*, Water Resources Publications, Fort

- Collins, CO., 1975.
- Molnar P. & Ramirez, J.A., Energy dissipation theories and optimal channel characteristics of river networks, *Water Resour. Res.*, 34, 1809-1818, 1998.
- Moore, I.D., Gessler, P., Nielsen, G. & Peterson, G., Soil attribute prediction using terrain analysis, *Soil Sci. Soc. Am. J.*, 57, 443-452, 1993.
- Moore, I.D., Larson, C.L., Estimating microrelief surface storage from point data, *Trans. ASAE.*, 20, 1073-1077, 1979.
- Nash, J.E. & Sutcliffe, J.V., River flow forecasting through conceptual model, *J. Hydrol.*, 10, 282-290, 1970.
- Onstad, C.A., Depressional storage on tilled soil surfaces, *Trans. ASAE.*, 27, 729-732, 1984.
- Perrier, A., Land surface processes : vegetation, ed., Eagleson, P., *Land Surface Processes in Atmospheric General Circulation Models*, 395-348, Cambridge Univ. Press, 1982.
- Pfister, L., Humbert, J. & Hoffmann, L., Recent trends in rainfall-runoff characteristics in the Alzette river basin, Luxembourg, *Climate Change*, 45(2), 323-337, 2000.
- Ragab, R. & Cooper, J.D., Variability of unsaturated zone water transport parameters: implications for hydrological modelling, *J. Hydrol.*, 148, 109-131, 1993.
- Rawls, W.J. & Brakensiek, D.L., Prediction of Soil Water Properties for Hydrological Modelling, *Watershed Management in the Eighties*, ASCE, 293-299, 1985.
- Rawls, W.J., Brakensiek, D.L. & Saxton, K.E., Estimation of soil water properties, *Trans. Amer. Soc. of Agric. Engin.*, 25(5), 1316-1320, 1328, 1982.
- Rowe, L.K., Rainfall interception by an evergreen beech forest, *J. Hydrol.*, 66, 143-158, 1983.
- Saghafian, B., Julián, P.Y., & Ogden, F.L., Similarity in catchment response 1. Stationary rainstorms, *Water Resour. Res.*, 31, 1533-1541, 1995.
- Sharma, K.D., Runoff behaviour of water harvesting microcatchment. *Agric. Water Manage.*, 11, 137-144, 1986.
- Sheaffer, J.R., K.R. Wright, W.C. Taggart & R.M. Wright, *Urban Storm Drainage Management*, Marcel Dekker, New York, 1982.
- Shuttleworth, W.J., Micrometeorology of temperate and tropical forest, *Phil. Trans. Roy. Meteorol. Soc.*, 110, 1143-1162, 1989.

- Simons D.B., Storm water and Sediment runoff simulation for a system of multiple watersheds, Volume II, Sediment routing and yield. Prepared for USDA Forest Service, Rocky Mountain Range Experiment Station, Flagstaff, Arizona, 1981.
- SINCE, WatfloodSPL8, Flood Forecasting System, Developed for Surveys and Information Branch Ecosystem Science and Evaluation Directorate, Environment Canada, 1972.
- Singh, P., Kumar, N. & Arora, M., Degree-day factors for snow and ice for the Dokriani Glacier, Garhwal Himalayas, *J. Hydrol.*, 235, 1-11, 2000.
- Smakhtin, V.Y., Sami. K. & Hughes, D.A., Evaluating the performance of a deterministic daily rainfall-runoff model in a low flow context, *Hydrol. Process.*, 12, 797-811, 1998.
- Szeicz, G. & Long, I.F., Surface resistance of crop canopies, *Water Resour. Res.*, 5, 622-633, 1969.
- Thornthwaite, C.W. & Mather, J.R., The water balance, Laboratory of Climatology, Publ. No. 8, Centerton NJ., 1955.
- Ullah, W. & Dickinson, W.T., Quantitative description of depression storage using a digital surface model, I. Determination of depression storage, *J. Hydrol.* 42, 63-75, 1979a.
- Ullah, W. & Dickinson, W.T., Quantitative description of depression storage using a digital surface model, II. Characteristics of surface depressions, *J. Hydrol.* 42, 77-90, 1979b.
- USACE, HEC-1 Flood Hydrograph Package: User's Manual. U.S. Army Corps of Engineers, Davis, CA., 1998.
- Vieux, B.E. & Farajalla, N.S., Capturing the essential variability in distributed hydrological modelling: Hydraulic roughness, *Hydrol. Process.*, 8, 221-236, 1994.
- Vijay P.S. & Woolhiser, D.A., Mathematical modelling of watershed hydrology, *J. Hydrological Eng.*, 7(4), 270-292, 2002.
- Wang, Z.M., Batelaan, O. & De Smedt, F., A distributed model for water and energy transfer between soil, plants and atmosphere (WetSpa), *Phys. Chem. Earth*, 21(3), 189-193, 1997.
- Wittenberg, H. & Sivapalan, M., Watershed groundwater balance estimation using streamflow recession analysis and baseflow separation, *J. Hydrol.*, 219, 20-33, 1999.

- Wittenberg, H., Baseflow recession and recharge as nonlinear storage processes, *Hydrol. Process.*, 13, 715-726, 1999.
- Wu, Y., Woolhiser, D.A. & Yevjevich, V., Effects of spatial variability of hydraulic roughness on runoff hydrographs, *Agric. Forest Meteorol.*, 59, 231–248, 1982.
- Yen, B.C., *Channel Flow Resistance: centennial of Manning's Formula*, 43, Water Resources Publications, USA, 1992.
- Zinke, P.J., Forest interception studies in the United States, *International Symposium on Forest Hydrology*, eds., W.E. Sopper & H.W. Hull, 137-161, Pergamon Press, Oxford, 1967.